2018

Geochemical and Microbiological Controls on Mercury Methylation in Natural Waters

Alison M. Agather
Wright State University

GEOCHEMICAL AND MICROBIOLOGICAL CONTROLS ON MERCURY METHYLATION IN NATURAL WATERS

A dissertation submitted in partial fulfillment of the
requirements for the degree of
Doctor of Philosophy

ALISON M. AGATHER
B.A., Gustavus Adolphus College, 2013

2018
Wright State University

WRIGHT STATE UNIVERSITY

GRADUATE SCHOOL

November 9th, 2018

I HEREBY RECOMMEND THAT THE DISSERTATION PREPARED UNDER MY SUPERVISION BY Alison M. Agather ENTITLED Geochemical and microbiological controls on mercury methylation in natural waters BE ACCEPTED IN PARTIAL FULFILLMENT OF THE REQUIREMENTS FOR THE DEGREE OF Doctor of Philosophy.

_____

Chad Hammerschmidt, Ph.D.
Dissertation Director

_____

Donald Cipollini, Ph.D.
Director, ES Ph.D. Program

_____

Barry Milligan, Ph.D.
Interim Dean of the Graduate School

Committee on Final Examination:

_____

William Fitzgerald, Ph.D.

_____

Carl Lamborg, Ph.D.

_____

Mark McCarthy, Ph.D.

_____

Silvia Newell, Ph.D.

_____

Sarah Tebbens, Ph.D.

ABSTRACT

Agather, Alison M. Ph.D. Environmental Sciences Ph.D. Program, Wright State University, 2018. Geochemical and microbiological controls on mercury methylation in natural waters.

Mercury (Hg) is a global pollutant toxic to humans and wildlife. Monomethylmercury (MMHg) is a bioavailable compound that bioaccumulates and biomagnifies in food webs. Humans are primarily exposed to MMHg from seafood consumption (Sunderland 2007), and high quantities of the neurotoxin lead to reduced neurocognitive functioning in adults and the children of exposed mothers (Cohen et al. 2005, Yokoo et al. 2003). Negative effects from MMHg accumulation on the health of humans and wildlife requires a more complete understanding of the chemistry and microbiology driving Hg methylation in both marine and freshwater systems. This work focuses on water column distribution, speciation, and methylation of Hg. The aims of this dissertation are three-fold: (1) characterize the speciation and distribution of Hg in the western Arctic Ocean; (2) examine seasonal variations in Hg speciation, methylation, and demethylation, and the microbial communities of Hg methylators in Crystal Lake, Ohio; and (3) quantify Hg methylation rates and characterize methylating microbial communities in waters on the continental shelf of the northwest Atlantic Ocean. While Hg methylation has been studied for decades, this work is built upon recent improvements in Hg detection limits, and

newly discovered genes responsible for Hg methylation. In conjunction with U.S. Arctic GEOTRACES (GN01), the western Arctic Ocean was sampled in the summer of 2015. Although Hg concentrations in the Canada and Eurasian Basins were low relative to the Atlantic and Pacific Oceans, higher MMHg concentrations were observed in Arctic seawater that recently interacted with continental margins. We estimate that the Arctic Ocean receives 4–71 kmol Hg yr^{-1} from the Bering Strait, which is likely to interact with sediments of the shallow continental shelves before entering into the Arctic Ocean. This is potentially important, because while the estimated atmospheric input to the Arctic Ocean is ~400 kmol Hg yr^{-1}, inflowing Hg from the Bering Strait may still be an important source of Hg that can be methylated on the Chukchi Shelf. Mercury methylation potentials were measured in a stratified freshwater system, Crystal Lake, in Dayton, Ohio (objective #2). Mercury methylation occurred in both oxic and anoxic portions of the water column, but methylation potentials were greatest at the oxic/anoxic boundary layer. Mercury methylating genes were found throughout the water column and had the greatest copy number in the hypolimnion. Similarly, previous marine work showed that sediments and the microbial communities therein are large sources of MMHg to near shore marine systems (Fitzgerald et al. 2007), which led to methylation and demethylation studies along the northwest Atlantic shelf (objective #3). Greater abundance of Hg methylating microbes were observed in water overlying sediment as opposed to shallower waters, but methylation potentials did not significantly differ. Together, these results suggested that (1) Archaea may be responsible for Hg methylation in oxic waters; and (2) redox transition zones in the water column and the sediment-water interface are important sources of bioavailable MMHg. These studies improve our

understanding of Hg cycling in natural waters and suggest possible conditions and organisms that stimulate Hg methylation.

TABLE OF CONTENTS

LIST OF FIGURES

LIST OF TABLES

ACKNOWLEDGMENTS

I thank my advisor, Chad, who asked me to stay and get a Ph.D., even after I blew up the lab microwave. With your mentorship, I have become a better scientist and have had many opportunities that would not have been possible otherwise. I have learned a lot in my five and a half years at Wright State, and I expect our friendship will continue after I leave.

Thank you Bill, Carl, and Katlin for welcoming me to team Hg with open arms. Carl and Katlin: from the North Pole to Marseille, there are no two scientists I would rather travel and study Hg with. Thanks for always being great mentors and lab-mates at sea. And to Bill: thanks for teaching me that any oceanographer worth her salt needs a drink or two now and then. I will always appreciate your Boston-accented advice.

Thank you to my committee, Silvia Newell, Sarah Tebbens, and Mark McCarthy, for a lot of help and support along the way. I have appreciated your candor and diverse perspectives, as sometimes Team Hg can get a bit carried away. Thank you, Silvia, for teaching me everything I wanted to know about PCR, and then some. It has improved this work immeasurably.

Thank you to Jeff Jeremiason, for allowing me to work in your lab and trusting me to use and maintain the ICP-MS. I learned a lot about Hg, instrumentation, and being a good lab mate and teammate while working in your lab.

Thank you to past and present students in the WSU Hg lab. You made lab work and hanging out in the dungeon fun. Thank you to past and present EES students and ES Ph.D. students, I appreciate the diverse skills and interests that have inspired many good conversations and led to lots of fun. Thank you to the staff in the Earth & Environmental Sciences Department and the Environmental Sciences Ph.D. Department.

Thank you to my friends and family, who have supported me through my academic career and the ups and downs of grad school. You always knew how to brighten my day and make me smile.

Lastly, I acknowledge my funding sources: Wright State Graduate School's Wright Fellowship, the EES and ES Ph.D. Departments, and National Science Foundation Grant OCE-1434650 funded me throughout the past five and a half years.

Chapter 1: INTRODUCTION

1.1. Importance

Mercury (Hg) is pollutant that impacts human and ecosystem health. Hg speciation dictates the environmental fate of the metal, and its uptake, metabolism and accumulation in humans. The toxicity of elemental Hg (Hg^0) differs from monomethylmercury (MMHg) due to chemical differences between species. Hg^0 is a monoatomic gas that vaporizes from liquid Hg. Hg^0 poisoning is less common now, but remains an occupational hazard for some jobs. From the 17th to mid-20th century, hatters were a common example of Hg^0 toxicity. Animal hides were felted together with mercuric nitrate ($Hg(NO_3)_2$), and hatters typically worked in poorly ventilated spaces. The phrase "mad as a hatter" resulted from neurocognitive loss from repeated Hg^0 exposure. Hg^0 easily crosses the blood-brain barrier which results in neurodegeneration (Farina et al., 2013). Awareness of the ill effects of Hg^0 has reduced its use and improved workplace safety. Today, Hg^0 exposure mostly results from dental amalgams and small-scale artisanal gold mining (Ha et al., 2017).

Most humans are exposed to Hg in the form of MMHg, which is a neurotoxin and the most bioavailable form of Hg. Attention turned to MMHg in the early 20th century, when an environmental disaster in Minimata, Japan highlighted an extreme incident of MMHg poisoning. Minimata residents noticed many fishermen had developed symptoms

of a neurological disease and cats were “dancing” in the streets. The source of the problem was an acetaldehyde manufacturing plant that discharged MMHg waste directly into the bay. MMHg bioaccumulated in the local food web, exposing consumers to high MMHg concentrations. This environmental disaster highlights the risks associated with MMHg bioaccumulation and human exposure through the consumption of seafood (Clarkson, 1998).

Unfortunately Minimata was not the last incident of mass MMHg exposure. In the early 1970s, crop yields in Iraq were low. To ensure high crop yields the following season, the Iraqi government ordered fungicide-fortified grains. In error, the seeds sent to Iraq were treated with a fungicide containing MMHg. When Iraqis made bread from wheat grown from treated seeds, they exposed themselves to high MMHg concentrations (Clarkson, 1998). While this incident is unlikely to be repeated, it bears mentioning because of the common theme that anthropogenic alteration of Hg has led to detrimental side effects.

These stories are extreme cases of MMHg exposure, but they have increased visibility and justified the need for Hg research. Today the dangers of MMHg exposure are low, and mostly depend on food consumption habits. Humans primarily accumulate MMHg from seafood consumption (Clarkson et al., 2003; Sunderland, 2007). Populations largely dependent on marine animals as a primary protein source tend to accumulate more MMHg (Choi and Grandjean, 2008; Van Oostdam et al., 1999). Arctic communities such as Faroe Islanders and other Arctic populations, consume traditional diets comprised of animals at high trophic-levels, which often contain high concentrations of MMHg (Choi and Grandjean, 2008; Van Oostdam et al., 1999). At lower latitudes, humans

consuming locally caught seafood risk MMHg accumulation (Lincoln et al., 2010), and freshwater fish can be a route of MMHg exposure (Johnsson et al., 2004).

1.2. Negative health effects

Elevated blood MMHg concentration is a human health concern because of its neurotoxicity. Depending on an individual's dosage and sensitivity, Hg may adversely affect the renal, cardiovascular, nervous, and immune systems (Yokoo et al., 2003; Zahir et al., 2005). Humans with the greatest risk of MMHg exposure are fetuses exposed in utero, who can succumb to developmental delays (Cohen et al., 2005).

Accumulation and neurotoxicity of MMHg are caused by the compound's chemical properties. First, the entry rate of MMHg into the central nervous system is faster than the entry rate of inorganic Hg compounds (Farina et al., 2013). Once in the central nervous system, the electrophilic properties of MMHg negatively impact homeostasis. MMHg oxidizes sulfhydryl groups (-SH/-S^{-}), proteins with thiol groups, and non-protein thiols (Farina et al., 2013). Oxidation of sulfur groups alters their function (Kim et al., 2002). MMHg can also oxidize glutathione and selenoproteins, which are more nucleophilic than thiols (Farina et al., 2013).

Redox state modification within the central nervous system has cascading effects on the body that lead to neurodegeneration. Changes in the redox state of the nucleophilic group cause both oxidative stress (Farina et al., 2011), and glutamate dyshomeostasis (Aschner et al., 2007). MMHg uptake increases the amount of extracellular glutamate by inhibiting glutamate uptake (Aschner et al., 2000; Brookes and Kristt, 1989), and stimulating gultamate release (Reynolds and Racz, 1987). Glutamate is the most

important excitatory neurotransmitter in the mammalian central nervous system, but excessive amounts damage neurons (Aschner et al., 2007; Farina et al., 2013). Increases in glutamate correlate with increases Ca^{2+} and Na^{+}, which stimulate nitric oxide (NO) production (Farina et al., 2013). These biochemical reactions cause neurodegeneration in cerebral and cerebellar cortices (Uchino et al., 1995).

Plainly, excessive amounts of MMHg accumulation negatively impacts the chemical equilibrium of the central nervous system. To prevent neurodegeneration, dose and exposure frequency should be monitored. Body burden estimates from measuring Hg in hair, blood, or toenails can help estimate MMHg vulnerability. Exposure levels can identify populations at risk of excessive MMHg accumulation from either diet or environment. The World Health Organization suggests a maximum weekly intake of 1.6 $\mu g\ kg^{-1}$ (Poulin and Gibb, 2008), and the U.S. Environmental Protection Agency sets a more conservative intake guideline of 0.1 $\mu g\ kg^{-1}$ (US EPA, 2016). Still, better mechanistic understanding of the effect of MMHg on the body and dose-response assessments do not fully answer questions regarding MMHg formation. Our knowledge and understanding of Hg cycling has improved, but many questions remain regarding Hg methylation in the environment.

1.3. Aquatic mercury (Hg) cycle

Mercury enters the environment from a variety of natural sources such as volcanic outgassing, submarine hydrothermal vents and the mineral cinnabar. These sources are overshadowed by human alteration of the Hg cycle. Anthropogenic activities such as artisanal gold mining, mining, and fossil fuel burning have increased Hg in the environment by a factor of three since the industrial revolution (Fitzgerald et al., 2005,

1998). Anthropogenic emissions have increased Hg stored in the atmosphere and ocean. It is estimated that about 300 million moles of Hg have been added to the global ocean, and two-thirds of the oceanic Hg is in the thermocline, where active chemical cycling takes place (Lamborg et al., 2014). Mercury is present as four species in natural waters: elemental Hg (Hg^0), divalent inorganic Hg (Hg(II)) complexed to inorganic and organic molecules, MMHg, (CH_3Hg^+), and dimethylmercury (DMHg, CH_3Hg_2). These species undergo many biotic and abiotic reactions in the water column and sediments. A brief overview of Hg^0, Hg^{2+}, and DMHg cycling follows, as well as a more in depth look at MMHg cycling in the water column.

1.3.1. Hg cycling

Mercury is the only metal that is a liquid at room temperature, and volatilizes to the monoatomic gas Hg^0. With an atmospheric lifetime of 6 to 12 months (Horowitz et al., 2017; Slemr et al., 1985), Hg^0 can travel long distances from its emission source before removal from the atmosphere (Figure 1.1). Hg^0 acts as a direct link between the atmosphere and water column, as it can diffuse into and efflux out of surface waters. Photochemical oxidation of atmospheric Hg^0 to Hg^{2+} allows particles to scavenge Hg^{2+}, which are subsequently washed out of the atmosphere by precipitation (Lindqvist et al., 1991; Nriagu and Pacyna, 1988). Wet and dry atmospheric deposition is the largest source of Hg to the ocean (Fitzgerald et al., 2007; Horowitz et al., 2017; Sunderland and Mason, 2007).

Divalent Hg deposition leads to various biotic and abiotic reactions. Inorganic and organic ligands may complex with Hg^{2+}, and much of Hg in the aquatic water column is bound to dissolved organic carbon (Fitzgerald et al., 2007). Depending on the

complexation of Hg^{2+}, it may be reduced to Hg^0 by photochemical reactions (Rolfhus and Fitzgerald, 2004) or biotic reduction via the *mer* operon (Boyd and Barkay, 2012). Hg^{2+} may associate with particles which may be deposited to sediments, or methylated to either MMHg or DMHg (Figure 1.1). While methylation and demethylation occur biotically and abiotically, the most important source of MMHg is hypothesized to be biomethylation (Benoit et al., 2002; Compeau and Bartha, 1985). Complexation of Hg^{2+} may dictate the formation of MMHg and DMHg.

Once methylated, Hg can enter the food web and bioaccumulate in higher trophic levels. Most of the Hg in fish tissue exists as MMHg (Bloom, 1992). Little is known about DMHg, but it is thought to be a relatively short-lived gas. The mechanism for DMHg formation is unknown, but has been observed in marine waters (Lehnherr et al., 2011). DMHg may be the product of methylation of MMHg or Hg(II). Similarly, the process governing DMHg demethylation is uncertain, but MMHg may be a product of DMHg disintegration. Few studies have measured DMHg in freshwater lakes (Bloom and Effler, 1990; Vandal et al., 1991), indicating DMHg may be more important to marine Hg cycles. In the ocean, DMHg is mainly found in cold, deep waters (Mason et al., 1995).

1.3.2. MMHg cycling

Biotic and abiotic transformation pathways synthesize and demethylate MMHg. Methylation has been attributed to biotic transformation pathways for some time, but only recently has the microbial pathway responsible for MMHg formation been discovered (Parks et al., 2013). This recent discovery has propelled research into MMHg formation regarding which microbes methylate Hg and what conditions are ideal for Hg

methylation (Sections 1.3.3, 1.3.4). Abiotic transformation pathways will be discussed in brief, and biotic methylation will be examined in deeper detail.

1.3.3. Abiotic methylation

Abiotic reactions are thought to be a minor contributor to MMHg formation in aquatic systems. A methyl donor may be the product of biotic mechanisms; but enzyme activity distinguishes a biotic reaction from an abiotic methylation reaction. Three potential abiotic Hg methylation mechanisms have been identified: (1) molecules such as methyl iodide, dimethylsulfide, and fulvic and humic acids may methylate Hg^{2+} via oxidative addition (Celo et al., 2006), (2) transmethylation occurs when compounds such as methylcobalamin, methyltin, or methyliodide react with Hg^{2+} (Celo et al., 2006), and (3) an acetic acid solution in aerated water, such as rain, may form MMHg (Gårdfeldt et al., 2003; Hammerschmidt et al., 2007). Abiotic methylation is conditionally dependent on pH, temperature, and presence of complexing agents, including dissolved organic matter (Celo et al., 2006). These requirements decrease the likelihood of abiotic methylation and result in biotic methylation being more prevalent. Lastly, sediment work has shown potential for abiotic methylation in sediment (Hammerschmidt and Fitzgerald, 2001), which may account for up to 5% of Hg methylation (Compeau and Bartha, 1985).

1.3.4. Biotic methylation

The processes and mechanisms involved in biotic Hg methylation were elucidated with the discovery of the genes responsible for Hg methylation (Parks et al., 2013). Similarity within a sequence of the large subunit CFeSP (CfsA, locus tag CHY_1223) was found between the binding domain of CfsA and the N terminus of DND132_1056 (Parks et al., 2013). The corresponding genes are *hgcA* and *hgcB*, respectively, in the

hgcAB cluster. Confirming the presence of *hgcAB* in known methylators and their absence in non-methylators suggested their possible role in methylating Hg (Parks et al., 2013).

The presence of both *hgcA* and *hgcB* are necessary for MMHg formation (Qian et al., 2018). *hgcA* and its orthologues encode a corrinoid protein, which facilitates the transfer of a methyl group to Hg (Parks et al., 2013). *hgcB* and its orthologues encodes 2[4Fe-4S] ferrodoxin, which reduces the corrinoid protein. The discovery of the gene pair and mechanism for Hg methylation was consistent with a pervious hypothesis that methylating microbes can identify Hg^{2+} as a substrate (Choi et al., 1994b), but instead identifies CH_3-H_4-Folate as a possible methyl donor. The CH_3-H_4-Folate molecule donates a CH_3^+ to cob(I)alamin-HgcA to form CH_3-cob(III)alamin-HgcA. The protein HgcB performs the thermodynamically challenging oxidation of Co(II) to Co(III). The protein HgcA is thought to allow the coordination of Co-S (Parks et al., 2013).

BLASTP (Basic Local Alignment Search Tool for Proteins) and Pfam (a collection of protein families) searches have been used to confirm the presence of *hgcAB* orthologues in previously sequenced microbial genomes (Gilmour et al., 2013). *hgcAB* orthologues led to phylogeny reconstruction of *hgcAB.* Methylation most likely developed as a method of detoxification rather than a method of resistance to Hg^{2+} and or Hg^0 (Graham et al., 2012). *hgcAB* is present in two phyla of bacteria, Protobacteria and Firmicutes, and one phylum of archaea, Euryarchaeota (Parks et al., 2013). A follow up investigation further divided orthologues into five clades, three within *Deltaproteobacteria*: *Geobacter, Desulfovibrionales and Desulfobacterales*. The other

clades were evolutionarily distant, including methanogens (*Archaea*), and *Clostridia* (*Firmicutes*; Gilmour et al., 2013; Parks et al., 2013).

Within *Deltaproteobacteria*, most of the identified Hg methylators are in the genera *Desulfovibrio* and *Geobacter* (Gilmour et al., 2013). Three other families within the *Deltaproteobacteria* contain methylating genes; the *Desulfobacteracceae*, *Desulfoobulbaceae*, and *Desulfomicrobiaceae.* Many studies have concluded that the ability to methylate Hg is strain specific and not dependent upon species, genus, or metabolic group (Ranchou-Peyruse et al., 2009).

Genetic screening for *hgcAB* has identified microbes that were previously unknown Hg methylators. For example, *Firmicutes* are a diverse, typically gram-positive bacteria. Methylating *Firmicutes* includes fermentative (*Ethanoligenens harbinense*), acetogenic (*Acetonema longum*), cellulolytic, acidiphilic (*Desulfosporosinus acidiphilus*), and haloalkaliphilic (*Dethiobacter alkaliphilus*) species. Most *Firmicutes* use partially reduced sulfur species as an electron acceptor, but one was found to use Fe(III) (*Desulfitobacterium metallireducens*). Within *Deltaproteobacteria*, previously unknown Hg methylators include an obligate alkaliphile (*Desulfonatronospira thiodismutans*), metal reducer (*Anaeromyxobacter dehalogenans*), reductive dechlorinator (*Desulfomonile tiedjei*), syntrophs (*Syntrophus aciditrophicus* and *Syntrophorhabdus aromaticivorans*) and a deep-sea vent thermophile (*Desulfacinum hydrothermale*). The *hgcAB* gene cluster in methanogens is currently confined to *Methanomicrobia*, which contains methylotrophic and hydrogenotrophic species (Gilmour et al., 2013).

A comparative analysis of microbiomes identified homologues (related by an ancestral DNA sequence) and orthologues (related by an ancestral gene) of the gene pair

hgcAB (Podar et al., 2015). Identifying relatives of *hgcAB* may identify microbes without the gene pair that might be capable of methylation via alternate mechanisms. Currently, about 3,100 of 33,000 microbiome sequences have the Pfam3599 superfamily of proteins, which encodes the HgcA protein (Podar et al., 2015). The range of these sequences varies from fragments with the conserved domain to full length *hgcAB*. Some sequences contain the necessary sequence for the corrionid FeS protein, suggesting the acetyl-CoA pathway does not equate to methylating capability (Podar et al., 2015).

Analysis of *hgcAB* prevalence throughout various environments revealed diverse methylating communities (Podar et al., 2015). Engineered environments for either biomass fermentation or chlorinated-compound degradation had less microbial diversity of Hg methylators compared to natural environments such as wetlands, dead zones, permafrost, and marine sediment. In locations with high methylation rates, diverse microbial communities had increased abundance of *hgcA*. The broad phylogenetic diversity of these sites had a representative of every microbial taxon related to Hg methylation. Analysis of community genetics identified previously unknown sites of Hg methylation, including: thawing permafrost, coastal hypoxic zones, bioreactors for contaminant degradation, saturated agricultural soils and extreme anaerobic environments (Podar et al., 2015).

Development of polymerase chain reaction (PCR) primers has helped identify *hgcAB* in the environment. Broad range primers confirm the presence of *hgcAB*, while clade-specific primers allow quantification of *hgcA* gene copies in environmental samples (Christensen et al., 2016). These primers identifed and characterized methylating

microbial populations in rice paddy soils in China (Liu et al., 2018; Vishnivetskaya et al., 2018).

1.4. Goals and Hypotheses

The following hypotheses were developed to better understand the distribution of Hg species, and the geochemical and microbiological controls on Hg cycling and MMHg formation in marine and freshwater systems. A brief discussion of each hypothesis and methods for testing the hypothesis ensue.

Hypothesis 1: Mercury methylation occurs in the oxic water column of lakes and coastal marine ecosystems.

Water column profiles in the Atlantic, Pacific, and Southern Oceans, and the Mediterranean Sea show subsurface MMHg, DMHg, or total methylated-Hg (MeHg, the sum of MMHg and DMHg) maxima (Bowman et al., 2016, 2015; Cossa et al., 2011, 2009; Heimbürger et al., 2010). Recent isotopic tracer studies have shown that MeHg production occurs in oceanic and estuarine surface waters (Blum et al., 2013; Lehnherr et al., 2011; Monperrus et al., 2007; Schartup et al., 2015), but these studies have not confirmed the mechanism behind Hg methylation in oxygenated marine regions. They have provided a useful biogeochemical framework and scientific justification for the search and identification of Hg methylating biological communities in oxic aqueous environments.

I investigated water column Hg methylation in two different aquatic environments: Crystal Lake, Ohio, and the continental margin of the northwest Atlantic Ocean. Crystal Lake is seasonally stratified and has high concentrations of sulfide in the

hypolimnion during the summer and fall. MMHg production was examined throughout the water column during the late summer and fall, highlighting variations and controls on Hg methylation.

Additionally, I tested this hypothesis in productive shelf waters of the northwest Atlantic Ocean. Biologically productive waters may contain more MeHg (Cossa et al., 2009), so I set out to determine if communities in productive waters could methylate more MMHg than the 0.3–3.8% per day reported in the Mediterranean Sea (Monperrus et al., 2007), or the 0.2–1.3% reported in the Canadian Arctic Archipelago (Lehnherr et al., 2011).

In addition to methylation assays, DNA was collected from both Crystal Lake and the northwest Atlantic Ocean. DNA was screened for the presence of *hgcAB*, and *hgcA* was quantified for *Deltaproteobacteria, Archaea*, and *Firmicutes* to determine which clades were potentially involved with Hg methylation (Christensen et al., 2016).

Hypothesis 2: Sea ice cover alters Hg speciation and concentration in the upper water column, compared to open (ice-free) water.

Models predict Hg^0 evasion is the largest pathway for Hg loss from the ice-free Arctic water column (Soerensen et al., 2016). I hypothesized that ice acts as a physical barrier preventing Hg species from degassing to the atmosphere. Ice cover has been shown to affect surface concentrations of MMHg by reducing photodemethylation of MMHg (Point et al., 2011). Sea ice may also be a source of MMHg to the upper water column (50 m), either from methylation associated with sea ice (Gionfriddo et al., 2016),

or from melting multi-year ice, which provides Hg(II) substrate for methylation (Beattie et al., 2014).

This hypothesis was tested by taking high-resolution samples of four dissolved Hg species (MMHg, DMHg, Hg^0, and HgT) during the U.S. GEOTRACES Arctic cruise (GN01) in the summer and fall of 2015. Surface water samples at ice-free and ice-covered stations were collected to compare differences. For ice-covered stations, samples were collected at 1, 5, and 20 meters to characterize interactions between sea ice and surface waters. Surface water at ice-free stations were sampled at 1 and 20 m.

Hypothesis 3: Hg speciation and vertical distributions result from water circulation and age differences between the Makarov, Canada, and Fram Basins.

Pacific water flows through the Bering Strait into the Arctic Ocean. Anticyclonic (clockwise) surface circulation of Pacific water in the Beaufort Sea is driven by high atmospheric pressure above the Beaufort Sea. Shallow and intermediate layers circulate cyclonically. Each of the Arctic Ocean's four basins have distinct cyclonic cells in the intermediate layer (Talley et al., 2011). Deep circulation in the Arctic is influenced by the Lomonosov Ridge, which prevents a continuous rim current and separates Eurasian and Canadian Basin deep water masses (Talley et al., 2011).

The distribution of trace elements and their speciation in the oceans is governed by geochemical and biological processes, and ocean mixing. Water mass identification has helped corroborate Hg speciation differences due to varying water mass ages and nutrient concentrations in other ocean basins (Bowman et al., 2016, 2015; Cossa et al., 2011). Apparent oxygen utilization, nitrate, and phosphate have been used to explain

differences in Hg cycling (Bowman et al., 2015; Cossa et al., 2011, 2009; Heimbürger et al., 2010; Sunderland et al., 2009). For example, total Hg concentrations are proportional to those of nutrients in ocean deep waters, except in the North Atlantic Ocean (Lamborg et al., 2014). Water age is likely important, because young (0.6-1 year; Kipp, 2017) Eurasian Basin sourced water at the North Pole contains signatures of permafrost melt and recent shelf interaction, which likely affect Hg concentrations in the upper water column.

Hypothesis 4: Interactions between sulfide and Hg in the hypolimnion of Crystal Lake form HgS complexes that decrease in situ MMHg concentrations, but do not affect methylation potential.

Sulfur plays varied, but important roles in the Hg cycle. Sulfate additions stimulate MeHg production (Compeau and Bartha, 1985; Gilmour et al., 1992; Jeremiason et al., 2006; Mitchell et al., 2008; Strickman et al., 2016). Sulfate reduction produces sulfide, and high concentrations of sulfide can inhibit Hg methylation (Benoit et al., 2001a, 2001b; Gilmour et al., 1998). Inhibition of Hg methylation in highly sulfidic (300–3,000 μg/L; Benoit et al., 2001b; Gilmour et al., 1998) waters results from a change in the speciation and/or size of Hg-S complexes, which appears to influence bioavailability to methylating microbes (Benoit et al., 2001b; Graham et al., 2012). Methylating bacteria prefer either HgS^0 or nanoparticle $HgS_{(S)}$, as opposed to other Hg-S species, because it can cross cell membranes for MMHg production (Benoit et al., 1999a, 1999b, 2001b). One study has shown HgS complexes to be reactive or reducible in situ (Mason et al., 1993), but study results may have been site specific due to either geochemical factors or microbial community composition.

I addressed this hypothesis in two ways. First, I seasonally sampled water from Crystal Lake to measure distributions of sulfide and Hg, and Hg speciation throughout the water column. Second, I performed methylation assays with additions of isotopically labeled Hg^{2+} to water from various depths of the water column and incubated the water samples in situ. I expected reduced Hg methylation potentials and low MMHg concentrations in sulfidic water as compared to oxic water.

Goal: Investigate the diversity, abundance, and distribution of methylating communities in the water columns of Crystal Lake and the northwest Atlantic Ocean.

Hypothesis 5: There will be a greater abundance of *hgcA* where higher methylation potentials are measured.

Newly developed tools have successfully identified methylating organisms in rice paddy soils in China (Liu et al., 2018; Vishnivetskaya et al., 2018), but these tools have not been used in conjunction with methylation studies. Hg methylation occurs in anoxic environments, and most Hg-methylating microorganisms are anaerobic microbes (Gilmour et al., 2013). Thus, I expected to find more *hgcA* and higher methylation rates in anoxic waters with low sulfide concentrations. To address this hypothesis I measured methylation potentials and abundance of *hgcA* DNA in Crystal Lake. I also measured methylation potentials in northwest Atlantic shelf waters, and I amended methylation assays with biological inhibitors. Inhibitor additions were used to study dominant methylators in productive shelf waters. qPCR quantified and confirmed the presence of clade-specific *hgcA* DNA, and supported results from inhibitor addition experiments.

1.6. References

Aschner, M., Syversen, T., Souza, D.O., Rocha, J.B.T., Farina, M., 2007. Involvement of glutamate and reactive oxygen species in methylmercury neurotoxicity. Braz. J. Med. Biol. Res. 40, 285–291. https://doi.org/10.1590/S0100-879X2007000300001

Aschner, M., Yao, C.P., Allen, J.W., Tan, K.H., 2000. Methylmercury alters glutamate transport in astrocytes. Neurochem. Int. 37, 199–206. https://doi.org/10.1016/S0197-0186(00)00023-1

Beattie, S.A., Armstrong, D., Chaulk, A., Comte, J., Gosselin, M., Wang, F., 2014. Total and Methylated Mercury in Arctic Multiyear Sea Ice. Environ. Sci. Technol. 48, 5575–5582. https://doi.org/10.1021/es5008033

Benoit, J.M., Gilmour, C.C., Heyes, A., Mason, R.P., Miller, C.L., 2002. Geochemical and Biological Controls over Methylmercury Production and Degradation in Aquatic Ecosystems, in: Biogeochemistry of Environmentally Important Trace Elements, ACS Symposium Series. American Chemical Society, pp. 262–297. https://doi.org/10.1021/bk-2003-0835.ch019

Benoit, J.M., Gilmour, C.C., Mason, R.P., 2001a. The Influence of Sulfide on Solid-Phase Mercury Bioavailability for Methylation by Pure Cultures of *Desulfobulbus propionicus* (1pr3). Environ. Sci. Technol. 35, 127–132. https://doi.org/10.1021/es001415n

Benoit, J.M., Gilmour, C.C., Mason, R.P., 2001b. Aspects of Bioavailability of Mercury for Methylation in Pure Cultures of Desulfobulbus propionicus (1pr3). Appl. Environ. Microbiol. 67, 51–58. https://doi.org/10.1128/AEM.67.1.51-58.2001

Benoit, J.M., Gilmour, C.C., Mason, R.P., Heyes, A., 1999a. Sulfide Controls on Mercury Speciation and Bioavailability to Methylating Bacteria in Sediment Pore Waters. Environ. Sci. Technol. 33, 951–957. https://doi.org/10.1021/es9808200

Benoit, J.M., Mason, R.P., Gilmour, C.C., 1999b. Estimation of mercury-sulfide speciation in sediment pore waters using octanol-water partitioning and implications for availability to methylating bacteria. Environ. Toxicol. Chem. 18, 2138–2141. https://doi.org/10.1002/etc.5620181004

Bloom, N.S., 1992. On the Chemical Form of Mercury in Edible Fish and Marine Invertebrate Tissue. Can. J. Fish. Aquat. Sci. 49, 1010–1017. https://doi.org/10.1139/f92-113

Bloom, N.S., Effler, S.W., 1990. Seasonal variability in the Mercury speciation of Onondaga Lake (New York). Water. Air. Soil Pollut. 53, 251–265. https://doi.org/10.1007/BF00170741

Blum, J.D., Popp, B.N., Drazen, J.C., Anela Choy, C., Johnson, M.W., 2013. Methylmercury production below the mixed layer in the North Pacific Ocean. Nat. Geosci. 6, 879.

Bowman, K.L., Hammerschmidt, C.R., Lamborg, C.H., Swarr, G., 2015. Mercury in the North Atlantic Ocean: The U.S. GEOTRACES zonal and meridional sections. Deep Sea Res. Part II Top. Stud. Oceanogr. 116, 251–261. https://doi.org/10.1016/j.dsr2.2014.07.004

Bowman, K.L., Hammerschmidt, C.R., Lamborg, C.H., Swarr, G.J., Agather, A.M., 2016. Distribution of mercury species across a zonal section of the eastern

tropical South Pacific Ocean (U.S. GEOTRACES GP16). Mar. Chem. 186, 156–166. https://doi.org/10.1016/j.marchem.2016.09.005
Boyd, E., Barkay, T., 2012. The Mercury Resistance Operon: From an Origin in a Geothermal Environment to an Efficient Detoxification Machine. Front. Microbiol. 3. https://doi.org/10.3389/fmicb.2012.00349
Brookes, N., Kristt, D.A., 1989. Inhibition of Amino Acid Transport and Protein Synthesis by HgCl2 and Methylmercury in Astrocytes: Selectivity and Reversibility. J. Neurochem. 53, 1228–1237. https://doi.org/10.1111/j.1471-4159.1989.tb07419.x
Celo, V., Lean, D.R.S., Scott, S.L., 2006. Abiotic methylation of mercury in the aquatic environment. Sci. Total Environ. 368, 126–137. https://doi.org/10.1016/j.scitotenv.2005.09.043
Choi, A.L., Grandjean, P., 2008. Methylmercury exposure and health effects in humans. Environ. Chem. 5, 112–120. https://doi.org/10.1071/EN08014
Christensen, G.A., Wymore, A.M., King, A.J., Podar, M., Hurt, R.A., Santillan, E.U., Soren, A., Brandt, C.C., Brown, S.D., Palumbo, A.V., Wall, J.D., Gilmour, C.C., Elias, D.A., 2016. Development and Validation of Broad-Range Qualitative and Clade-Specific Quantitative Molecular Probes for Assessing Mercury Methylation in the Environment. Appl. Environ. Microbiol. 82, 6068–6078. https://doi.org/10.1128/AEM.01271-16
Clarkson, T.W., 1998. Human toxicology of Mercury. J. Trace Elem. Exp. Med. 11, 303–317. https://doi.org/10.1002/(SICI)1520-670X(1998)11:2/3<303::AID-JTRA18>3.0.CO;2-V
Clarkson, T.W., Magos, L., Myers, G.J., 2003. The Toxicology of Mercury — Current Exposures and Clinical Manifestations. N. Engl. J. Med. 349, 1731–1737. https://doi.org/10.1056/NEJMra022471
Cohen, J., Bellinger, D., Shaywitz, B., 2005. A Quantitative Analysis of Prenatal Methyl Mercury Exposure and Cognitive Development. Am. J. Prev. Med. 29, 353–353. https://doi.org/10.1016/j.amepre.2005.06.007
Compeau, G.C., Bartha, R., 1985. Sulfate-Reducing Bacteria: Principal Methylators of Mercury in Anoxic Estuarine Sediment. Appl Env. Microbiol 50, 498–502.
Cossa, D., Averty, B., Pirrone, N., 2009. The origin of methylmercury in open Mediterranean waters. Limnol. Oceanogr. 54, 837–844. https://doi.org/10.4319/lo.2009.54.3.0837
Cossa, D., Heimbürger, L.-E., Lannuzel, D., Rintoul, S.R., Butler, E.C.V., Bowie, A.R., Averty, B., Watson, R.J., Remenyi, T., 2011. Mercury in the Southern Ocean. Geochim. Cosmochim. Acta 75, 4037–4052. https://doi.org/10.1016/j.gca.2011.05.001
Farina, M., Aschner, M., Rocha, J.B.T., 2011. Oxidative stress in MeHg-induced neurotoxicity. Toxicol. Appl. Pharmacol., Environmental Chemicals and Neurotoxicity 256, 405–417. https://doi.org/10.1016/j.taap.2011.05.001
Farina, M., Avila, D.S., da Rocha, J.B.T., Aschner, M., 2013. Metals, oxidative stress and neurodegeneration: A focus on iron, manganese and mercury. Neurochem. Int., Special Issue: Oxidative Stress and Neurodegeneration 62, 575–594. https://doi.org/10.1016/j.neuint.2012.12.006

Fitzgerald, W.F., Engstrom, D.R., Lamborg, C.H., Tseng, C.-M., Balcom, P.H., Hammerschmidt, C.R., 2005. Modern and Historic Atmospheric Mercury Fluxes in Northern Alaska: Global Sources and Arctic Depletion. Environ. Sci. Technol. 39, 557–568. https://doi.org/10.1021/es049128x

Fitzgerald, W.F., Engstrom, D.R., Mason, R.P., Nater, E.A., 1998. The Case for Atmospheric Mercury Contamination in Remote Areas. Environ. Sci. Technol. 32, 1–7. https://doi.org/10.1021/es970284w

Fitzgerald, W.F., Lamborg, C.H., Hammerschmidt, C.R., 2007. Marine Biogeochemical Cycling of Mercury. Chem. Rev. 107, 641–662. https://doi.org/10.1021/cr050353m

Gårdfeldt, K., Munthe, J., Strömberg, D., Lindqvist, O., 2003. A kinetic study on the abiotic methylation of divalent mercury in the aqueous phase. Sci. Total Environ. 304, 127–136. https://doi.org/10.1016/S0048-9697(02)00562-4

Gilmour, C.C., Henry, E.A., Mitchell, R., 1992. Sulfate stimulation of mercury methylation in freshwater sediments. Environ. Sci. Technol. 26, 2281–2287. https://doi.org/10.1021/es00035a029

Gilmour, C.C., Podar, M., Bullock, A.L., Graham, A.M., Brown, S.D., Somenahally, A.C., Johs, A., Hurt, R.A., Bailey, K.L., Elias, D.A., 2013. Mercury Methylation by Novel Microorganisms from New Environments. Environ. Sci. Technol. 47, 11810–11820. https://doi.org/10.1021/es403075t

Gilmour, C.C., Riedel, G.S., Ederington, M.C., Bell, J.T., Gill, G.A., Stordal, M.C., 1998. Methylmercury concentrations and production rates across a trophic gradient in the northern Everglades. Biogeochemistry 40, 327–345. https://doi.org/10.1023/A:1005972708616

Gionfriddo, C.M., Tate, M.T., Wick, R.R., Schultz, M.B., Zemla, A., Thelen, M.P., Schofield, R., Krabbenhoft, D.P., Holt, K.E., Moreau, J.W., 2016. Microbial mercury methylation in Antarctic sea ice. Nat. Microbiol. 1, 16127.

Graham, A.M., Aiken, G.R., Gilmour, C.C., 2012. Dissolved Organic Matter Enhances Microbial Mercury Methylation Under Sulfidic Conditions. Environ. Sci. Technol. 46, 2715–2723. https://doi.org/10.1021/es203658f

Ha, E., Basu, N., Bose-O'Reilly, S., Dórea, J.G., McSorley, E., Sakamoto, M., Chan, H.M., 2017. Current progress on understanding the impact of mercury on human health. Environ. Res. 152, 419–433. https://doi.org/10.1016/j.envres.2016.06.042

Hammerschmidt, C.R., Fitzgerald, W.F., 2001. Formation of Artifact Methylmercury during Extraction from a Sediment Reference Material. Anal. Chem. 73, 5930–5936. https://doi.org/10.1021/ac010721w

Hammerschmidt, C.R., Lamborg, C.H., Fitzgerald, W.F., 2007. Aqueous phase methylation as a potential source of methylmercury in wet deposition. Atmos. Environ. 41, 1663–1668. https://doi.org/10.1016/j.atmosenv.2006.10.032

Heimbürger, L.-E., Cossa, D., Marty, J.-C., Migon, C., Averty, B., Dufour, A., Ras, J., 2010. Methyl mercury distributions in relation to the presence of nano- and picophytoplankton in an oceanic water column (Ligurian Sea, North-western Mediterranean). Geochim. Cosmochim. Acta 74, 5549–5559. https://doi.org/10.1016/j.gca.2010.06.036

Horowitz, H.M., Jacob, D.J., Zhang, Y., Dibble, T.S., Slemr, F., Amos, H.M., Schmidt, J.A., Corbitt, E.S., Marais, E.A., Sunderland, E.M., 2017. A new mechanism for

atmospheric mercury redox chemistry: implications for the global mercury budget. Atmospheric Chem. Phys. 17, 6353–6371. https://doi.org/10.5194/acp-17-6353-2017

Jeremiason, J.D., Engstrom, D.R., Swain, E.B., Nater, E.A., Johnson, B.M., Almendinger, J.E., Monson, B.A., Kolka, R.K., 2006. Sulfate Addition Increases Methylmercury Production in an Experimental Wetland. Environ. Sci. Technol. 40, 3800–3806. https://doi.org/10.1021/es0524144

Johnsson, C., Sällsten, G., Schütz, A., Sjörs, A., Barregård, L., 2004. Hair mercury levels versus freshwater fish consumption in household members of Swedish angling societies. Environ. Res. 96, 257–263. https://doi.org/10.1016/j.envres.2004.01.005

Kim, S.O., Merchant, K., Nudelman, R., Beyer, W.F., Keng, T., DeAngelo, J., Hausladen, A., Stamler, J.S., 2002. OxyR: A Molecular Code for Redox-Related Signaling. Cell 109, 383–396. https://doi.org/10.1016/S0092-8674(02)00723-7

Lamborg, C.H., Hammerschmidt, C.R., Bowman, K.L., Swarr, G.J., Munson, K.M., Ohnemus, D.C., Lam, P.J., Heimbürger, L.-E., Rijkenberg, M.J.A., Saito, M.A., 2014. A global ocean inventory of anthropogenic mercury based on water column measurements. Nature 512, 65–68. https://doi.org/10.1038/nature13563

Lehnherr, I., Louis, V.L.S., Hintelmann, H., Kirk, J.L., 2011. Methylation of inorganic mercury in polar marine waters. Nat. Geosci. 4, 298–302. https://doi.org/10.1038/ngeo1134

Lincoln, R.A., Shine, J.P., Chesney, E.J., Vorhees, D.J., Grandjean, P., Senn, D.B., 2010. Fish Consumption and Mercury Exposure among Louisiana Recreational Anglers. Environ. Health Perspect. 119, 245–251. https://doi.org/10.1289/ehp.1002609

Lindqvist, O., Johansson, K., Bringmark, L., Timm, B., Aastrup, M., Andersson, A., Hovsenius, G., Håkanson, L., Iverfeldt, Å., Meili, M., 1991. Mercury in the Swedish environment ? Recent research on causes, consequences and corrective methods. Water. Air. Soil Pollut. 55, xi–261. https://doi.org/10.1007/BF00542429

Liu, X., Ma, A., Zhuang, G., Zhuang, X., 2018. Diversity of microbial communities potentially involved in mercury methylation in rice paddies surrounding typical mercury mining areas in China. MicrobiologyOpen 7, e00577. https://doi.org/10.1002/mbo3.577

Mason, R.P., Fitzgerald, W.F., Hurley, J., Hanson, A.K., Donaghay, P.L., Sieburth, J.M., 1993. Mercury biogeochemical cycling in a stratified estuary. Limnol. Oceanogr. 38, 1227–1241. https://doi.org/10.4319/lo.1993.38.6.1227

Mason, R.P., Morel, F.M.M., Hemond, H.F., 1995. The role of microorganisms in elemental mercury formation in natural waters. Water. Air. Soil Pollut. 80, 775–787. https://doi.org/10.1007/BF01189729

Mitchell, C.P.J., Branfireun, B.A., Kolka, R.K., 2008. Assessing sulfate and carbon controls on net methylmercury production in peatlands: An in situ mesocosm approach. Appl. Geochem. 23, 503–518. https://doi.org/10.1016/j.apgeochem.2007.12.020

Monperrus, M., Tessier, E., Amouroux, D., Leynaert, A., Huonnic, P., Donard, O.F.X., 2007. Mercury methylation, demethylation and reduction rates in coastal and marine surface waters of the Mediterranean Sea. Mar. Chem., Mercury Cycling in Surface and Deep Waters of the Mediterranean Sea 107, 49–63. https://doi.org/10.1016/j.marchem.2007.01.018

Nriagu, J.O., Pacyna, J.M., 1988. Quantitative assessment of worldwide contamination of air, water and soils by trace metals. Nature 333, 134.
Parks, J.M., Johs, A., Podar, M., Bridou, R., Hurt, R.A., Smith, S.D., Tomanicek, S.J., Qian, Y., Brown, S.D., Brandt, C.C., Palumbo, A.V., Smith, J.C., Wall, J.D., Elias, D.A., Liang, L., 2013. The Genetic Basis for Bacterial Mercury Methylation. Science 339, 1332–1335. https://doi.org/10.1126/science.1230667
Podar, M., Gilmour, C.C., Brandt, C.C., Soren, A., Brown, S.D., Crable, B.R., Palumbo, A.V., Somenahally, A.C., Elias, D.A., 2015. Global prevalence and distribution of genes and microorganisms involved in mercury methylation. Sci. Adv. 1, e1500675–e1500675. https://doi.org/10.1126/sciadv.1500675
Point, D., Sonke, J.E., Day, R.D., Roseneau, D.G., Hobson, K.A., Vander Pol, S.S., Moors, A.J., Pugh, R.S., Donard, O.F.X., Becker, P.R., 2011. Methylmercury photodegradation influenced by sea-ice cover in Arctic marine ecosystems. Nat. Geosci. 4, 188.
Poulin, J., Gibb, H. 2008. Mercury: Assessing the environmental burden of disease at national and local levels. Editor, Pruss-Ustun, A. World Health Organization, Geneva. WHO Environmental Burden of Disease Series No. 16.
Qian, C., Chen, H., Johs, A., Lu, X., An, J., Pierce, E.M., Parks, J.M., Elias, D.A., Hettich, R.L., Gu, B., 2018. Quantitative Proteomic Analysis of Biological Processes and Responses of the Bacterium Desulfovibrio desulfuricans ND132 upon Deletion of Its Mercury Methylation Genes. Proteomics 18, 1700479. https://doi.org/10.1002/pmic.201700479
Ranchou-Peyruse, M., Monperrus, M., Bridou, R., Duran, R., Amouroux, D., Salvado, J.C., Guyoneaud, R., 2009. Overview of Mercury Methylation Capacities among Anaerobic Bacteria Including Representatives of the Sulphate-Reducers: Implications for Environmental Studies. Geomicrobiol. J. 26, 1–8.
Reynolds, J.N., Racz, W.J., 1987. Effects of methylmercury on the spontaneous and potassium-evoked release of endogenous amino acids from mouse cerebellar slices. Can. J. Physiol. Pharmacol. 65, 791–798. https://doi.org/10.1139/y87-127
Rolfhus, K.R., Fitzgerald, W.F., 2004. Mechanisms and temporal variability of dissolved gaseous mercury production in coastal seawater. Mar. Chem. 90, 125–136. https://doi.org/10.1016/j.marchem.2004.03.012
Schartup, A.T., Balcom, P.H., Soerensen, A.L., Gosnell, K.J., Calder, R.S.D., Mason, R.P., Sunderland, E.M., 2015. Freshwater discharges drive high levels of methylmercury in Arctic marine biota. Proc. Natl. Acad. Sci. 112, 11789–11794. https://doi.org/10.1073/pnas.1505541112
Slemr, F., Schuster, G., Seiler, W., 1985. Distribution, speciation, and budget of atmospheric mercury. J. Atmospheric Chem. 3, 407–434. https://doi.org/10.1007/BF00053870
Soerensen, A.L., Jacob, D.J., Schartup, A.T., Fisher, J.A., Lehnherr, I., St. Louis, V.L., Heimbürger, L.-E., Sonke, J.E., Krabbenhoft, D.P., Sunderland, E.M., 2016. A mass budget for mercury and methylmercury in the Arctic Ocean. Glob. Biogeochem. Cycles 30, 560–575. https://doi.org/10.1002/2015GB005280
Strickman, R.J.S., Fulthorpe, R.R., Coleman Wasik, J.K., Engstrom, D.R., Mitchell, C.P.J., 2016. Experimental sulfate amendment alters peatland bacterial

community structure. Sci. Total Environ. 566–567, 1289–1296. https://doi.org/10.1016/j.scitotenv.2016.05.189
Sunderland, E.M., 2007. Mercury Exposure from Domestic and Imported Estuarine and Marine Fish in the U.S. Seafood Market. Environ. Health Perspect. 115, 235–242. https://doi.org/10.1289/ehp.9377
Sunderland, E.M., Krabbenhoft, D.P., Moreau, J.W., Strode, S.A., Landing, W.M., 2009. Mercury sources, distribution, and bioavailability in the North Pacific Ocean: Insights from data and models. Glob. Biogeochem. Cycles 23, GB2010. https://doi.org/10.1029/2008GB003425
Sunderland, E.M., Mason, R.P., 2007. Human impacts on open ocean mercury concentrations. Glob. Biogeochem. Cycles 21, GB4022. https://doi.org/10.1029/2006GB002876
Talley, L.D., Pickard, G.L., Emery, W.J. (Eds.), 2011. Descriptive physical oceanography: an introduction, 6th ed. ed. Academic Press, Amsterdam ; Boston.
Uchino, M., Okajima, T., Eto, K., Kumamoto, T., Mishima, I., Ando, M., 1995. Neurologic Features of Chronic Minamata Disease (Organic Mercury Poisoning) Certified at Autopsy. Intern. Med. 34, 744–747. https://doi.org/10.2169/internalmedicine.34.744
US EPA, O., 2016. EPA-FDA Fish Advice: Technical Information [WWW Document]. US EPA. URL https://www.epa.gov/fish-tech/epa-fda-fish-advice-technical-information (accessed 9.25.18).
Van Oostdam, J., Gilman, A., Dewailly, E., Usher, P., Wheatley, B., Kuhnlein, H., Neve, S., Walker, J., Tracy, B., Feeley, M., Jerome, V., Kwavnick, B., 1999. Human health implications of environmental contaminants in Arctic Canada: a review. Sci. Total Environ. 230, 1–82. https://doi.org/10.1016/S0048-9697(99)00036-4
Vandal, G.M., Mason, R.P., Fitzgerald, W.F., 1991. Cycling of volatile mercury in temperate lakes. Water. Air. Soil Pollut. 56, 791–803. https://doi.org/10.1007/BF00342317
Vishnivetskaya, T.A., Hu, H., Nostrand, J.D.V., Wymore, A.M., Xu, X., Qiu, G., Feng, X., Zhou, J., Brown, S.D., Brandt, C.C., Podar, M., Gu, B., Elias, D.A., 2018. Microbial community structure with trends in methylation gene diversity and abundance in mercury-contaminated rice paddy soils in Guizhou, China. Environ. Sci. Process. Impacts 20, 673–685. https://doi.org/10.1039/C7EM00558J
Yokoo, E.M., Valente, J.G., Grattan, L., Schmidt, S.L., Platt, I., Silbergeld, E.K., 2003. Low level methylmercury exposure affects neuropsychological function in adults. Environ. Health 2. https://doi.org/10.1186/1476-069X-2-8
Zahir, F., Rizwi, S.J., Haq, S.K., Khan, R.H., 2005. Low dose mercury toxicity and human health. Environ. Toxicol. Pharmacol. 20, 351–360. https://doi.org/10.1016/j.etap.2005.03.007

Figures

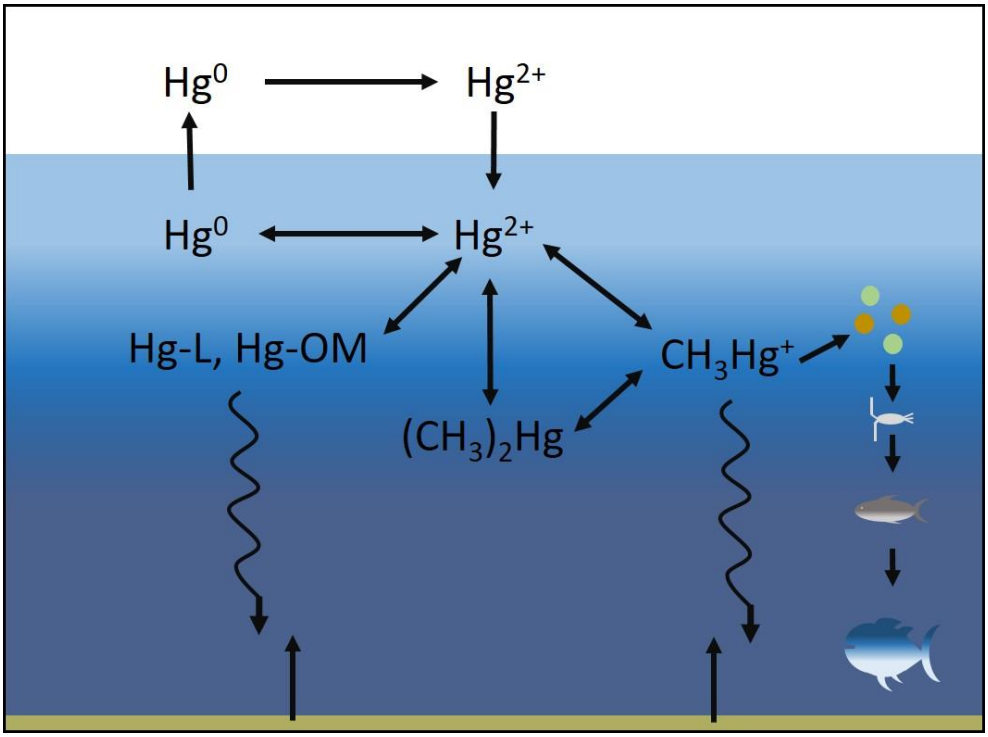

Figure 1.1 The biogeochemical cycle of mercury in aquatic systems.

Chapter 2: DISTRIBUTION OF MERCURY SPECIES IN THE WESTERN ARCTIC OCEAN (U.S. GEOTRACES GN01)

Alison M. Agather, Katlin L. Bowman, Carl H. Lamborg, Chad R. Hammerschmidt

2.1. Abstract

Mercury (Hg) in the Arctic Ocean is a concern due to unusually high concentrations of monomethylmercury (MMHg) in fish and marine animals. Increased human exposure from consumption of these animals is a significant health concern that is related to Hg contamination in nature. Most Arctic marine Hg research has investigated the amounts, distributions, and cycling in animals, snow, and ice, while few studies have examined the aqueous behavior and fate of Hg in the polar ocean. Here we present the most comprehensive dataset detailing Hg speciation and distribution of elemental Hg (Hg^0), dimethylmercury (DMHg), and filtered and particulate total Hg and MMHg in the western Arctic Ocean. This data was obtained as part of the U.S. Arctic GEOTRACES cruise (GN01) in 2015. Major findings indicate that the amount of Hg supplied to the Arctic Ocean through the Bering Strait has not increased over the last two decades (4–71 kmol HgT yr^{-1}), and many water masses appeared to be enriched with anthropogenic Hg. The Transpolar Drift supplied HgT and Hg^0 to the central Arctic Ocean, but not methylated Hg. Gaseous Hg^0, but not DMHg, was elevated in surface waters under the ice cover. Monomethylmercury levels, which averaged 0.054 ± 0.050 pM, are lower than other major ocean basins, suggesting ambient MMHg levels in western Arctic Ocean seawater do not by themselves explain anomalously high Hg in Arctic animals.

2.2. Introduction

Monomethlymercury (MMHg) is a bioaccumulating neurotoxin that, at current environmental exposures, poses a health risk to humans (Mergler et al., 2007) and wildlife (Scheuhammer et al., 2015). Human exposure to MMHg is primarily from seafood consumption (Sunderland, 2007), and the rate and quantity of seafood consumed may predict which individuals and populations are adversely affected by MMHg exposure (Grandjean et al., 1995; Ha et al., 2017; Karagas et al., 2012; Mahaffey et al., 2009; Mergler et al., 2007; Sheehan et al., 2014; Van Oostdam et al., 2005). Exposures of women of child-bearing age are of particular concern because MMHg can be maternally transferred to their children while in utero and nursing (Mergler et al., 2007; Oskarsson et al., 1996). Arctic populations have an increased risk of accumulating high levels of MMHg. Concentrations of mercury (Hg), mostly as MMHg, in Arctic animals are often greater than those in animals of similar trophic status at lower latitudes (Dietz et al., 1998; Dietz et al., 2009). Dietary exposures and subsequent blood MMHg concentrations of some Arctic and sub-Arctic populations exceed the threshold for negative effects on childhood development (Choi and Grandjean, 2008). This is contrary to a hypothesis suggesting Hg accumulation decreases with temperature (Dijkstra et al., 2013). And although the mechanisms for exacerbated MMHg in Arctic biota are unknown, there are many factors that have been hypothesized to contribute to the complex cycling of Hg in the Arctic, including atmospheric Hg depletion events (Lindberg et al., 2002; Schroeder et al., 1998; Steffen et al., 2007), presence of snow pack (Kirk et al., 2006; St. Louis et al., 2007) and sea ice (Beattie et al., 2014), and potential for Hg methylation in ice brine (Gionfriddo et al., 2016).

Exacerbating these unique Arctic Hg cycling mechanisms are anthropogenic Hg emissions. The relatively long atmospheric residence time of Hg (~ 0.5–1 year, Horowitz et al., 2017; Slemr et al., 1985) coupled to its tendency to re-volatize following deposition allows for long range transport of the contaminant before it is deposited (Fitzgerald et al., 1998; Mason et al., 2012; Slemr and Langer, 1992; Swain et al., 1992). There are no large point sources of Hg in the Arctic, however, atmospheric transport of elemental Hg (Hg^0) to the region is a significant source of the metal (Outridge et al., 2008). Emissions from human activities since the Industrial Revolution have increased Hg deposition in the Arctic by a factor of three (Fitzgerald et al., 1998; Fitzgerald et al., 2005). Mercury levels in Arctic animals have increased over the same period of time, 92% of which has been attributed to anthropogenic emissions (Dietz et al., 2009). Unlike other ocean basins, Arctic Ocean mass balance estimates suggest that sources other than atmospheric deposition may be important, including rivers, melting permafrost, and exchange with the Pacific and Atlantic Oceans (Outridge et al., 2008; Soerensen et al., 2016). These sources supply Hg to the oceanic water column, where it undergoes a complex series of biotic and abiotic reactions, forming dissolved Hg^0, MMHg and dimethylmercury (DMHg).

A series of hypotheses have attempted to address the difference between Hg cycling in the Arctic Ocean and other basins. Atmospheric depletion events are unique to polar regions and are a large source of Hg(II) to the Arctic environment (Schroeder et al., 1998; Steffen et al., 2007). Riverine discharge provides another significant supply of Hg entering the Arctic (Fisher et al., 2012), and both of these sources are frequently used to explain recent biotic Hg trends. Delivery of Hg into the Arctic Ocean is worsened by climate change and melting permafrost, which supplements already substantial riverine

Hg loads (Soerensen et al., 2016). Warming air and sea temperatures likely affect Hg cycling between the ocean, atmosphere and sea ice (Outridge et al., 2008). Ice-free waters increase vertical mixing which brings MMHg and DMHg to the surface. After mixing, DMHg can efflux from the surface ocean into the atmosphere and be deposited as MMHg (Kirk et al., 2008; St. Louis et al., 2007). Mixing also brings MMHg to the surface ocean, where it is likely to enter the food chain (Kirk et al., 2008). And while it has not been directly addressed in the Arctic, MMHg accumulation in coastal food webs can largely be attributed to methylation in near-shore and shelf sediments (Hammerschmidt, et al., 2004; Hammerschmidt and Fitzgerald, 2006a), which may be important over the vast Arctic shelves.

Yet still, a lack of sufficient ocean data adjudicate these hypotheses. To better understand Hg cycling in the Arctic Ocean, we measured filtered gaseous Hg^0 and DMHg, filtered total Hg (HgT) and MMHg, and particulate total Hg (HgT_{Part}) and MMHg ($MMHg_{Part}$) in the western Arctic Ocean. This U.S. GEOTRACES transect (GN01) was part of the first large-scale effort to examine Hg speciation and distribution in the Arctic Ocean. Contemporaneous GEOTRACES cruises were conducted in the Canadian Arctic Archipelago and in the eastern Arctic Ocean. Here, we present results of the U.S. GEOTRACES cruise in the western Arctic Ocean.

2.3. Methods

2.3.1. Sampling

Water and particles were sampled between August 9th and October 12th, 2015 during the U.S. Arctic GEOTRACES (GN01) section (Figure 2.1). The section began in the Bering Sea and passed through the Bering Strait, traversed the Makarov Basin,

reached the North Pole (Eurasian Basin), and returned southeast through the Canada Basin. Water samples were collected by deploying a trace-metal clean rosette attached to a plastic-coated hydrowire fitted with 12-L Teflon-coated GO-Flo bottles (Cutter and Bruland, 2012). Water was sampled at twenty-two full depth stations (24 depths) and five marginal ice zone stations (MIZ, 3–5 depths). The MIZ was identified as the region where sea ice was loose and broken. Immediately following rosette recovery, GO-Flo bottles were transferred to a clean laboratory van, and filtered (0.2 μm Pall AcroPak-200) without degassing into 2-L Teflon bottles for Hg^0, MMHg, and DMHg analysis (Lamborg et al., 2012); and into 0.25-L borosilicate glass bottles for HgT analysis. Sample bottles were acid cleaned (Hammerschmidt et al., 2011) and trace-metal clean techniques were followed (Bishop et al., 2012). In addition to GO-Flo samples, seawater from six stations was sampled at 1, 5 and 20 m below the ice with a pump and acid washed plastic tubing. Under-ice samples were collected upwind of the ship and pumped under the protection of a tent. Seawater collected this way was filtered (0.2 μm Pall AcroPak-200) in a clean lab on board the ship and dispensed into clean bottles for Hg analysis.

Suspended particles (1–51 μm) were sampled from 16 depths at 20 stations with McLane in situ pumps (Bishop et al., 2012; Whatman QMA). Filters were subsampled in two 13 mm diameter punches and stored frozen until analysis (Bowman et al., 2015). The total volume of filtered seawater varied between 16 and 164 L, with larger volumes generally collected at deeper depths.

2.3.2. Mercury Analysis

Elemental Hg, DMHg, and HgT were measured in a shipboard laboratory. Within two hours of collection, samples were purged with Hg-free N_2 gas to quantitatively strip Hg^0 and DMHg from solution (Bowman and Hammerschmidt, 2011). Bond Elut ENV (Agilent; Baya et al., 2013) traps were used to concentrate DMHg from effluent upstream of Hg^0-collecting gold traps (Bloom and Fitzgerald, 1988; Bowman et al., 2016). Elemental Hg was quantified by dual Au-amalgamation cold vapor atomic fluorescence spectrometry (CVAFS; Bloom and Fitzgerald, 1988), with a method detection limit of 0.04 pM. When extra water was available, duplicate samples were analyzed for Hg^0, with a relative percent difference (RPD) of 14 ± 11 (n = 8). In contrast to previous U.S. GEOTRACES cruises, DMHg was not analyzed by gas chromatographic-CVAFS; (Baya et al., 2013; Bloom, 1989; Bowman and Hammerschmidt, 2011; Bowman et al., 2015; Bowman et al., 2016), because the cold temperature of the compressed argon (stored on deck) resulted in insufficient pressure in the gas chromatographic column. Instead, DMHg was thermally desorbed from the Bond Elut traps, thermally decomposed to Hg^0, collected on an in-line Au trap, and quantified via CVAFS. Calibration of at-sea measurements of Hg^0, HgT, and DMHg were performed with gaseous Hg^0 standards. Trapping efficiency for each analytical Bond Elut trap was determined with an ethylated MMHg standard (methylethylmercury; Bowman and Hammerschmidt, 2011), that was validated against TORT-2 reference material (lobster hepatopancreas, Canadian Research Council). The method detection limit for DMHg was 0.012 pM, and duplicates averaged 15 ± 5 RPD (n = 4).

Seawater for analysis of total Hg was oxidized with bromine monochloride (BrCl; Bloom and Crecelius, 1983) and neutralized with NH_2OH prior to reduction with $SnCl_2$. Samples were quantified by dual Au-amalgamation CVAFS (Bloom and Fitzgerald, 1988; Fitzgerald and Gill, 1979). The method detection limit for HgT was 0.10 pM. Reproducibility between analytical duplicates averaged 11 ± 5 RPD (*n* = 17).

While at sea, variable gas pressure in the gas chromatograph caused irregular MMHg peak retention times, making it indecipherable from the inorganic Hg peak. Accordingly, seawater samples ranging from 0.25 to 2 L, were acidified to 1% with sulfuric acid and shipped frozen to Wright State University for analysis. Samples were thawed >12 hours in the dark at room temperature, acidity neutralized with KOH, buffered with acetate, amended with ascorbic acid (Munson et al., 2014), derivatized with sodium tetraethylborate, and analyzed via flow injection GC-CVAFS (Bowman and Hammerschmidt, 2011; Tseng et al., 2004). The method detection limit was 0.025 pM MMHg for 0.22-L and 0.020 pM MMHg for 0.4-L samples. Agreement between analytical replicates averaged 11 ± 8 RPD (*n* = 5).

Particulate samples were digested in 2N HNO_3 in a 60 °C water bath for 12 hours (Hammerschmidt and Fitzgerald, 2006b). Aliquots of the digestate (5-mL) were analyzed for particulate MMHg by flow- injection GC-CVAFS (Bowman et al., 2015; Tseng et al., 2004). Sample measurements were calibrated against similarly digested MMHg standards, which were validated versus digestates of TORT-2 reference material (lobster hepatopancreas, Canadian Research Council). For particulate HgT, 2-mL aliquots of the same filter digestates were oxidized with BrCl for >12 hours. Samples were neutralized with NH_2OH, reduced with $SnCl_2$, and analyzed via CVAFS that was calibrated with

aqueous Hg(II) standards traceable to the U.S. National Institute of Standards and Technology (Bloom and Fitzgerald, 1988). The estimated detection limits for analysis of $MMHg_{Part}$ and HgT_{Part} were 0.002 and 0.02 pM, respectively, agreement between analytical replicates of HgT_{Part} averaged 7 ± 6 RPD (n = 16). Insufficient volume and low sample concentration did not allow for $MMHg_{Part}$ duplicates. Statistical comparisons between water masses were performed with Mann-Whitney Rank Sum Test.

2.4. Results and Discussion

2.4.1. Physical Oceanography

The Arctic Ocean is the smallest (1.56×10^7 km^2) and shallowest (mean depth = 1200 m) ocean basin, characterized by broad continental shelves contributing to 53% of its area (Jakobsson, 2002). Salty waters enter the Arctic Ocean from both sides of Greenland, while fresher North Pacific water flows through the Bering Strait. The ocean basin is split by the Lomonsov Ridge, separating the Canadian Basin (max depth ~3800 m) from the Eurasian Basin (max depth ~4200 m; Rudels, 2001). Subdivisions of the Canadian Basin include the Makarov and Canada Basins, while the Eurasian Basin is subdivided into the Nansen and Amundsen Basins.

The water column of the Arctic Ocean can be divided into three distinct density layers. Polar Surface Water (PSW; $\sigma_\theta \leq 27.70$) consists of the fresh Polar Mixed Layer (PML, < 51 m depth) and the halocline (Figure 2.2). The intermediate layer ($27.70 < \sigma_\theta > 30.444$) is composed of Atlantic Water (AW) and upper Polar Deep Water (uPDW). Deep water ($\sigma_\theta > 30.444$) results from slope convection and is differentiated on either side of the Lomonsov Ridge as Eurasian Basin Deep Water (EBDW) and Canada Basin Deep Water (CBDW; Rudels, 2001).

Circulation in the Arctic Ocean varies by depth. In surface and intermediate layers, rim currents dictate water movement. Surficial flow is cyclonic in the Eurasian Basin and anticyclonic in the Beaufort Gyre in the Canadian Basin. Atmospheric high pressure over the Beaufort Sea drives the Transpolar Drift (TPD), which flows from the Laptev and East Siberian Seas to the Fram Strait, along a similar path as the Lomonosov Ridge (Rudels, 2001). The TPD bisects the Arctic, shuttling ice, Siberian shelf and river water laden with nutrients and trace metals across the basin and out through the Fram Strait (Barrie et al., 1998; Gordienko and Laktionov, 1969; Klunder et al., 2012), though the exact path of the TPD varies year to year due to the Arctic Oscillation index (Macdonald et al., 2005). Intermediate waters move cyclonically throughout the basin, with individual cyclonic cells in the Makarov, Canada, Nansen, and Amundsen Basins. Similar to intermediate layers, deep water circulation is also cyclonic, but the Lomonosov Ridge impedes a continuous rim current (Talley et al., 2011).

Riverine discharge to the Arctic Ocean delivers freshwater, nutrients, metals and carbon. Although the Arctic Ocean comprises only 1.4% of the world ocean volume (Jakobsson, 2002), it receives 11% of global riverine discharge (Lammers et al., 2001). Pan-arctic rivers drain 22.4×10^6 km^2 of land, an area of about one and a half times the size of the Arctic Ocean (Lammers et al., 2001). Rivers average an annual runoff of 3200 km^3 per year, and most of their discharge (46–66%) occurs during the spring freshet (Lammers et al., 2001; McClelland et al., 2006). Although these data provide a good estimate of riverine inflow, overall Arctic river discharge has increased since 1932, and is expected to continue to increase with climate change (McClelland et al., 2006; Peterson et al., 2002).

Sea ice differentiates the Arctic Ocean from other basins. First-year ice forms in late summer in regions of open water, while multi-year ice lasts year round. Multi-year ice exists in the central Arctic, Canadian Basin and around Greenland. Outside the central Arctic, ice consists of more first- than multi-year ice. The outer region of the first-year ice makes up the Marginal Ice Zone (MIZ), where broken ice attenuates wave energy, leading to upwelling, eddies, and jets. The MIZ typically has higher rates of primary production than surrounding water (Talley et al., 2011).

Water along the GN01 transect in the Bering Strait, Makarov and Canada Basins is influenced by inflow from the Pacific and Atlantic Oceans. With the exception of the TPD, surface water throughout this section of the western Arctic Ocean originated from the Pacific Ocean, entering through the Bering Strait as Bering Strait Modified Water (BSMW), which is characterized as having lower salinity with increased silicate and nutrients. Nutrient enrichment results from riverine discharge and inputs from the shelf. In contrast to water from the Pacific, Atlantic water is colder with a higher oxygen content. The surface water sampled from above 85°N (Stations 30–43) was relatively young meteoric water with transport time of 0.5–1 year, and hypothesized to be transported to the central Arctic Ocean from the East Siberian Arctic Shelf by the TPD (Kipp et al., 2018).

2.4.2. Filtered total Hg

Filtered HgT in seawater along the Arctic GN01 section ranged from 0.21 to 3.69 pM, and averaged 0.86 ± 0.45 pM among all depths and locations (n = 338; Table 1). Throughout the section, the highest average concentrations of HgT were in the Bering Sea and Strait (1.06 ± 0.59 pM, n = 31; Figure 2.3 A) and over the Chukchi shelf (1.06 ±

0.60 pM, $n = 47$, where "shelf" stations have a water depth < 200 m). Water on the shelf is more likely to be influenced by sediment resuspension and continental inputs of HgT, however, absence of Ra and Th anomalies indicate insignificant direct riverine input along the entire GN01 section (Personal communication, Erin Black, Dalhousie University).

Filtered HgT in the PML was variable, ranging from 0.41 to 2.9 pM. There was no HgT enrichment in the ice-covered PML when compared to surface water elsewhere in the section and sea ice (DiMento, 2017). However, greater amounts of HgT were measured in the TPD (1.36 ± 0.38 pM, $n = 21$) than in the ice-capped PML (0.89 ± 0.27 pM $n = 13$; $p < 0.001$). A relationship between HgT and fraction of meteoric water (derived from $\delta^{18}O$, Figure 2.4, Pasqualini et al., 2017) suggests that HgT in Arctic meteoric water is 4.0 ± 1.7 pM. This estimate is within the range of HgT measurements in Arctic sea ice (0.7–60.8 pM, unfiltered; Beattie et al., 2014) and Russian river water (0.7–13.3 pM; Coquery et al., 1995), but less than Arctic Alaskan rainwater (5–130 pM; Fitzgerald et al., 2005). It is unlikely that increased HgT in meteoric water is due to ice melt, because $\delta^{18}O$ values indicate brine formation rather than freshening of the surface waters (Personal communication, A. Pasquilini, LDEO). Thus, if the HgT in meteoric water is not fully explained by Arctic rivers and melting sea ice and associated snow, then vertical mixing over the thawing East Siberian Shelf, as hypothesized by Kipp et al. (2018) for ^{228}Ra, may be the source of increased HgT in the TPD.

Although Arctic deep waters (> 2000 m) along the GN01 section had increased HgT near the sediments, average concentrations were lower than either deep Atlantic or Pacific Ocean waters (Bowman et al., 2015; Bowman et al., 2016; Laurier et al., 2004;

Mason et al., 1998; Munson et al., 2015; Table 2.1). Filtered and particulate HgT increased near the sediment at stations 14, 19, 26, 30, and 52 (Figure 2.5), which suggests some vertical mixing with an efflux of HgT from the sediment. Similarly, aluminum concentrations were greater near the bottom, and may also be resuspended from the sediments (Personal communication, M. Hatta and C. Measures, University of Hawai'i). Sediments may be a localized source of HgT to deep Arctic waters, but deep water averages remain low. Bottom water HgT in the Canada (0.58 ± 0.24 pM; n = 38) and Eurasian Basins (0.50 ± 0.16 pM; n = 6) did not differ significantly (p = 0.442). These levels are in marked contrast to those in young North Atlantic Deep Water (1.04 ± 0.17 pM; Bowman et al. 2015), modified Pacific Deep Water (1.25 ± 0.23 pM, Bowman et al., 2016), and Antarctic Bottom Water in the Southern Ocean (1.35 ± 0.39 pM; Cossa et al., 2011). Deep water in the Canada and Eurasian Basins was last ventilated about 450 and 240 years ago, respectively (Schlosser et al., 1997). As such, based solely on age, these deep water masses are unlikely to contain much anthropogenic Hg. Sinking particles may add anthropogenic Hg to these water masses, however, due to low primary productivity, we would expect particle-driven sinking of anthropogenic Hg to be low. Thus, compared to other oceans, decreased particle pumping and little pollution enhancement in the Arctic Ocean leads to decreased HgT in deep water.

Many of the shallow Arctic Ocean water masses within the GN01 section have the fingerprint of anthropogenic Hg. According to Lamborg et al. (2014), concentrations of non-anthropogenic HgT can be estimated using remineralized phosphate (P_{remin}, Apparent Oxygen Utilization divided by 170; Anderson and Sarmiento, 1994), with a HgT:P_{remin} ratio of 1.02×10^{-6}. By extension, water masses with a HgT:P_{remin} ratio greater

than 1.02×10^{-6} contain anthropogenic Hg. HgT:P_{remin} ratios in the upper Arctic Ocean are about double this ratio and suggest that Hg emissions over the last 300 years have increased Hg concentrations (Figure 2.6). Of the water masses sampled, BSMW ($2.8 \pm 2.4 \times 10^{-6}$), ATL ($2.4 \pm 0.5 \times 10^{-6}$), EBDW ($1.4 \pm 0.1 \times 10^{-6}$), CBDW ($1.5 \pm 0.2 \times 10^{-6}$) contained more HgT than would be expected from remineralization of pre-industrial particulate matter alone. Deep waters in both the Canada and Eurasian Basins exhibit the least amount of anthropogenic impact, with ~1.4 times the amount of Hg we would expect from remineralization alone. As previously discussed, sediment resuspension supplies deep Arctic waters with Hg, however, it is unlikely this process impacts the entirety of the deep water masses.

Pacific water entering the Bering Strait contains about the same concentration of HgT leaving the Strait. Previous research from the VERTEX (1986-1987) and IOC cruises (2002) reported unfiltered HgT concentrations of 0.58 ± 0.37 pM and 0.64 ± 0.26 pM in North Pacific upper water (Laurier et al., 2004). If we assume these upper waters entered the Bering Strait without much alteration to HgT content, and compare these values to our Bering Strait upper water column mean of 1.3 ± 0.81 pM (sum of filtered and particulate HgT), there has not been an increase of HgT entering the Arctic Ocean from the North Pacific over the last two decades. From concentrations measured in this study and an estimate of Pacific inflow of 0.83 ± 0.66 Sv (Roach et al., 1995), we estimate the range of HgT entering the Arctic Ocean from the Bering Strait to be 4–71 kmol yr^{-1}. This range encompasses previous estimates of 20 kmol yr^{-1} (Outridge et al., 2008) and 27.5 kmol yr^{-1} (Soerensen et al., 2016). However, the flux of HgT into the

Arctic Ocean from the Bering Strait is small source compared to other sources (Outridge et al., 2008; Soerensen et al., 2016).

2.4.3. Elemental Hg

Filtered Hg^0 in the Arctic GN01 section ranged from below detection limit (0.04 pM) to 1.03 pM, with an average of 0.20 ± 0.16 pM (*n* = 269; Table 2.1). Similar mean concentrations and ranges have been reported for waters in the Canadian Arctic Archipelago, Nordic seas, and central Arctic Ocean (Andersson et al., 2008; Kirk et al., 2008; Sommar et al., 2007; St. Louis et al., 2007). Hg^0 distributions had nutrient-type profiles in ice-free waters, similar to other oceans (Bowman et al., 2015; Bowman et al., 2016; Cossa et al., 2011; Mason et al., 1995), but ice-covered waters had a surface maximum, which may be unique to polar seas (Figure 2.5). Hg^0 in BSMW (0.25 ± 0.19 pM, *n* = 79) suggests it may be transported into the central Arctic Ocean from the Bering Strait and Chukchi shelf (Figure 2.3 B). It is possible that the broad shallow shelves host microbes possessing *merA*, a gene responsible for reducing Hg^{2+} to Hg^0 (Summers and Sugarman, 1974; Summers and Silver, 1978). Hg^0 in PML (0.21 ± 0.19 pM, *n* = 63) is similar to AW (0.21 ± 0.15 pM, *n* = 29), and deep waters contain lower levels. Average amounts of Hg^0 in CBDW (0.11 ± 0.06 pM, 21 ± 13% of HgT as Hg^0, *n* = 27) and EBDW (0.13 ± 0.03 pM, 25 ± 8%, *n* = 5) were comparable, despite a water mass age difference of >200 years. This is in contrast to previous reports of decreasing Hg^0 with increasing water mass age (Bowman et al., 2015; Bowman et al., 2016), suggesting that Hg^0 production rates are slower in cold, and deep polar waters.

Surface waters at ice-covered stations had the highest Hg^0 measured along the GN01 section (Figure 2.7). Hg^0 in ice-covered surface waters (< 21 m, 0.37 ± 0.26 pM, *n*

= 17) were greater than in ice-free surface waters (0.074 ± 0.050 pM, n = 15; p < 0.001; Figure 2.7). Similar under-ice surface concentrations have been reported in the Arctic (Andersson et al., 2008), and greater levels have been documented in surface waters from the North Pacific, most likely due to a highly reductive environment (Mason et al., 1998). Ice-covered waters were supersaturated with Hg^0 (230 ± 228%; DiMento, 2017). Hg^0 was a larger fraction of HgT (24 ± 13%, n = 12) in ice-capped waters than in ice-free waters (12 ± 11%, n = 21; p = 0.001). Greater levels of Hg^0 under sea ice have been observed by others (St. Louis et al., 2007), and may be due to limited gas exchange between the PML and the atmosphere. It is unlikely that excess Hg^0 results from photoreduction of Hg (II), as sea ice reflects and attenuates much of the incident sunlight. Ice may also interfere with any re-oxidation processes that occur in surface waters, preventing excess Hg^0 from being transformed into another more reactive Hg species. Elemental Hg is therefore most likely formed in situ by microbes, perhaps attached under ice. Microbial communities with the *merA* operon can reduce Hg^{2+} to Hg^0 and have been found in ice-covered Arctic waters (Poulain et al., 2007), however, *merA* was not found in the GN01 section (Bowman et al., *In prep.*). Diversity of microbial communities and irregular ice thickness and cover might explain the variability of Hg^0 at ice stations. In addition, leads and breaks in ice cover may allow for degassing and contribute to variable Hg^0 content in the PML (Figure 2.7).

Unlike HgT, the TPD did not significantly influence Hg^0 in surface waters. Ice-covered waters within the TPD did not contain more Hg^0 (0.37 ± 0.30 pM, n = 9) than ice-covered waters outside of the TPD (0.35 ± 0.27 pM, n = 6; p = 1.0). But, if we consider the entire extent of the TPD (<100 m) and not solely the surface waters, Hg^0 is

affected by meteoric water. A correlation between the fraction of meteoric water and Hg^0 was found ($r = 0.78$, $p = 0.0002$), and the coefficient of determination suggests the meteoric water is not the only factor influencing Hg^0 concentration ($r^2 = 0.60$; Figure 2.4). Ice and an influx of meteoric water influences Hg^0 in ice-covered surface waters of the TPD.

2.4.4. Filtered MMHg

Monomethylmercury concentrations along the GN01 section ranged from below detection limit (0.020 pM) to 0.36 pM, and averaged 0.054 ± 0.050 pM (*n* = 164; Figure 2.3 C; Table 2.1). Surface water MMHg (0.064 ± 0.065 pM, *n* = 44) was about 50% lower than those observed in the Canadian Arctic Archipelago (0.12 ± 0.050 pM, Kirk et al., 2008). Monomethylmercury averaged 0.047 ± 0.033 pM (*n* = 16) in CBDW and 0.030 ± 0.034 pM (*n* = 4) in EBDW. Several stations (i.e., 14, 26, 32, 48, 52, 57) had increased MMHg just above the ocean floor (Figure 2.5), suggesting mobilization from sediments may be a source of MMHg to overlying water (Hammerschmidt et al., 2004; Hammerschmidt and Fitzgerald, 2006a; Hollweg et al., 2010). The fraction of HgT as MMHg and DMHg (%MeHg) averaged 12 ± 6 % (*n* = 12) in the PML, 12 ± 9 % (*n* = 19) in the halocline, 16 ± 10 % (*n* = 21) in AW, and 18 ± 17% (*n* = 17) in deep water. Previous observations of unfiltered Arctic Ocean water in the central Arctic, Beaufort Sea, and the Archipelago observed a %MeHg maximum in the halocline (10–49%, Heimbürger et al., 2015; Wang et al., 2012). Our observations of %MeHg (sum of filtered and particulate) agree with previous reports, but we also observe a %MeHg maximum in AW. An increase in %MeHg in AW might result from its circulation and interaction with the Arctic's broad shelves, where water masses might accumulate MeHg.

MMHg concentrations in the Arctic Ocean were unrelated to AOU, unlike the Pacific Ocean (Bowman et al., 2016; Munson et al., 2015; Sunderland et al., 2009), Southern Ocean (Cossa et al., 2011), and Mediterranean Sea (Cossa et al., 2009; Heimbürger et al., 2010). The lack of correlation is likely due to the absence of an oxygen minimum zone, which is hypothesized to provide an anaerobic environment for methylating bacteria. Ice coverage in the Arctic Ocean leads to variable phytoplankton growth and activity (Arrigo and van Dijken, 2011; Arrigo et al., 2012), which might also explain the lack of correlation between MMHg and AOU, and also between MMHg and phytoplankton pigment concentration. Phytoplankton blooms occur under single year ice (Arrigo et al., 2012), but thick multi-year ice results in decreased light and low primary production (Arrigo and van Dijken, 2011). Primary production under ice tends to be at a shallower depth than in open water, which may explain irregularities in these biological proxies for MMHg distribution. The AOU in the Arctic is advected from the broad, nutrient-rich shelves. Therefore, no correlation between MMHg and AOU maxima may indicate in situ MMHg production, rather than advection from the shelves (Heimbürger et al., 2015; Wang et al., 2012).

Both the TPD and ice cover affect MMHg in surface water of the central Arctic Ocean (Figure 2.3 C). MMHg in the upper 20 m of the ice-covered TPD (0.069 ± 0.070 pM, n = 13) and ice-covered waters outside of the TPD (0.064 ± 0.024, n = 3) were greater than ice-free waters (0.036 ± 0.009 pM, n = 3). While MMHg was elevated in the TPD, concentrations in the upper 100 m of the water column did not exhibit a strong relationship with meteoric water (Figure 2.4). MMHg levels on the Siberian Shelf are unknown, but if we assume concentrations are similar to the Chuckchi Shelf (0.028 ±

0.007 pM, $n = 2$), and use a demethylation rate of 0.36 ± 0.09 d^{-1} (derived from polar marine waters, Lehnherr et al., 2011), and the estimated transport time of TPD water from the Siberian Shelf (6 – 12 months; Kipp et al. 2018), then we would expect all shelf derived MMHg to be decomposed before reaching the central Arctic Ocean. The delivery of nutrients by the TPD likely fertilizes both methylating and demethylating microbial communities, which may result in variable MMHg that does not correlate with the fraction of meteoric water. There is also the possibility of localized, under-ice microbial communities which methylate Hg, which might explain why the TPD only affects the upper 20 m.

MMHg in the western Arctic Ocean is less than the Atlantic Ocean (Bowman et al., 2015) and similar to the Pacific Ocean (Bowman et al., 2016; Table 2.1). One explanation for the relatively lower MMHg is that the demethylation rate constant in polar marine waters is greater than the methylation rate constant (Lehnherr et al., 2011). Thus, while Hg methylation may be active by under-ice microbial communities and in the halocline, it is likely that demethylation lowers the steady-state concentration of MMHg. Returning to the central hypothesis for this study, it is possible that the majority of MMHg in the Arctic Ocean is produced on the shelves and in the archipelago, but very little is exported into the central ocean. For example, the Chukchi shelf is very productive, and 80% of the POC remains over the shelf and slope (Moran et al., 2005). The shelves and continental inputs might be sources of MMHg to the Arctic, but very little of it is transported via the TPD and AW into the central Arctic Ocean. Low MMHg concentrations in the western Arctic Ocean do not explain anomalous MMHg

concentrations in Arctic animals, and suggests other regions should be studied for MMHg production and assimilation into the food chain.

2.4.5. DMHg

DMHg ranged from below the detection limit (0.012 pM) to 0.23 pM with an average concentration of 0.040 ± 0.029 pM (*n* = 199; Table 2.1). As with MMHg, DMHg concentrations were lower than those measured in either the North Atlantic (Bowman et al., 2015) or the eastern tropical Pacific (Bowman et al., 2016), but comparable to those measured in the Canadian Arctic (Kirk et al., 2008; St. Louis et al., 2007). The average ratio of MMHg:DMHg in the Arctic Ocean was 2.1 ± 2.5 (*n* = 108). The MMHg:DMHg ratio remained relatively consistent from the upper 150 m of the water column (3.0 ± 4.0, *n* = 33) through intermediate and deep waters (1.6 ± 1.4, *n* = 57; 1.7 ± 1.0, *n* = 18). Upper water column mean values are similar to North Pacific waters (Bowman et al., 2016; Hammerschmidt and Bowman, 2012), but much less than in the North Atlantic (Bowman et al., 2015). Meanwhile, the deep water mean ratio suggests that in the Arctic Ocean, DMHg is not necessarily the dominant methylated species below the thermocline, which has been found to be the case in other oceans (Cossa et al., 1997; Mason et al., 1993; Mason et al., 1995). DMHg concentrations were unrelated to pigment concentrations, AOU, N* (a proxy for denitrification), and P_{remin}. The mechanism for DMHg production is unknown, but if the primary source of DMHg were from MMHg methylation, low MMHg in the Arctic Ocean may limit DMHg.

Vertical distributions of DMHg in the Arctic Ocean (Figures 2.3 D and 2.5) had a similar shape to other oceans, with a low surface water average (0.024 ± 0.016 pM, *n* = 21), a subsurface maximum in the halocline (0.041 ± 0.024, *n* = 45), and homogenized

levels below 1000 m, with similar average concentrations in EBDW (0.034 ± 0.019 pM, n = 6) and CBDW (0.030 ± 0.017, n = 22). The subsurface DMHg maxima is more prominent in the Canada Basin, and may be partially due to AW (0.041 ± 0.021 pM, n = 28; Figures 2.3 D, 2.5). Atlantic Water increases in density and circulates in a rim current, therefore it is possible the water mass accumulates nutrients beneficial for MMHg formation from the continental shelf, that are subsequently methylated to form DMHg. Interactions with the shelf may also allow AW to accumulate organic matter with reduced sulfide groups that are conducive to DMHg formation (Jonsson et al., 2016). The maximum follows the 300 μmol kg^{-1} oxygen contour, whereas in other oceans, the DMHg maximum occurs at depths with lower amounts of oxygen (Bowman et al., 2015; Bowman et al., 2016).

Unlike Hg^0, DMHg did not exhibit a surface maxima under sea ice in the Arctic Ocean. As described above, the presence of sea ice prevents degassing of Hg^0, but DMHg was not observed to concentrate in water under the ice in an analogous way. Ice likely prohibits DMHg evasion, so some under ice processes must prevent the buildup of DMHg. Under ice communities are either incapable of forming DMHg or demethylation rates are similar in magnitude to methylation rates. Demethylation of DMHg may occur either via biotic processes, or photodecomposition that leaves Hg^0 either undisturbed or indistinguishable from high Hg^0 concentrations under the ice, or a combination of all these processes. The influx of young shelf water does not yield higher DMHg concentrations. The TPD had a negative effect on DMHg concentration, as fraction of meteoric water and DMHg are inversely related with a correlation coefficient of 0.69 (Figure 2.4). An inverse relationship between DMHg and meteoric water supports the

idea that DMHg is more likely to form in the marine water column as opposed to freshwater systems.

2.4.6. Particulate HgT

The average concentration of particulate HgT (HgT_{Part}) along the GN01 transect was 0.1 ± 0.1 pM (n = 141; Table 2.1). HgT_{Part} concentrations were greatest in surface waters, and declined with depth to about 1000 m, and were homogenous throughout deep waters (Figure 2.8 A). Profiles and average concentrations of HgT in the Arctic Ocean are not similar to those observed in the North Atlantic Ocean (Bowman et al., 2015; Mason et al., 1998) and eastern tropical South Pacific Ocean (Bowman et al., 2016; Table 2.1). The average for the Arctic Ocean is greater than other oceans studied presumably due to the broad shelves supplying HgT_{Part} to the central Arctic. The largest source of HgT_{Part} to the Arctic Ocean is BSMW which has a distinct shelf fingerprint consisting of tracers such as filtered Cd extending into the central Arctic Ocean (Personal communication, Laramie Jensen, Texas A&M, and Laura Whitmore, University of Southern Mississippi). Particulate HgT in BSMW (0.13 ± 0.15 pM, n = 63) is significantly greater than HgT_{part} in the central Arctic, including the TPD (0.04 ± 0.04, n = 33; $p < 0.001$). The relatively young age of the TPD and the combined shelf and riverine source would suggest high HgT_{Part} concentrations in the TPD. However, HgT_{Part} measured in the TPD (0.09 ± 0.05 pM, n = 14) is significantly lower than HgT_{Part} in the upper 100 m outside of the TPD (0.22 ± 0.21 pM, n = 37; p = 0.019). This is likely due to particles in BSMW, and those particles were accumulated on the shelf.

2.4.7. Particulate MMHg

Particulate MMHg ($MMHg_{Part}$) concentrations varied widely, with 93% of samples being below the detection limit. The average concentration for $MMHg_{Part}$ in the Arctic was 0.004 ± 0.003 pM (n = 17), and $MMHg_{Part}$ constituted 0–86% of the HgT_{Part}. Mean measurements of Arctic $MMHg_{Part}$ are an order of magnitude greater than mean values for $MMHg_{Part}$ in the North Atlantic Ocean (Bowman et al., 2015) and the eastern tropical South Pacific Ocean (Bowman et al., 2016; Table 2.1). The sample average is disproportionately weighted by $MMHg_{Part}$ concentrations from shelf particles, and few quantifiable particles from the open ocean (Figure 2.8 B). Chukchi Shelf waters have high $MMHg_{Part}$ concentrations, and are advected with BSMW into the open ocean. These trends mirror those of HgT_{Part}, indicating sources of particulate MMHg and HgT to the Arctic are the Bering Strait and Chukchi Shelf. Some station profiles exhibited resuspension of $MMHg_{Part}$ in nephloid layers, but the magnitude of resuspension varied depending on the local bathymetry. The vertical distribution of $MMHg_{Part}$ was low in the surface, with a subsurface maxima and homogeneous below 1000 m, except for resuspension from the sediment or where water had recently interacted with a sill.

Particulate MMHg in the TPD was below detection limit, and lower than $MMHg_{Part}$ concentrations measured in the PML (0.003 ± 0.002 pM, n = 4). One possible explanation for differences in concentration might be a difference in particle lability due to the particle source, affecting $MMHg_{Part}$ to a greater extent than HgT_{Part}. Settling rate of particles from the Siberian Shelf might also be greater than that of particles from the Chukchi Shelf.

2.5. Conclusions

Four species of Hg were analyzed in seawater from the Bering Sea and Strait, Canada and Makarov Basins, and just over the Lomonosov Ridge in the Eurasian Basin in the western Arctic Ocean. Total Hg concentrations were the greatest in the Bering Sea and Strait and under ice in the TPD. Elemental Hg in surface water was greater under the ice than in ice-free waters, especially in the TPD. Methylated forms of Hg in water were greater over the shelf compared to open ocean, and vertical profiles exhibit a subsurface maxima in both MMHg and DMHg, neither of which were related to either oxygen consumption or nutrient levels. Unlike HgT and Hg^0, the TPD was not a source of MMHg or DMHg to the central Arctic Ocean. The Chukchi Shelf appears to be an important source of particulate HgT and MMHg to the Arctic, and may be an important part of the Arctic Hg food chain. All forms of filtered Hg in the Arctic Ocean had lower average concentrations than found in either the Atlantic or Pacific Oceans, while particles coming off of the shelf had higher HgT and MMHg than average particle concentrations in the Pacific or Atlantic Oceans. Low MMHg in the western Arctic Ocean suggest that Arctic animals are exposed to Hg primarily in coastal regions.

2.6. Acknowledgments

We thank chief scientists David Kadko and William Landing; the Captain, officers, and crew of the U.S. Coast Guard cutter *Healy* (HLY1502). We thank the GEOTRACES sampling team: Greg Cutter, Kyle McQuiggan, Peter Morton, Sarah Rauschenberg, Gabi Weiss, Simone Moos, and Lisa Oswald; the pump team: Phoebe Lam, Maija Heller, Yang Xiang, Steven Pike, Erin Black, and Lauren Kipp; and the small boat operations, ice, and melt pond teams: Ana Aguilar-Islas, Rob Rember, Neil Wyatt,

and Chris Marsay. We thank Brian DiMento for sharing total gaseous mercury data. We thank Kim Vaeth and William Fitzgerald for looking at earlier versions of this draft and providing helpful feedback. We also thank Kelly Muterspaw, Kayla Haman, Kortney Mullen and Katelynn Alcorn for help in the lab. This work was funded by the National Science Foundation grants OCE-1434650, 1434653, and 1534315.

Filtered Hg (https://www.bco-dmo.org/dataset/738136) and particulate Hg datasets (https://www.bco-dmo.org/dataset/738307) are available for download from the Biological and Chemical Oceanography Data Management Office.

2.7. References

Anderson, L.A., Sarmiento, J.L., 1994. Redfield ratios of remineralization determined by nutrient data analysis. Global Biogeochem. Cycles 8, 65–80.

Andersson, M.E., Sommar, J., Gårdfeldt, K., Lindqvist, O., 2008. Enhanced concentrations of dissolved gaseous mercury in the surface waters of the Arctic Ocean. Mar. Chem. 110, 190–194.

Arrigo, K.R., van Dijken, G.L., 2011. Secular trends in Arctic Ocean net primary production. J. Geophys. Res. 116, C09011.

Arrigo, K.R., Perovich, D.K., Pickart, R.S., Brown, Z.W. van Dijken, G.L., Lowry, K.E., Mills, M.M., Palmer, M.A., Balch, W.M., Bahr, F., Bates, N.R., Benitez-Nelson, C., Bowler, B. Brownlee, E., Ehn, J.K., Frey, K.E., Garley, R., Laney, S.R., Lubelczyk, L., Mathis, J., Matsuoka, A., Mitchell, B.G., Moore, G.W.K., Ortega-Retuerta, E., Pal, S., Polashenski, C.M., Reynolds, R.A., Schieber, B., Sosik, H.M., Stephens, M., Swift, J.H., 2012. Massive phytoplankton blooms under Arctic sea ice. Science 336, 1408.

Barrie, L., Flack, E., Gregor, D.J., Iversen, T., Loeng, H., Macdonald, R., Pfirman, S., Skotvold, T., Wartena, E., 1998. The influence of physical and chemical processes on contaminant transport into and within the Arctic, in: Gregor, D.J., Loeng, H., Barrie, L. (Eds.), AMAP Assessment Report: Arctic Pollution Issues. Arctic Monitoring and Assessment Programme, Oslo, Norway; pp. 25–116.

Baya, P.A., Hollinsworth, J.L., Hintelmann, H., 2013. Evaluation and optimization of solid adsorbents for the sampling of gaseous methylated mercury species. Anal. Chim. Acta 786, 61–69.

Beattie, S.A., Armstrong, D., Chaulk, A., Comte, J., Gosselin, M., Wang, F., 2014. Total and methylated mercury in Arctic multiyear sea ice. Environ. Sci. Technol. 48, 5575–5582.

Bishop, J.K., Lam, P.J., Wood, T.J., 2012. Getting good particles: Accurate sampling of particles by large volume in-situ filtration. Limnol. Oceanogr.: Methods 10, 681–710.

Bloom, N.S., Crecelius, E.A., 1983. Determination of mercury in seawater at sub-nanogram per liter levels. Mar. Chem. 14, 49–59.

Bloom, N., Fitzgerald, W.F., 1988. Determination of volatile mercury species at the picogram level by low-temperature gas chromatography with cold-vapour atomic fluorescence detection. Anal. Chim. Acta 208, 151–161.

Bloom, N., 1989. Determination of pictogram levels of methylmercury by aqueous phase ethylation, followed by cryogenic gas chromatography with cold vapour atomic fluorescence detection. Can. J. Fish. Aquat. Sci. 46, 1131–1140.

Bowman, K.L., Hammerschmidt, C.R., 2011. Extraction of monomethylmercury from seawater for low-femtomolar determination. Limnol. Oceanogr.: Methods 9, 121–128.

Bowman, K.L., Hammerschmidt, C.R., Lamborg, C.H., Swarr, G., 2015. Mercury in the North Atlantic Ocean: The U.S. GEOTRACES zonal and meridional sections. Deep Sea Res. II 116, 251–261.

Bowman, K.L., Hammerschmidt, C.R., Lamborg, C.H., Swarr, G.J., Agather, A.M., 2016. Distribution of mercury species across a zonal section of the eastern tropical South Pacific Ocean (U.S. GEOTRACES GP16). Mar. Chem. 186, 156–166.

Bowman, K.L., Collins, E., Agather, A.M., Lamborg, C.H., Hammerschmidt, C.R., Christensen, G., Elias, D., Podar, M., Kaul, D., Dupont, C., Saito, M.A., In preparation. Presence and distribution of mercury-cycling genes in the Arctic and Pacific Oceans and their relationship to mercury speciation.

Choi, A.L., Grandjean, P., 2008. Methylmercury exposure and health effects in humans. Environ. Chem. 5, 112–120.

Coquery, M., Cossa, D., Martin, J.M., 1995. The distribution of dissolved and particulate mercury in three Siberian estuaries and adjacent Arctic coastal waters. Water, Air, Soil Pollut. 80, 653–664.

Cossa, D., Martin, J-M., Takayanagi, K., Sanjuan, J., 1997. The distribution and cycling of mercury species in the western Mediterranean. Deep Sea Res. II 44(3–4), 721–740.

Cossa, D., Averty, B., Pirrone, N., 2009. The origin of methylmercury in open Mediterranean waters. Limnol. Oceanogr. 54(3), 837–844.

Cossa, D., Heimbürger, L.-E., Lannuzel, D., Rintoul, S.R., Butler, E.C.V., Bowie, A.R., Averty, B., Watson, R.J., Remenyi, T., 2011. Mercury in the Southern Ocean. Geochim. Cosmochim. Acta 75, 4037–4052.

Cutter, G.A., Bruland, K.W., 2012. Rapid and noncontaminating sampling system for trace elements in global ocean surveys. Limnol. Oceanogr.: Methods 10, 425–436.

Dietz, R., Pacyna, J., Thomas, D.J., Asmund, G., Gordeev, V.V., Johansen, P., Kimstach, V., Lockhart, L., Pfirman, S., Riget, F., Shaw, G., Wagemann, R., White, M., 1998. Heavy metals, in: Dietz, R., Pacyna, J., Thomas, D.J., (Eds.), AMAP Assessment Report: Arctic Pollution Issues. Arctic Monitoring and Assessment Programme, Oslo, Norway; pp. 373–453.

Dietz, R., Outridge, P.M., Hobson, K.A., 2009. Anthropogenic contributions to mercury levels in present-day Arctic animals—A review. Sci. Tot. Environ. 407, 6120–6131.

Dijkstra, J.A., Buckman, K.L., Ward, D., Evans, D.W., Dionne, M., Chen, C.Y., 2013. Experimental and natural warming elevates mercury concentrations in estuarine fish. PLoS ONE 8(3):e58401.

DiMento, B.P., 2017. An investigation of the major transformations and loss mechanisms of mercury and selenium in the surface ocean. Ph.D. Thesis, University of Connecticut.

[Dataset] Fetterer, F., Knowles, K., Meier, W., Savoie, M., Windnagel, A.K., 2017, updated daily. *Sea Ice Index, Version 3*. Monthly Sea Ice Extent, September 2015.

Boulder, CO, USA. NSDIC: National Snow and Ice Data Center. [Data set] doi: https://doi.org/10.7265/N5K072F8. Accessed 04/17/16.

Fisher, J.A., Jacob, D.J., Soerensen, A.L., Amos, H.M., Steffen, A., Sunderland, E.M., 2012. Riverine source of Arctic Ocean mercury inferred from atmospheric observations. Nat. Geosci. 5, 499–504.

Fitzgerald, W.F., Gill, G.A., 1979. Subnanogram determination of mercury by two-stage gold amalgamation and gas phase detection applied to atmospheric analysis. Anal. Chem. 51(11), 1714–1720.

Fitzgerald, W.F., Engstrom, D.R., Mason, R.P., Nater, E. A., 1998. The case for atmospheric mercury contamination in remote areas. Environ. Sci. Technol. 32(1), 1–7.

Fitzgerald, W.F., Engstrom, D.R., Lamborg, C.H., Tseng, C.-M., Balcom, P.H., Hammerschmidt, C.R., 2005. Modern and historic atmospheric mercury fluxes in Northern Alaska: Global sources and Arctic depletion. Environ. Sci. Technol. 39, 557–568.

Gionfriddo, C.M., Tate, M.T., Wick, R.R., Schultz, M.B., Zelma, A., Thelen, M.P., Schofield, R., Krabbenhoft, D.P., Holt, K.E., Moreau, J.W., 2016. Microbial mercury methylation in Antarctic sea ice. Nat. Microbiol. 16127, doi: 10.1038/NMICROBIOL2016.127

Gordienko, P.A., Laktionov, A.F., 1969. Circulation and physics of the Arctic Basin waters, in: Gordon, A.L., Baker, F.W.G. (Eds.), Oceanography: Annals of the International Geophysical Year, vol. 46. Pergamon Press, London, pp. 94–112.

Grandjean, P., Weihe, P., Needham, L.L., Burse, V.W., Patterson, Jr., D.G., Sampson, E.J., Jørgensen, P.J., Vahter, M., 1995. Relation of a seafood diet to mercury, selenium, arsenic, and polychlorinated biphenyl and other organochlorine concentrations in human milk. Environ. Res. 71, 29–38.

Ha, E., Basu, N., Bose-O'Reilly, S., Dórea, J.G., McSorley, E., Sakamoto, M., Chan, H.M., 2017. Current progress on understanding the impact of mercury on human health. Environ. Res. 152, 419–433.

Hammerschmidt, C.R., Fitzgerald, W.F., Lamborg, C.H., Balcom, P.H., Visscher, P.T., 2004. Biogeochemistry of methylmercury in sediments of Long Island Sound. Mar. Chem. 90, 31–52.

Hammerschmidt, C.R., Fitzgerald, W.F., 2006a. Methylmercury cycling in sediments on the continental shelf of southern New England. Geochim. Cosmochim. Acta 70, 918–930.

Hammerschmidt, C.R., Fitzgerald, W.F., 2006b. Bioaccumulation and trophic transfer of methylmercury in Long Island Sound. Arch. Environ. Contam. Toxicol. 51, 416–424.

Hammerschmidt, C.R., Bowman, K.L., Tabatchnick, M.D., Lamborg, C.H., 2011. Storage bottle material and cleaning for determination of total mercury in seawater. Limnol. Oceanogr.: Methods 9, 426–431.

Hammerschmidt, C.R., Bowman, K.L., 2012. Vertical methylmercury distribution in the subtropical North Pacific Ocean. Mar. Chem. 132–133, 77–82.

Heimbürger, L.-E., Sonke, J.E., Cossa, D., Point, D., Lagane, C., Laffont, L., Galfond, B.T., Nicolaus, M., Rabe, B., Rutgers van der Loeff, M., 2015. Shallow methylmercury production in the marginal sea ice zone of the central Arctic Ocean. Sci. Rep. 5, 10318; doi: 10.1038/srep10318.

Hollweg, T.A., Gilmour, C.C., Mason, R.P., 2010. Mercury and methylmercury cycling in sediments of the mid-Atlantic continental shelf and slope. Limnol. Oceanogr. 55(6), 2703–2722.

Horowitz, H.M., Jacob, D.J., Zhang, Y., Dibble, T.S., Slemr, F., Amos, H.M., Schmidt, J.A., Corbitt, E.S., Marais, E.A., Sunderland, E.M., 2017. A new mechanism for atmospheric mercury redox chemistry: Implications for the global mercury budget. Atmos. Chem. Phys. 17, 6353–6371.

Jakobsson, M., 2002. Hypsometry and volume of the Arctic Ocean and its constituent seas. Geochem. Geophys. Geosyst. 3(5), 1–18.

Jonsson, S., Mazrui, N.M., Mason, R.P., 2016. Dimethylmercury formation mediated by inorganic and organic reduced sulfur surfaces. Sci. Rep. 6, 27958; doi: 10.1038/srep27958.

Karagas, M.R., Choi, A.L. Oken, E., Horvat, M., Schoeny, R., Kamai, E., Cowell, W., Grandjean, P., Korrick, S., 2012. Evidence on the human health effects of low-level methylmercury exposure. Environ. Health Perspect. 120(6), 799–806.

Kipp, L.E., Charette, M.A., Moore, W.S., Henderson, P.B., Rigor, I.G., 2018. Increased fluxes of shelf-derived materials to the central Arctic Ocean. Sci. Adv. 4, eaao1302.

Kirk, J.L., St. Louis, V.L., Sharp, M.J., 2006. Rapid reduction and reemission of mercury deposited into snowpacks during atmospheric mercury depletion events at Churchill, Manitoba, Canada. Environ. Sci. Technol. 40, 7590–7596.

Kirk, J.L., St. Louis, V.L., Hintelmann, H., Lehnherr, I., Else, B., Poissant, L., 2008. Methylated mercury species in marine waters of the Canadian High and Sub Arctic. Environ. Sci. Technol. 42, 8367–8373.

Klunder, M.B., Bauch, D., Laan, P., de Baar, H.J.W., van Heuven, S., Ober, S., 2012. Dissolved iron in the Arctic shelf seas and surface waters of the central Arctic Ocean: Impact of Arctic river water and ice-melt. J. Geophys. Res. 117, C01027.

Lamborg, C.H., Hammerschmidt, C.R., Gill, G.A., Mason, R.P., Gichuki, S., 2012. An intercomparison of procedures for the determination of total mercury in seawater and recommendations regarding mercury speciation during GEOTRACES cruises. Limnol. Oceanogr.: Methods 10, 90–100.

Lamborg, C.H., Hammerschmidt, C.R., Bowman, K.L., Swarr, G.J., Munson, K.M., Ohnemus, D.C., Lam, P.J., Heimbürger, L.-E., Rijkenberg, M.J.A., Saito, M.A., 2014. A global ocean inventory of anthropogenic mercury based on water column measurements. Nature 512, 65–68.

Lammers, R.B., Shiklomanov, A.I., Vörösmarty, C.J., Fekete, B.M., Peterson, B.J., 2001. Assessment of contemporary Arctic river runoff based on observational discharge records. J. Geophys. Res. 106(D4), 3321–3334.

Laurier, F.J.G., Mason, R.P., Gill, G.A., Whalin, L., 2004. Mercury distributions in the North Pacific Ocean—20 years of observations. Mar. Chem. 90, 3–19.

Lehnherr, I., St. Louis, V.L., Hintelmann, H., Kirk, J.L., 2011. Methylation of inorganic mercury in polar marine waters. Nat. Geosci. 4, 298–302.

Lindberg, S.E., Brooks, S., Lin, C.-J., Scott, K.J., Landis, M.S., Stevens, R.K., Goodsite, M., Richter, A., 2002. Dynamic oxidation of gaseous mercury in the Arctic troposphere at polar sunrise. Environ. Sci. Technol. 36, 1245–1256.

Macdonald, R.W., Harner, T., Fyfe, J., 2005. Recent climate change in the Arctic and its impact on contaminant pathways and interpretation of temporal trend data. Sci. Tot. Environ. 342 5–86.

Mahaffey, K.R., Clickner, R.P., Jeffries, R.A., 2009. Adult women's blood mercury concentrations vary regionally in the United States: Association with patterns of fish consumption (NHANES 1999–2004). Env. Health Perspect. 117(1), 47–53.

Mason, R.P., Fitzgerald, W.F., Hurley, J., Hanson, A.K., Donaghay, P.L., Sieburth, J.M., 1993. Mercury biogeochemical cycling in a stratified estuary. Limnol. Oceanogr. 38(6), 1227–1241.

Mason, R.P., Rolfhus, K.R., Fitzgerald, W.F., 1995. Methylated and elemental mercury cycling in surface and deep ocean waters of the North Atlantic. Water, Air, and Soil Pollut. 80, 665–677.

Mason, R.P., Rolfhus, K.R., Fitzgerald, W.F., 1998. Mercury in the North Atlantic. Mar. Chem. 61, 37–53.

Mason, R. P., Choi, A.L., Fitzgerald, W.F., Hammerschmidt, C.R., Lamborg, C.H., Soerensen, A.L., Sunderland, E.M., 2012. Mercury biogeochemical cycling in the ocean and policy implications. Environ. Res. 119, 101–117.

McClelland, J.W., Déry, S.J., Peterson, B.J., Holmes, R.M., Wood, E.F., 2006. A pan-arctic evaluation of changes in river discharge during the latter half of the 20th century. Geophys. Res. Lett. 33, L06715, 1–4.

Mergler, D., Anderson, H.A., Hing Man Chan, L., Mahaffey, K.R., Murray, M., Sakamoto, M., Stern, A.H., 2007. Methylmercury exposure and health effects in humans: A worldwide concern. Ambio 36(1) 3–11.

Moran, S.B., Kelly, R.P., Hagstrom, K., Smith, J.N., Grebmeier, J.M., Cooper, L.W., Cota, G.F., Walsh, J.J., Bates, N.R., Hansell, D.A., Maslowski, W., Nelson, R.P., Mulsow, S., 2005. Seasonal changes in POC export flux in the Chukchi Sea and implications for water column-benthic coupling in Arctic shelves. Deep Sea Res. II 52, 3427–3451.

Munson, K.M., Babi, D., Lamborg, C.H., 2014. Determination of monomethylmercury from seawater with ascorbic acid-assisted direct ethylation. Limol. Oceanogr.: Methods 12, 1–9.

Munson, K.M., Lamborg, C.H., Swarr, G.J., Saito, M.A., 2015. Mercury species concentrations and fluxes in the Central Tropical Pacific Ocean. Global Biogeochem. Cycles 29, 656–676.

Oskarsson, A., Schültz, A., Skerfving, S., Hallén, I.P., Ohlin, B., Lagerkvist, B.J., 1996. Total and inorganic mercury in breast milk in relation to fish consumption and amalgam fillings in lactating women. Arch. Environ. Health 51(3), 234–41.

Outridge, P.M., Macdonald, R.W., Wang, F., Stern, G.A., Dastoor, A.P., 2008. A mass balance inventory of mercury in the Arctic Ocean. Environ. Chem. 5, 89–111.

[Dataset] Pasqualini, A., Schlosser, P., Newton, R., Koffman, T.N., 2017. U.S. GEOTRACES Artic Section Ocean Water Hydrogen and Oxygen Stable Isotope Analyses (version 1.0) [Data set]. IEDA, doi:10.1594/IEDA/100633.

Peterson, B.J., Holmes, R.M., McClelland, J.W., Vörösmarty, C.J., Lammers, R.B., Shiklomanov, A.I., Shiklomanov, I.A., Rahmstorf, S., 2002. Increasing river discharge to the Arctic Ocean. Science 298, 2171–2173.

Poulain, A.J., Ní Chadhain, S.M., Ariya, P.A., Amyot, M., Garcia, E., Campbell, P.G.C., Zylstra, G.J., Barkay, T., 2007. Potential for mercury reduction by microbes in the high Arctic. Appl. Environ. Microbiol. 73(7), 2230–2238.

Roach, A.T., Aagaard, K., Pease, C.H. Salo, S.A., Weingartner, T., Pavlov, V., Kulakov, M., 1995. Direct measurements of transport and water properties through the Bering Strait. J. Geophys. Res. 100 (9) 18443–18457.

Rudels, B., 2001. Arctic Basin circulation, in: Steele, J.H., Thorpe, S.A., Turekian, K.K. (Eds.), Encyclopedia of Ocean Sciences. Elsevier Science Ltd.: Oxford, UK pp. 177–187.

Scheuhammer, A., Braune, B., Chan, H.M., Frouin, H., Krey, A., Letcher, R., Loseto, L., Noël, M., Ostertag, S., Ross, P., Wayland, M., 2015. Recent progress on our understanding of the biological effects of mercury in fish and wildlife in the Canadian Arctic. Sci. Tot. Environ. 509–510, 91–103.

Schlosser, P., Kromer, B., Ekwurzel, B., Bönisch, G., McNichol, A., Schneider, R., von Reden, K., Östlund, H.G., Swift, J.H., 1997. The first trans-Arctic ^{14}C section: comparison of the mean ages of the deep waters in the Eurasian and Canadian basins of the Arctic Ocean. Nuc. Instr. And Meth. in Phys. Res. B 123, 431–437.

Schroeder, W.H., Anlauf, K.G., Barrie, L.A., Lu, J.Y., Steffen, A., Schneeberger, D.R., Berg, T., 1998. Arctic springtime depletion of mercury. Nature 394, 331–332.

Sheehan, M.C., Burke, T.A., Navas-Acien, A., Breysse, P.N., McGready, J., Fox, M.A., 2014. Global methylmercury exposure from seafood consumption and risk of developmental neurotoxicity: a systematic review. Bull. World Health Organ. 92(4), 254–269F.

Slemr, F., Schuster, G., Seiler, W., 1985. Distribution, speciation, and budget of atmospheric mercury. J. Atmos. Chem. 3, 407–434.

Slemr, F., Langer, E., 1992. Increase in global atmospheric concentrations of mercury inferred from measurements over the Atlantic Ocean. Nature 355, 434–437.

Soerensen, A.L., Jacob, D.J., Schartup, A.T., Fisher, J.A., Lehnherr, I., St. Louis, V.L., Heimbürger, L.-E., Sonke, J.E., Krabbenhoft, D.P., Sunderland, E.M., 2016. A mass budget for mercury and methylmercury in the Arctic Ocean. Global Biogeochem. Cycles 30, doi:10.1002/2015GB005280.

Sommar, J., Wängberg, I., Berg, T., Gårdfelt, K., Munthe, J., Richter, A., Urba, A., Wittrock, F., Schroeder, W.H., 2007. Circumpolar transport and air-surface exchange of atmospheric mercury at Ny-Ålesund (79° N), Svalbard, spring 2002. Atmos. Chem. Phys. 7, 151–166.

St. Louis, V.L., Hintelmann, H., Graydon, J.A., Kirk, J.L., Barker, J., Dimock, B., Sharp, M.J., Lehnherr, I., 2007. Methylated mercury species in Canadian High Arctic marine surface waters and snowpacks. Environ. Sci. Technol. 41, 6433–6441.

Steffen, A., Douglas, T., Amyot, M., Ariya, P., Aspmo, K., Berg, T., Bottenheim, J., Brooks, S., Cobbett, F., Dastoor, A., Dommergue, A., Ebinghaus, R., Ferrari, C., Kardfeldt, K., Goodsite, M.E., Lean, D., Poulain, A., Scherz, C., Skov, H., Sommar, J., Temme, C., 2007. A synthesis of atmospheric mercury depletion event chemistry linking atmosphere, snow and water. Atmos. Chem. Phys. Discuss. 7, 10837–10931.

Summers, A.O., Sugarman, L.I., 1974. Cell-free mercury(II)-reducing activity in a plasmid-bearing strain of *Escherichia coli.* J. Bacteriol. 119 (1), 242–249.

Summers, A.O., Silver, S., 1978. Microbial Transformations of metals. Ann. Rev. Microbiol. 32, 637–672.

Sunderland, E. M., 2007. Mercury exposure from domestic and imported estuarine and marine fish in the U.S. seafood market. Environ. Health Perspect. 115(2), 235–242.

Sunderland, E.M., Krabbenhoft, D.P., Moreau, J.W., Strode, S.A., Landing, W.M., 2009. Mercury sources, distribution, and bioavailability in the North Pacific Ocean: Insights from data and models. Global Biogeochem. Cycles 23, GB2010, doi: 10.1029/2008GB003425.

Swain, E.B., Engstrom, D.R., Brigham, M.E., Henning, T. A., Brezonik, P.L., 1992. Increasing rates of atmospheric mercury deposition in midcontinental North America. Science 257, 784–787.

Talley, L.D., Pickard, G.L., Emery, W.J., Swift, J.H., 2011. Arctic Ocean and Nordic Seas, in: Talley, L.D., Descriptive Physical Oceanography (6 Ed). Academic Press, London, pp. 401–436.

Tseng, C.-M., Hammerschmidt, C.R., Fitzgerald, W.F., 2004. Determination of methylmercury in environmental matrixes by on-line flow injection and atomic fluorescence spectrometry. Anal. Chem. 76 (23), 7131–7136.

Van Oostdam, J., Donaldson, S.G., Feeley, M., Arnold, D., Ayotte, P., Bondy, G., Chan, L., Dewaily, É., Furgal, C.M., Kuhnlein, H., Loring, E., Muchle, G., Myles, E., Receveur, O., Tracy, B., Gill, U., Kalhok, S., 2005. Human health implications of environmental contaminants in Arctic Canada: A review. Sci. Tot. Environ. 351–352, 165–246.

Wang, F., Macdonald, R.W., Armstrong, D.A., Stern, G.A., 2012. Total and methylated mercury in the Beaufort Sea: The role of local and recent organic remineralization. Environ. Sci. Technol. 46, 11821–11828.

FIGURES

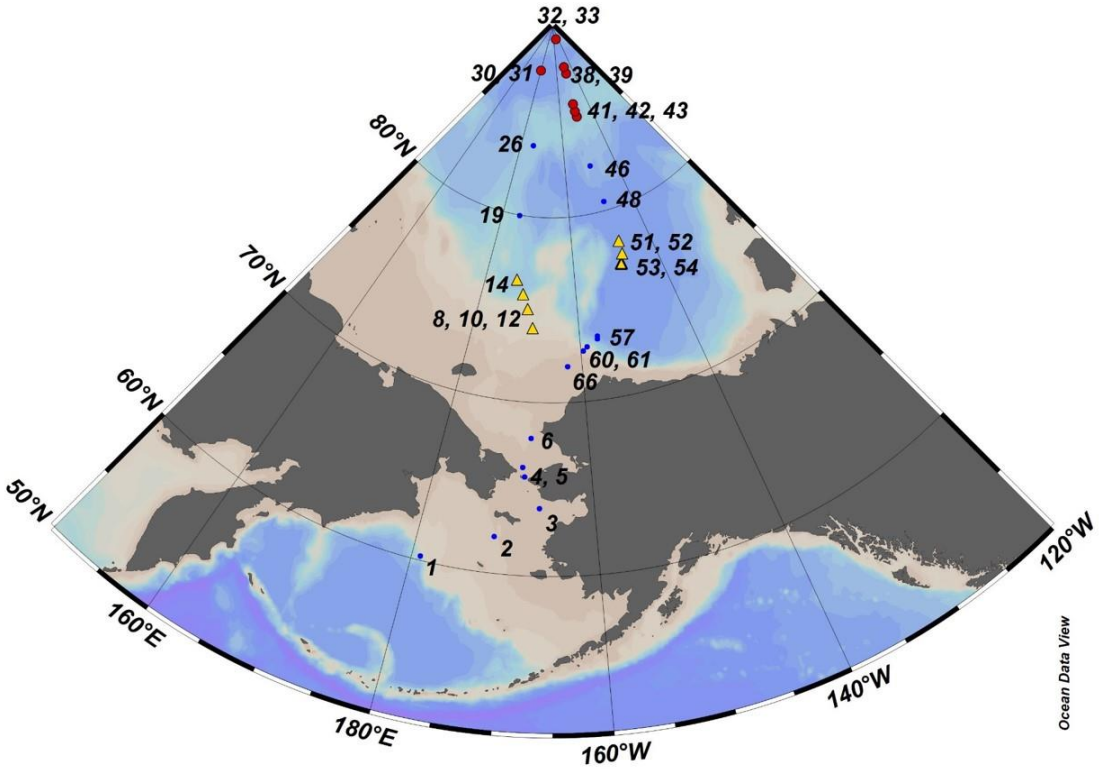

Figure 2.1. Water-sampling stations along the U.S. GEOTRACES western Arctic section (GN01). Transpolar drift (TPD) stations denoted by red dots and marginal ice zone (MIZ) stations are indicated with yellow triangles. Stations north of the MIZ were ice covered, while stations south of the MIZ were ice-free.

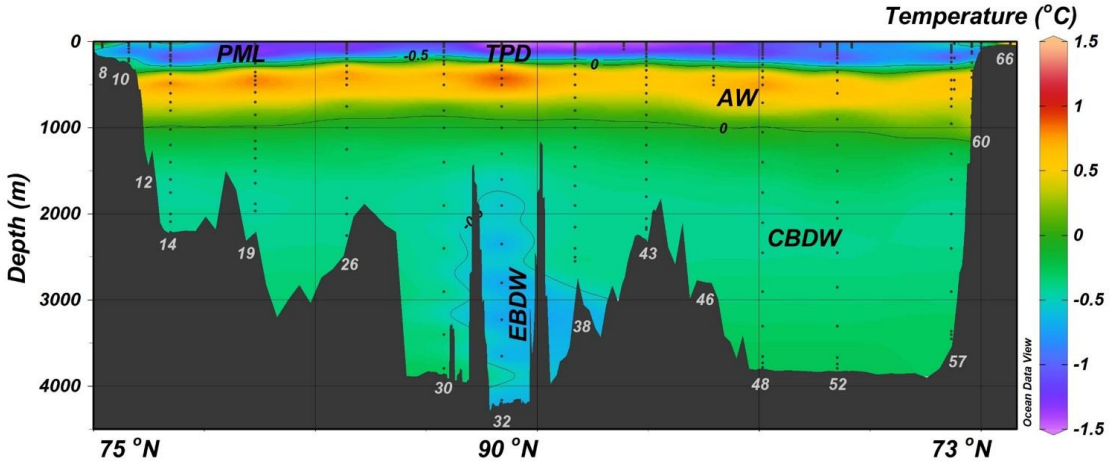

Figure 2.2. Water temperature in the GN01 Arctic section, with 0 and −0.5 °C contour lines noted. Water masses sampled are labeled, including: Polar Mixed Layer (PML), Atlantic Water (AW), Canada Basin Deep Water (CBDW), and Eurasian Basin Deep Water (BDW). The Transpolar Drift (TPD) is also indicated, extending from station 30 to station 43 in the surface layer. Station numbers are indicated in grey numbering along the bathymetry.

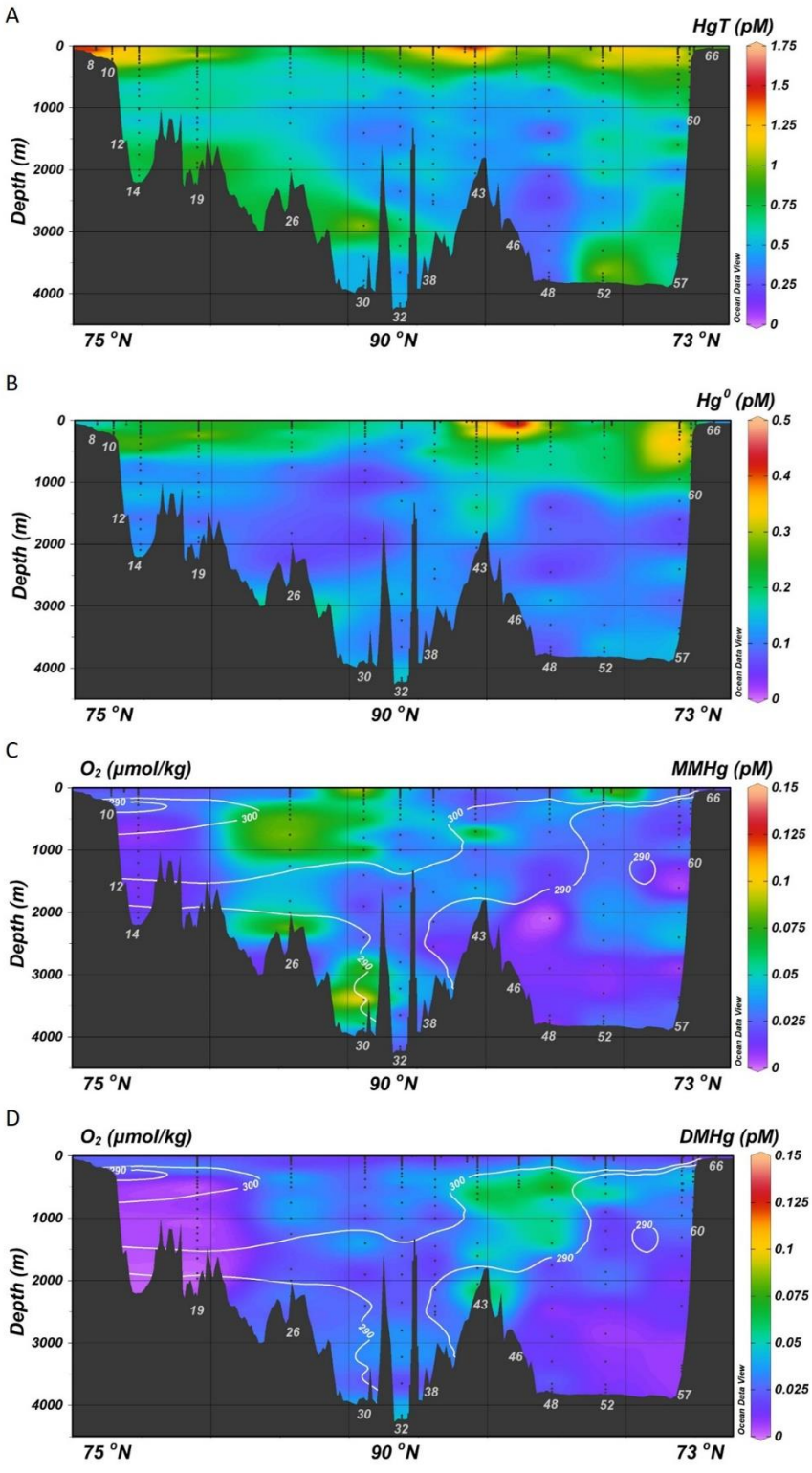
A
HgT (pM)
B
Hg0 (pM)
C
O2 (µmol/kg)
MMHg (pM)
D
O2 (µmol/kg)
DMHg (pM)
Depth (m)
75 °N
90 °N
73 °N
Ocean Data View

Figure 2.3. Filtered total Hg (HgT, A), elemental Hg (Hg^0, B), monomethyl-Hg (MMHg, C), and dimethyl-Hg (DMHg, D) in the western Arctic Ocean. Dots indicate water sample depth, and the numbers listed in the bathymetry indicate station number.

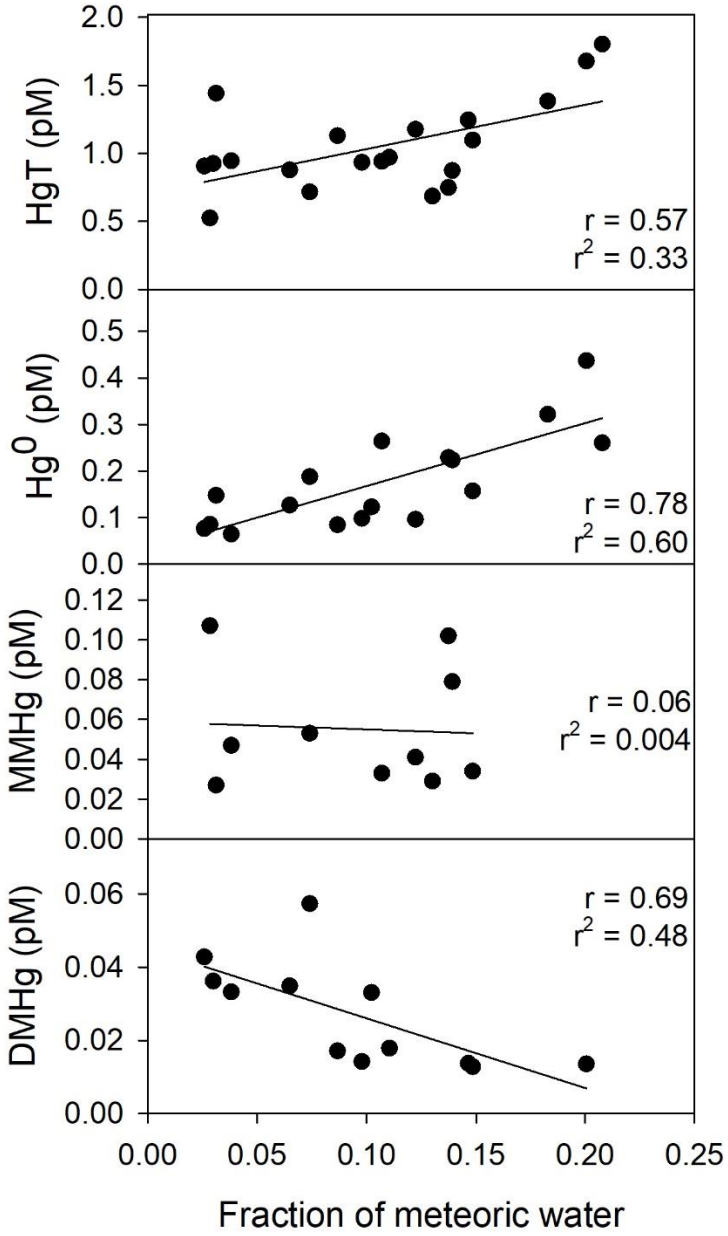

Figure 2.4. HgT, Hg^0, MMHg and DMHg plotted versus the fraction of meteoric water in the upper 100 m of stations above 85°N (Stations 30–43), in the Transpolar Drift (Pasqualini et al., 2017). The equation from the HgT regression line, y = 3.2569 x + 0.7062, can be used to extrapolate HgT content in 100% meteoric water.

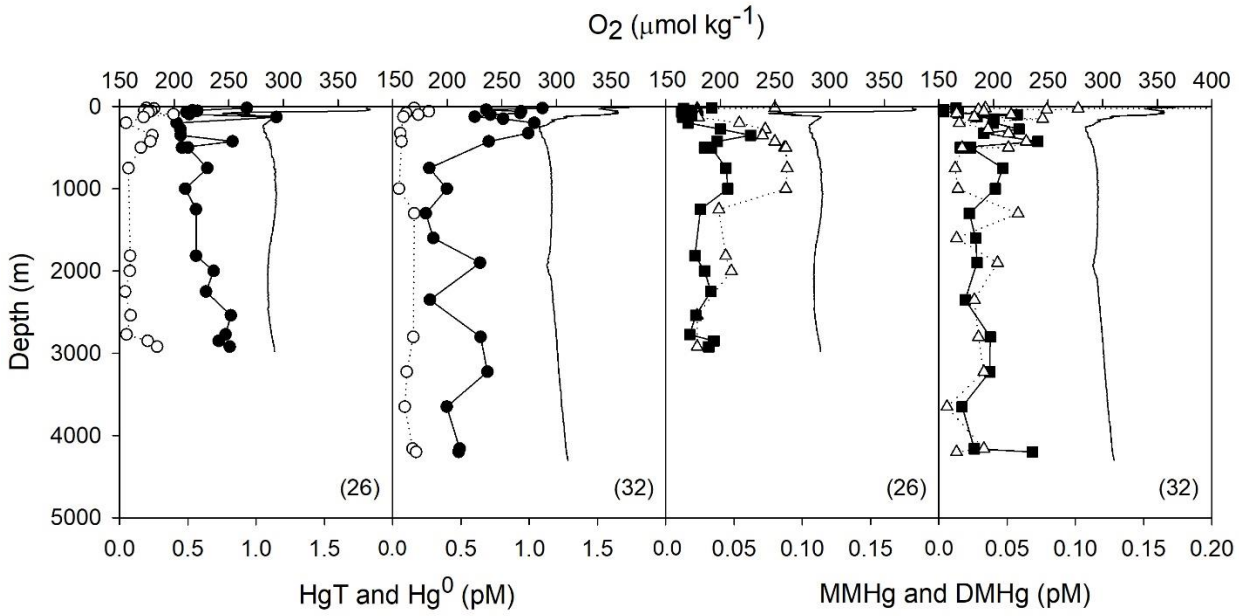

Figure 2.5. Filtered mercury species at ice-covered stations in the Makarov (26) and Eurasian Basins (32). Left panels contain filtered total mercury (black circles), elemental mercury (open circles), and right panels show filtered monomethylmercury (black squares) and dimethylmercury (open triangles). All panels show dissolved oxygen (black line).

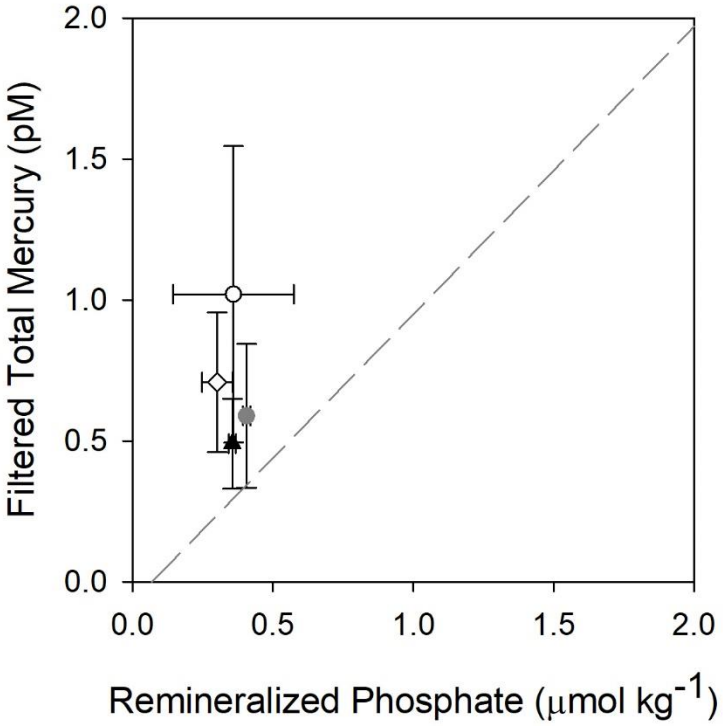

Figure 2.6. Filtered total mercury (HgT) measured in the western Arctic Ocean, compared to remineralized phosphate. Bering Strait Modified Water (open circle), Eurasian Basin Deep Water (black triangle), Canada Basin Deep Water (grey circle), and Atlantic Water (open diamond) have HgT:P ratios greater than those in unaffected water masses, suggesting they contain anthropogenic mercury.

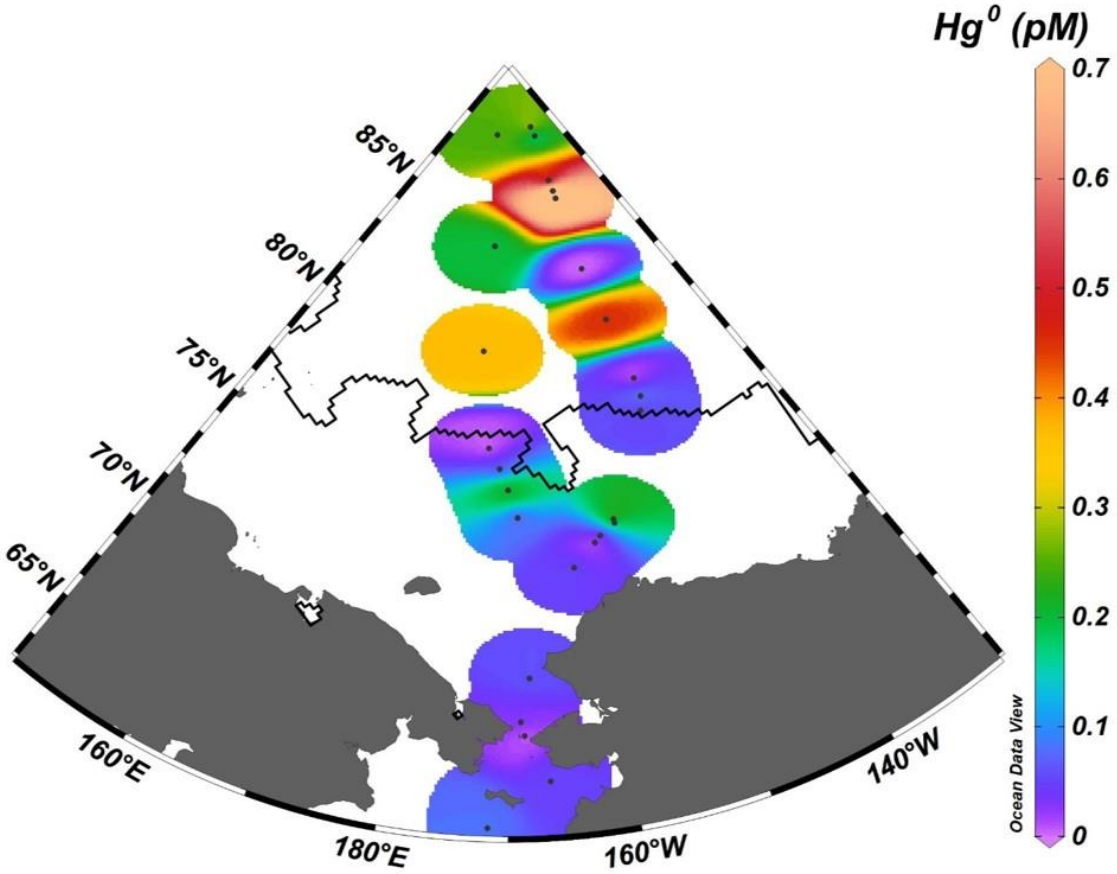

Figure 2.7. Elemental Hg measurements at the shallowest depth sampled. The black line indicates the average ice extent for the month of September 2015 (Fetterer et al., 2017).

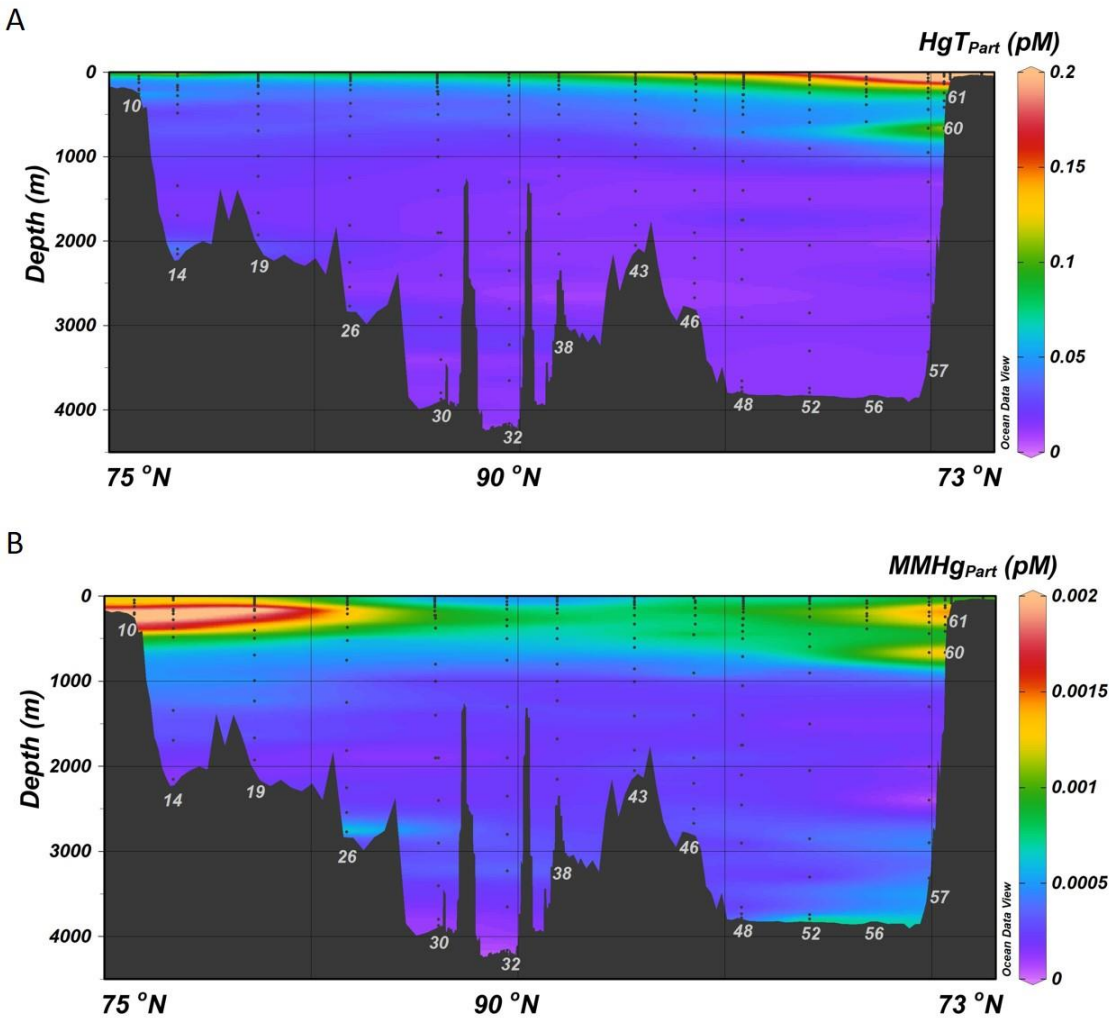

Figure 2.8. Particulate total Hg (HgT_{Part}, A) and particulate monomethyl-Hg ($MMHg_{Part}$, B) in the GN01 transect. Station numbers are denoted by numbers in the bathymetry, and black dots throughout the water column indicate sampling depth.

TABLES

Table 2.1. Summary of filtered and particulate species in the GN01 section, compared to average values from the Atlantic Ocean ([a]Bowman et al. 2015, [b]Mason et al., 1998), Pacific Ocean (Bowman et al., 2016), Mediterranean Sea (Cossa et al., 2009), and Southern Ocean (Cossa et al., 2011).

Hg Species	Mean ± SD (pM)	Range (pM)	*n*	Atlantic Ocean (pM)	Pacific Ocean (pM)	Mediterranean Sea (pM)	Southern Ocean (pM)
Total Hg	0.86 ± 0.45	0.21–3.69	338	0.89 ± 0.31[a] 2.4 ± 1.6[b]	0.78 ± 0.41	1.19 ± 0.48	1.33 ± 0.45
Hg0	0.20 ± 0.16	< DL–1.03	269	0.48 ± 0.31[b]	0.045 ± 0.061	-	-
MMHg	0.054 ± 0.050	< DL–0.36	164	0.095 ± 0.098[a]	0.07 ± 0.06	-	-
DMHg	0.040 ± 0.029	< DL–0.23	199	0.18 ± 0.12[a] 0.07 ± 0.04[a]	0.07 ± 0.07	-	-
Particulate HgT	0.1 ± 0.1	< DL–0.75	141	0.038 ± 0.039[a] 0.035 ± 0.02[b]	0.075 ± 0.094	-	-
Particulate MMHg	0.004 ± 0.003	< DL–0.011	17	0.0007 ± 0.001[a]	0.0007 ± 0.001	-	-

Chapter 3: VERTICAL AND SEASONAL VARIATION OF MERCURY METHYLATION AND SPECIATION IN A EUTROPHIC KETTLE LAKE IN SOUTHWEST OHIO

3.1. Abstract

Aquatic systems are ideal locations for mercury (Hg) methylation to neurotoxic monomethylmercury (MMHg). We measured Hg speciation in a eutrophic kettle lake (Crystal Lake, Clark County, Ohio) throughout one year and performed Hg methylation assays during the summer and early fall. Throughout the year, unfiltered total Hg averaged 5.4 ± 0.43 pM (± 1 SE), elemental Hg averaged 0.14 ± 0.037 pM, and mean concentrations of MMHg were 1.0 ± 0.15 pM. Total Hg maxima were located at the oxic/anoxic boundary and in the hypolimnion, and MMHg maxima were located along the oxic/anoxic boundary during summer stratification. Dimethylmercury was not detected throughout the duration of this study. Specific methylation potentials averaged 0.9 ± 0.4 % d^{-1} in the epilimnion, 0.4 ± 0.1 % d^{-1} in the oxic/anoxic boundary, and 5 ± 3 % d^{-1} in the hypolimnion. Demethylation potentials were below detection limit, but estimated to be < 5 % d^{-1}. Hypolimnetic sulfide exceeded 150 μM during the late summer and early fall, likely preventing Hg methylation due to the formation of Hg-sulfide complexes that are not bioavailable for methylation. To evaluate Hg-methylating community structure, DNA was collected from the water column and screened for *hgcAB*, and *hgcA* abundance for all three known methylating clades (*Deltaproteobacteria, Archaea, and Firmicutes*). All three clades were present, and *Archaea* was the most abundant methylating clade at all depths. *hgcA* was most abundant

in the anoxic hypolimnion, where Hg methylation rates were greatest. *Archaeal* genes were most abundant in the epilimnion, suggesting a possible mechanism for oxic methylation in freshwater systems. However, greater methylation rates and gene abundance suggest that anoxic water and sediment production are more important for Hg methylation in Crystal Lake.

3.2. Introduction

Mercury (Hg) is a toxic metal with natural and anthropogenic sources. Since the Industrial Revolution, fossil fuel combustion has increased the amount of Hg in the environment by a factor of three (Fitzgerald et al., 1998). Fossil fuel use, artisanal gold mining, and natural sources release elemental Hg (Hg^0) into the atmosphere, where it can persist and disperse for up to a year before it is oxidized to Hg^{2+} and scavenged (Horowitz et al., 2017; Slemr et al., 1985). Once deposited, Hg^{2+} can be transformed by biotic and/or abiotic processes, including addition of a methyl group to form monomethylmercury (MMHg), a bioaccumulating neurotoxin. Humans are exposed to MMHg primarily by consumption of fish (Johnsson et al., 2004; Karagas et al., 2012; Mergler et al., 2007; Sheehan et al., 2014). MMHg bioaccumulation is relatively well studied, but many questions remain about Hg methylation in the water column.

Hypolimnetic waters (Eckley et al., 2005; Eckley and Hintelmann, 2006; Watras et al., 1995) and anaerobic lake sediments (Gilmour et al., 1992; Gilmour and Henry, 1991; Pak and Bartha, 1998) provide ideal conditions for Hg methylation. MMHg produced in lakes may accumulate in fish and lead to consumption advisories. Lacustrine Hg methylation may be a source of MMHg to downstream ecosystems. To better

understand Hg cycling in lakes methylation studies with stable isotopes have been used to quantify methylation and demethylation rates (Eckley et al., 2005; Eckley and Hintelmann, 2006). Previous work has only measured methylation potentials in anoxic hypolimnia, and the greatest Hg methylation potentials occurred just below the oxycline, and after fall turnover no methylation was detected (Eckley and Hintelmann, 2006).

The gene pair *hgcAB* was recently identified to be responsible for Hg methylation by microbes (Parks et al., 2013). The first gene, *hgcA*, encodes a corrinoid-using methyltransferase, and the second gene, *hgcB*, encodes a ferrodoxin protein that reduces the corrinoid center of *hgcA* (Parks et al., 2013). Microorganisms containing the gene pair are thought to exist in three clades: *Deltaproteobacteria*, *Archaea* and *Firmicutes* (Gilmour et al., 2013). In culture, *Deltaproteobacteria* produce more MMHg than either *Archaea* or *Firmicutes*, and organisms associated with sulfate- and iron-reduction, including *Clostridia* (*Firmicutes*), are more productive than organisms in other environments (Gilmour et al., 2013). Recent development of microbiological tools to screen for *hgcAB* in environmental samples has identified and quantified clade-specific *hgcA* (Christensen et al., 2016). Although primer degeneracy remains a problem, the primers correctly identified Hg methylating communities in rice paddy soils in China and showed that gene copy number of *Deltaproteobacteria* and *Archaea* increased with HgT and MMHg (Vishnivetskaya et al., 2018). In high altitude lakes, the *hgcAB* primers have identified sulfate reducers and methanogens as the microbes methylating Hg (Bouchet et al., 2018).

The primary objective of this study is to better understand Hg cycling in the water column of a eutrophic, dimictic lake. The objectives of this study were to: (1) measure

ambient Hg speciation throughout one year; (2) quantify Hg methylation and MMHg demethylation potentials in the entire water column using stable isotopes; and (3) characterize the Hg-methylating microbial community with clade-specific *hgcA* primers. The combination of chemical and microbial techniques will help disentangle how water chemistry and microbial communities contribute to MMHg prodcution throughout different biogeochemical regimes within the water column. Together, these tools better constrain in situ Hg methylation and cycling in the water column.

3.3 Materials and Methods

3.3.1. Site description

Crystal Lake is located in Medway Township, Clark County Ohio (39.8888 N, 84.0239 W; Figure 3.1). The lake has four interconnected basins and we collected water from the deepest part of the main and largest basin. The main basin has an area of about 0.073 km^2, a maximum depth of 11.6 m, and a mean depth of 3.8 m (Woodruff, 1999). A stream feeds the lake from the north, and discharges into the Mad River at the south end (Meyer, 2014). Crystal Lake is eutrophic and dimictic, where seasonal stratification leads to oxygen depletion and sulfide accumulation in the hypolimnion. Low-oxygen conditions in the hypolimnion are thought to promote Hg methylation when sulfide concentrations are low (Eckley et al., 2005; Eckley and Hintelmann, 2006; Watras et al., 1995).

3.3.2. Water sampling

Water was sampled monthly from Crystal Lake from May through October of 2016, and January, March, April, and May of 2017. Sampling depths were identified from profiles of O_2, turbidity, chlorophyll fluorescence, pH, and temperature measured with a multiparameter sonde (Manta2, Eureka Water Probes). We targeted the chlorophyll maximum, turbidity maximum, O_2 maximum and minimum, oxic-anoxic boundary, and anoxic bottom water. The latter three horizons have been hypothesized to be locations of Hg methylation (Eckley et al., 2005; Eckley and Hintelmann, 2006; Herrin et al., 1998; Matilainen, 1995; Watras et al., 1995; Wollenberg and Peters, 2009). Water was sampled from depth with a peristaltic pump via acid-cleaned C-Flex^{TM} tubing attached to the sonde into two acid-cleaned, 2-L polycarbonate bottles, which were filled from the bottom to prevent degassing of dissolved Hg species (Lamborg et al., 2012). Samples were transported to Wright State University (WSU) in dark coolers.

Promptly after returning to WSU, water samples were subsampled for analysis of sulfide (40 mL) and total Hg (200 mL). Sulfide samples had no head space and were preserved with additions of KOH and zinc acetate (Standard Methods 4500-S^{2-}D). HgT samples were preserved by the addition of 0.4 mL BrCl (Bloom and Crecelius, 1983). One 2-L water sample per depth was subsampled and filtered with glass fiber filters for HgT (200 mL) and MMHg (1.5-L). Unfiltered samples were purged with ultra-high purity N_2 to collect DMHg and Hg^0 on Bond Elut and Au traps, respectively (Bowman and Hammerschmidt, 2011). After degassing, the same water samples were prepared for MMHg analysis by acidifying to 1% with trace-metal grade H_2SO_4 and stored for at least 12 hours before analysis.

During July, August and September of 2016, water was sampled for Hg methylation assays. Six 2-L samples were collected in polycarbonate bottles at depths of 1, 3, 6.5, 7.5, and 9 m, employing the same sampling method described above. Samples were amended with 10 pM $^{200}Hg^{2+}$ to quantify methylation potential of $CH_3{}^{200}Hg$, and 1 pM $CH_3{}^{201}Hg$ was added to measure demethylation. Amended water samples were suspended in bottles at the same depth from which the water was collected. A set of triplicates incubated for 4 hours, and the other for 24 hours. At the end of the incubation period, samples were amended with 1 pM $CH_3{}^{199}Hg$ for analysis by isotope dilution (Hintelmann and Evans, 1997) and acidified to 1% with H_2SO_4 to prevent further biological transformation of Hg.

In the field, water was sampled for DNA extraction from the same depths as water for Hg methylation assays. Microbes and associated DNA were preconcentrated on Sterivex filters (0.22 μm, Millipore). The volume of water passed through the filters ranged from 120 to 240 mL. Filters were preserved with RNAlater® (Invitrogen) and stored at −80 °C until extraction (Hampel et al., 2018).

3.3.3. Mercury analysis

Gaseous Hg species (DMHg and Hg^0) were purged and analyzed within four hours after sampling. Unfiltered samples were purged with Hg-free N_2 gas to quantitatively strip gaseous Hg species. Bond Elut ENV (Agilent) traps were placed upstream of Au traps for collection of DMHg and Hg^0, respectively (Baya et al., 2013; Bloom and Fitzgerald, 1988; Bowman et al., 2016). Dimethylmercury was analyzed by gas chromatographic cold vapor atomic fluorescence spectrometry (GC-CVAFS; Bowman and Hammerschmidt, 2011). Elemental Hg was quantified by dual Au-

amalgamation CVAFS (Bloom and Fitzgerald, 1988). Sample concentrations were calibrated against aqueous Hg (II) standards traceable to U.S. National Institute of Standards and Technology. The method detection limit was 0.03 pM.

Total mercury samples were oxidized with BrCl (Bloom and Crecelius, 1983) for >12 hours, neutralized with NH_2OH, reduced with $SNCl_2$, and analyzed via dual Au-amalgamation CVAFS (Fitzgerald and Gill, 1979; Bloom and Fitzgerald, 1988). Calibration was performed with aqueous Hg (II) standards traceable to U.S. National Institute of Standards and Technology. The method detection limit was 0.07 pM. Reproducibility between duplicates averaged 5 ± 1% RPD (± 1 SE; n = 19).

Water samples for MMHg analysis were acidified to 1% with H_2SO_4 for at least 12 hours, purged with air to remove H_2S, buffered to a pH of 4.9 and ethylated with sodium tetraethylborate, purged with high-purity N_2, and analyzed via CVAFS (Bowman and Hammerschmidt, 2011). Measurements were calibrated against aqueous CH_3HgCl standards that were calibrated versus TORT-2 reference material (lobster hepatopancreas, National Research Council of Canada). Analytical precision between duplicates of unfiltered water was 9 ± 4% RPD (n = 3), and the method detection limit was 0.02 pM.

Water samples amended with Hg isotopes were acidified to 1% with sulfuric acid for at least 12 hours immediately after incubation. Acidified samples from 7.5 and 9 m were purged with air to either volatilize or oxidize H_2S to improve MMHg recovery (Bowman and Hammerschmidt, 2011). Samples were buffered, ethylated, and purged onto Tenax traps and analyzed via isotope-dilution gas chromatography inductively coupled plasma mass-spectrometry (Perkin Elmer Elan 9000; Hintelmann et al., 1995; Hintelmann and Evans, 1997). Mercury isotope recovery was calculated as described by

Hintelmann and Evans (1997), and the detection limit for formed $MM^{200}Hg$ was 0.01 pM. Methylation potentials were calculated as described by Eckley et al. (2005) and are reported as percentage of added ^{200}Hg transformed into $CH_3{}^{200}Hg$ during the 24 hour incubation period. The detection limit for $MM^{201}Hg$ demethylation is constrained by the error associated with the isotopic addition technique, which was 4%, or 0.11 pM.

3.3.4. Sulfide analysis

Water was analyzed spectrophotometrically for sulfide (Standard Methods 4500-S^{S2-}D). The method detection limit for sulfide analysis was 0.051 μM, and precision between duplicate samples averaged 4 ± 3% RPD (n = 7).

3.3.5. Quantitative polymerase chain reaction analysis

DNA was extracted from Sterivex filters before quantification of *hgcA* via quantitative polymerase chain reaction (qPCR). The filters were washed with phosphate buffer to remove residual RNAlater, and genomic material was extracted with the Puregene® Core Kit A (Qiagen) with some modifications (Hampel et al., 2018; Newell et al., 2011). Sterivex filters were rinsed with phosphate buffered saline 1X solution, and 0.9 mL lysis buffer and 4 μL Proteinase K was added prior to incubation for one hour each at 55 and 65 °C. The extraction solution was removed and new aliquots of lysis buffer and Proteinase K were added prior to repeating the incubation (Hampel et al., 2018). The purity and mass of DNA extracted was quantified spectrophotometrically (NanoDrop ND 2000, Thermo Scientific). Samples were screened for *hgcAB* with broad range primers for polymerase chain reaction (PCR; Table 3.1; Christensen et al., 2016). After confirming the presence of hgc*AB*, qPCR standards were prepared for each clade from respective *hgcA* fragments cut from an agarose gel and cleaned with Wizard® SV

Gel & PCR Clean-Up System (Promega). Cleaned *hgcA* fragments were cloned with TOPO™ TA Cloning Kit (Invitrogen), and assimilated into a cell plasmid (One Shot™, Invitrogen). The plasmids containing *hgcA* were isolated with the UltraClean® Standard Mini Plasmid Prep Kit (Mo Bio Laboratories Inc.).

Sample assays included all samples to minimize set-to-set differentiation between analyses (Smith et al., 2006). Each assay contained three no template controls (NTC) and triplicate standards and samples containing 0.05–20 ng of DNA. Standards were prepared from serial dilutions of the isolated plasmid and ranged in efficiency from 95 to 110%, with R^2 values greater than 0.98. The *Archaea* primer efficiency was 71%, which was similar to the reported primer efficiency of the organism (*Methanomethylovorans hollandica*), 73% (Christensen et al., 2016). The qPCR amplification mixture contained Luna® qPCR Mastermix (NEB Labs). Christiansen et al.'s qPCR protocols (2016) were optimized for sample and primer concentration and denaturation, annealing, and extension times (Table 3.2). The NTC was not detected throughout the 50 cycles of the *Deltaproteobacteria* or *Firmicutes* assays. For the *Archaea* assay the number of cycles was increased to 50 (Lam et al., 2007). The NTC was detected five cycles after the lowest standard, at cycle 45. All analyses were followed by a melting curve, and single curves were observed to ensure formation of one product. Automatic settings on the thermocycler (Eppendorf Realplex) determined the threshold cycle value. Gene abundance was calculated by multiplying the quantity of DNA in the sample (ng) by Avogadro's number, and dividing it by the number of base pairs (bp) in the fragment multiplied by average mass of a DNA fragment.

$$Gene\ abundance = \frac{ng \cdot 6.0221\times10^{23}\frac{molecules}{mol}}{bp \cdot 10^{9}\frac{ng}{g} \cdot 650\frac{g}{mol}} \quad (1)$$

Gene abundance was normalized to sample volume, assuming 100% extraction efficiency. Based on the lowest standard concentration required to bracket *hgcA* concentrations within these environmental samples, assay detection limits (not method detection limits) for *Deltaproteobacteria* was 55100 copies mL^{-1}, 19700 copies mL^{-1} for *Firmicutes*, and 1.3×10^{10} copies mL^{-1} for *Archaea*. Assay detection limits for *Deltaproteobacteria* and *Firmicutes* are similar to literature values (Christensen et al., 2016) and less than half of the number of copies of the lowest standards. The calculated *Archaea* detection limit is higher due to the high concentration of archaeal *hgcA* detected throughout sampling events at this site.

3.4. Results and Discussion

3.4.1. Water chemistry

Crystal Lake was seasonally stratified with an anoxic hypolimnion through the spring, summer, and early fall. After fall turnover, the hypolimnion remained fully oxygenated until early spring (Figure 3.2 A). Throughout the summer the thermocline was centered at 5 m (Figure 3.2 B). Summer chlorophyll profiles had two subsurface maxima, at 3 and 6.5 m. The lake's pH ranged from 7 to 9, with lower pH values in the hypolimnion during stratification. In the summer, higher pH values coincided with subsurface chlorophyll maximums. Subsurface oxygen maxima coincided with chlorophyll and pH maxima at 3 and 6.5 m, which is biogeochemically consistent with increased photosynthesis at these depths (Figure 3.3). Turbidity profiles had surface

maxima, a mid-depth maximum at about 6.5 m, and increased over the benthos. The oxycline migrated up the water column throughout the summer. The 6.5 to 7.5 m depth marks the oxic-anoxic (O/A) boundary.

Sulfide concentrations in the hypolimnion increased from spring to summer until fall turnover (Figure 3.2 C). Hypolimnetic sulfide concentrations were below detection limit during winter until mid-spring. As the summer progressed and sulfide levels increased; quantifiable sulfide increased up the water column and was detected at shallower depths than the preceding months. While the majority of sulfide formation likely occurs in the sediment, as sulfate reduction is 10^3 times greater in sediments than the water column (Ingvorsen et al., 1981), sulfate reduction in the water column likely occurs throughout the spring and summer as the anoxic hypolimnion migrates up the water column (Eckley and Hintelmann, 2006).

3.4.2. Ambient Hg concentrations

Unfiltered HgT averaged 5.4 ± 0.43 pM (± 1 SE; *n* =74) throughout the water column during all sampling periods (Figure 3.4 A). This average is less than unfiltered HgT in many Wisconsin lakes (mean of 7.4 pM; Watras et al., 1995) and lakes in New York (5–25 pM; Driscoll et al., 1994). HgT in the upper 6 m of the lake was relatively constant, with a maximum in the O/A transition zone, and above the benthos, aligning with the turbidity maximum. The similarity between unfiltered HgT and turbidity suggests that HgT concentrations are associated with suspended particles (Figure 3.5). In estuarine and riverine systems, total suspended solids and turbidity was correlated to unfiltered HgT (Balcom et al., 2008; Conaway et al., 2003; Riscassi et al., 2011; Schoellhamer et al., 2007). To our knowledge, this relationship has only been addressed

in shallow lakes (< 1 m) or surface waters with respect to inflow from the watershed (Bloom et al., 2004; Mastrine et al., 1999; Watras et al., 1995), and not throughout the vertical water column. Particulate and filtered HgT maxima coincided, further suggesting particulate matter is an important phase of HgT. Dissolution, remineralization, or changing redox conditions may release particle bound HgT into surrounding waters (Chadwick et al., 2013; Rolfhus et al., 2003). Particulate matter increased in the O/A transition zone, which is likely explained by the presence of *Planktothrix rubescens*, cyanobacteria that make the toxin microcystin, during summer stratification (Meyer, 2014). Particulate Hg may also be supplied to the O/A transition zone from shallow sediment surrounding the relatively deep sampling location. Horizontal transport may be a source of HgT to *P. rubescens* and the lower water column.

Filtered HgT profiles were not collected throughout the sampling period due to contamination of some filtration methods. We tried filtering water with Sterivex filters (0.22 μm), Meissner filters (0.45 μm) with Barnstead attachments (0.2 μm), and in-line 0.7 μm GFF filters. The aforementioned filtration methods yielded contaminated blanks and filtered HgT concentrations were greater than unfiltered HgT. We think samples were contaminated with Hg-sulfides that dissolved during filtration. Vacuum filtration with glass fiber filters was the only method that did not yield contaminated samples, as indicated by blanks. Thus, April and May 2017 were the only months we collected non-contaminated filtered HgT data. For April and May, filtered HgT averaged 3.7 ± 0.53 pM (n =16), or 68 ± 20% of unfiltered HgT. Filtered HgT profiles exhibited a shallower subsurface maximum than the O/A boundary, around 4 to 5 m, and increased near the sediments similar to unfiltered HgT. These profiles suggest HgT is remobilized from the

sediments, and there is likely a mid-depth source of HgT that is transported laterally from the surrounding shallow sediments. Hg may efflux from the sediments around the maximum depth, leading to a mid-profile maximum, or scavenging within the community of organisms at the O/A boundary recycles particulate Hg.

The distribution of Hg^0 averaged 0.14 ± 0.04 pM (n =74) in Crystal Lake (Figure 3.4 B), and are comparable to reported ranges for Hg^0 in lakes (Siciliano et al., 2002; Tseng et al., 2004; Vandal et al., 1991). As illustrated, Hg^0 levels were low at the surface, with either a singular epilimnetic maximum or two maxima during the summer months. Throughout the entire year, Hg^0 decreased to below the detection limit in the hypolimnion. An exception to this profile was the sampling period in August, which had increased Hg^0 in the surface water, possibly due to rainfall during sampling. High concentrations of dissolved Hg^0 have been correlated to precipitation in oceans (Mason et al., 2017; Soerensen et al., 2014), and deposition is a dominant source of Hg to lacustrine surface water (Chen et al., 2016).

Subsurface Hg^0 maxima in the epilimnion co-occurred with chlorophyll maxima, suggesting photosynthesizers produce Hg^0 in surface waters (Mason et al., 1995; Poulain et al., 2004). It is also possible that epilimnetic communities reducing Hg^{2+} contain *merA*, bacterial mercuric reductase (Poulain et al., 2004; Schaefer et al., 2004), or some other unidentified biotic reduction. Assuming an average atmospheric Hg^0 concentration of 2 ng m^{-3} (Fitzgerald et al., 1991; Landis et al., 2002; Lyman and Gustin, 2008), and calculated Henry's law constants (Andersson et al., 2008), these subsurface maxima averaged 560 ± 180% Hg^0 saturation (range: 0 – 4,155%; as calculated in Vandal et al., 1991, and Andersson et al., 2008). Furthermore, we can extrapolate the flux of Hg^0 out of

Crystal Lake with a few assumptions. Average wind speeds for August and October 2016 were 3 and 4.3 m sec^{-1}, respectively (NWS, 2016). We estimate transfer velocity of 1.8 cm hr^{-1} for the summer (June, July, August) and 4.2 cm hr^{-1} for the spring/fall (March, April, May, September, October; Emerson, 1975; Wanninkhof et al., 1985; Fitzgerald et al., 1991), we estimate the flux of Hg^0 out of Crystal Lake to be 230 ± 110 pmol m^{-2} d^{-1} during the summer and 30 ± 50 pmol m^{-2} d^{-1} during the spring and fall. The flux is greatest during the summer, and the spring/fall flux encompasses zero, suggesting more Hg^0 is deposited from the atmosphere than evades from the lake during early spring and late fall. Assuming summer conditions persisted June through September, and spring and fall flux conditions were valid for the ice-free season of mid-February through May, and October through mid-December, the yearly flux of Hg^0 from Crystal Lake is 33 ± 3.4 nmol m^{-2} yr^{-1}. These saturation and flux estimates are slightly larger than, but in the same order of magnitude for lakes in Wisconsin (2–12 nmol m^{-2} yr^{-1}; Vandal et al., 1991) and Alaska (4–10 nmol m^{-2} yr^{-1}; Tseng et al., 2004), but greater than fluxes from Lake Ontario (0–46 pmol m^{-2} yr^{-1}; Poissant et al., 2000) and Canadian Arctic lakes (0.4–2.8 pmol m^{-2} yr^{-1}; Amyot et al., 1997).

Ambient unfiltered MMHg concentrations averaged 1.0 ± 0.15 pM (*n* =74; Figure 3.4 C). MMHg levels in Crystal Lake were comparable to other temperate lakes (0.34 – 3.1 pM; Driscoll et al., 1994; Fitzgerald et al., 1991; Verta and Matilainen, 1995), but higher than Lake Superior (0.008–0.064 pM; Rolfhus et al., 2003) and Arctic Lakes (0.05–0.315 pM; Hammerschmidt et al., 2006). Concentrations of MMHg were low in surface waters, with a maximum at the O/A boundary layer. Throughout much of the year MMHg was greatest in the O/A transition zone, except in the early spring (April and May

2017). A hypolimnetic MMHg maximum was only present in the spring prior to the accumulation of sulfide. In the summer and fall greater hypolimnetic sulfide concentrations prevented MMHg formation and accumulation, likely because Hg-S complexes prevented Hg methylation (Benoit et al., 1999a, 1999b). MMHg concentrations in the spring were an order of magnitude greater than summer, fall, or winter (Figure 3.5 C). Filtered MMHg for the months of April and May 2017 averaged 0.76 ± 0.23 pM (*n* =16). Similar to filtered HgT, filtered MMHg profiles had shallower subsurface maxima than the unfiltered species, but maxima for particulate MMHg and unfiltered MMHg coincided. Unfiltered, filtered, and particulate MMHg increased near the water-sediment interface, indicating the sediments are a source of MMHg to the hypolimnion.

As sulfide increased in the hypolimnion from spring to summer, and MMHg concentrations decreased. When sulfide concentrations exceeded 100 μM, MMHg was not detected in the hypolimnion, likely due to sulfidic complexes forming with Hg(II). Hg-S complexes prevent cellular uptake of Hg, inhibiting MMHg formation (Benoit et al., 1999a, 1999b; Eckley and Hintelmann, 2006; Gilmour et al., 2018). This may explain why MMHg concentrations increased in the O/A boundary layer as the summer progressed. The O/A boundary did not have sulfidic concentrations great enough to prevent biotic methylation.

No DMHg was detected at any depth throughout the duration of the study. Few measurements of DMHg in freshwater lakes have been reported (Bloom and Effler, 1990; Vandal et al., 1991). Recent work in the Arctic Ocean suggests that DMHg is inversely

related to meteoric water (Agather et al., in review), which may indicate that DMHg is unlikely to be found in shallow, well mixed lakes.

3.4.3. Mercury transformation assays

Mercury methylation potentials in Crystal Lake ranged from 0.1 to 10.1% d^{-1} in the summer and fall (Table 3.3). Methylation potentials were low in the epilimnion and metalimnion, and greatest in the hypolimnion. In July and September, there was no increase in methylation rate at the O/A boundary. But in August, the methylation potential increased at the O/A boundary. Across all months, methylation potentials in the hypolimnion were not significantly different than in the epilimnion and metalimnion (One-way ANOVA, $p = 0.406$). Epilimnion incubations at 1 and 3 m had greater methylation potentials in September than either July or August. This might be due to an increase in particulate matter in the epilimnion during the month of September. Marine particles may provide localized anaerobic environments conducive to metal cycling (Bianchi et al., 2018), and it is thus possible that the measured methylation in the epilimnion occurs within particulate matter.

Methylation potentials decreased in the hypolimnion from August to September. This may be a result of the increase in sulfide forming Hg-S complexes that cannot be taken up by biotic methylators (Benoit et al., 1999a, 1999b; Eckley and Hintelmann, 2006; Gilmour et al., 2018). An increase in sulfide at 7.5 and 9 m over the incubation period may explain the low recovery of methylation assay replicates. As opposed to previous lacustrine methylation studies with lower benthic sulfide concentrations (Eckley et al., 2005; Eckley and Hintelmann, 2006), Crystal Lake's hypolimnetic sulfide levels may make measurements difficult to quantify. In July, August, and September, sulfide

levels in the hypolimnion exceeded 150 μM. We suspect much of the Hg to be bound in disulfide complexes due to the high pH of the hypolimnion and sulfide concentrations. The formation of Hg-S compounds prevents passive uptake of Hg across cell membranes, which reduces or eliminates the possibility biotic methylation (Benoit et al., 1999b).

Throughout the transformation assays, most incubation samples increased $MM^{200}Hg$ concentrations over the 24 hour study, suggesting sustained linear methylation (Eckley et al., 2005; Eckley and Hintelmann, 2006; Lehnherr et al., 2011). The exception was the 6.5 m sample in September, where $MM^{200}Hg$ decreased between the 4 and 24 hour incubation, but all other incubation periods exhibited increased $MM^{200}Hg$ concentration. The decrease in $MM^{200}Hg$ at 6.5 m in September may reflect an imbalance between methylation and demethylation, where demethylation proceeded at a much greater rate than methylation, or methyl groups may have become depleted over the 24 hour incubation period. There is also the possibility of changing microbial community composition, or the depletion of available substrate or other integral components for biotic methylation. While Eckley and colleagues (2005) did not find altered bacterial communities over an incubation period of 25 hours, further research is needed for 24 hour incubations with specific focus on microbial communities with *hgcAB*.

Previous research identified late summer and early fall as the most productive time for Hg methylation in lakes (Eckley and Hintelmann, 2006), and our data supports summer and early fall as important times for Hg methylation in Crystal Lake. Hg methylation potentials at all depths increased from July to August, and in September epilimnion potentials increased, while metalimnion and hypolimnion potentials decreased. The epilimnetic increase may be due to methylation in the redox

microenvironments of particles (Bianchi et al., 2018). Another possibility is the vertical migration of the O/A boundary. In September, the water column was anoxic at 5 m, shallower than any other month studied. This vertical migration of the oxycline, O/A boundary, and anoxic water may impact methylation in the upper water column. As anoxic water and sulfide vertically migrate, methylation horizons may change and therefore methylation assays should be conducted at more frequent intervals throughout the water column, focusing specifically on the O/A boundary. We did not measure Hg methylation potentials because past research was unable to quantify methylation after fall turnover (Eckley et al., 2005). Mixing likely reduces water column methylation due to the re-oxidiation of the hypolimnion, likely removing ideal methylating conditions.

Demethylation potentials, measured as a decrease in $MM^{201}Hg$, were below detection limit (4%) at all depths for July, August, and September. Therefore, we assume a maximum demethylation potential of <5% per day (Eckley and Hintelmann, 2006). The average hypolimnion methylation potential, $5 \pm 3\%\ d^{-1}$, is statistically indistinguishable from the maximum possible demethylation potential. The mean methylation potential for the epilimnion, $0.9 \pm 0.4\ \%\ d^{-1}$, is slightly greater than, but not significantly different from, the potential we measured for the O/A boundary, $0.4 \pm 0.1\ \%\ d^{-1}$. The epilimnetic average is disproportionately weighted by the high methylation potential measured for September. Shallow sediments may produce MMHg which effluxes into overlying waters before surface waters are homogenized throughout the upper water column by wind driven mixing.

3.4.4. Genetic analyses

Bacterial and archaeal *hgcA* DNA was detected at all depths in Crystal Lake (Figure 3.6). Each of the three clades known to methylate Hg were present in water column samples (Table 3.3). At all depths, *Archaeal hgcA* copy numbers were greater than those associated with *Deltaproteobacteria*, which were greater than *Firmicutes hgcA* gene copy numbers. The abundance of *hgcA* genes was greater in the anoxic hypolimnion, which is consistent with past hypotheses that aquatic methylation mostly occurs in the anoxic hypolimnion (Eckley et al., 2005; Eckley and Hintelmann, 2006; Matilainen, 1995; Verta and Matilainen, 1995; Watras et al., 1995). Sulfate reducing bacteria (*Deltaproteobacteria*) and methanogens (*Archaea*) can live together syntrophically, which may occur in the hypolimnion. Metabolic interdependence between microorganisms transfers formate, acetate, and H_2 (Pak and Bartha, 1998; Vishnivetskaya et al., 2018), providing electrons and substrates to both species for MMHg production.

hgcA gene copies were less abundant in the epilimnion, and primarily consisted of *Archaea*. The presence of *hgcA*, mostly as *Archaea*, and measureable methylation rates, suggests that bioactive Hg methylation may occur in the oxic water column of Crystal Lake. *Archaea* dominates as the primary Hg methylator where iron and sulfide are not readily available (Gilmour et al., 2013), which is likely the case in the epilimnion. More *hgcA* copies were detected in surface water in September than August, coinciding with the increase in methylation potential at that depth compared to both July and August.

Methylation potentials did not significantly correlate with *hgcA* gene copy numbers (Table 3.4). *Firmicutes* gene copy number had the highest correlation with methylation potential (0.704), while *Deltaproteobacteria* gene copy number had a weak

negative correlation with methylation potential (−0.237), and *Archaea* gene copy number had a slight positive correlation (0.247). These correlation coefficients suggest that the detection and quantification of *hgcA* gene copies is not sufficient to indicate active methylation, but together with methylation potentials can better describe in-situ Hg cycling. Had we measured RNA rather than DNA, gene copy numbers may have been better predictors of Hg methylation potential. Regardless, similar conclusions have been drawn in lab experiments with methylation in sediments, and suggesting that Hg bioavailability might be a better indicator of methylation potential than gene abundance (Ndu et al., 2018).

As previously mentioned, *Archaeal hgcA* copy numbers were greater than either *Deltaproteobacteria* or *Firmicutes hgcA* gene copy numbers at all depths. Artificial inflation of *Archaea hgcA* gene copies is reported as a flaw of the primer set, because the primers can isolate and form two products (Christensen et al., 2016). However, under our optimized protocol, we observed a single curve in the melting curve, suggesting the formation of a singular product. Genetic sequencing of *hgcA* needs to be performed to confirm the product is *hgcA*, and indicate if the cells are known methylators. Sequencing will better describe the Hg methylating community within the lake.

hgcA abundance was greatest in the hypolimnion just above the sediment, suggesting that sediments may be a source of *hgcA* to the lower water column. If microbes containing *hgcA* come from the sediment, it is possible that as summer and fall progress, anaerobic microbes may migrate out of sediments as the anoxic layer expands. *Deltaproteobacteria* gene copies increased from August to September, suggesting sediments may be a source of *Deltaproteobacteria* to the hypolimnion. Vertical

migration from anoxic hypolimnetic waters to the oxic epilimnion is unlikely due to lake stratification and because many of the methylators are anaerobes (Gilmour et al., 2013; Podar et al., 2015).

We hypothesize that geochemical parameters, specifically sulfide concentrations, restrict and regulate MMHg formation in Crystal Lake. Gene presence and abundance supports Hg methylation potentials, but do not fully describe methylation trends. We measured methylation and detected *Archaeal hgcA* in oxic waters, suggesting an alternative method for oxic Hg methylation as opposed to methylation in particle transition zones (Bianchi et al., 2018). The anoxic hypolimnion supported the majority of microbial methylators, suggesting that in stratified eutrophic lakes, anoxic bottom water allows bacterial communities with *hgcAB* to flourish in the water column. More in situ work is necessary to determine regime limitations, and ideal conditions for these communities. Additionally, future work should include demethylation genes (*merB*) and their abundances in the water column, both in the epilimnion and hypolimnion, and demethylation should be measured with isotopically labeled carbon.

3.5. Acknowledgments

We thank Kortney Mullen, Kelly Muterspaw, Dane Boring, Ashley Livingston, Ngocminh Truong and Kayla Haman for help in the field and lab. We thank Katlin Bowman, Justyna Hampel, Benjamin Peterson, Desi Niewinski, Daniel Hoffman, and Megan Reed for help with microbiological protocols.

3.6. References

Agather, A.M., Bowman, K.L, Lamborg, C.H., Hammerschmidt, C.R. Distribution of mercury species in the Western Arctic Ocean (U.S. GEOTRACES GN01). *In review*.

Amyot, M., Lean, D., Mierle, G., 1997. Photochemical Formation of volatile mercury in high Arctic lakes. Environ. Toxicol. Chem. 16, 2054–2063. https://doi.org/10.1002/etc.5620161010

Andersson, M.E., Sommar, J., Gårdfeldt, K., Lindqvist, O., 2008. Enhanced concentrations of dissolved gaseous mercury in the surface waters of the Arctic Ocean. Mar. Chem. 110, 190–194. https://doi.org/10.1016/j.marchem.2008.04.002

Balcom, P.H., Hammerschmidt, C.R., Fitzgerald, W.F., Lamborg, C.H., O'Connor, J.S., 2008. Seasonal distributions and cycling of mercury and methylmercury in the waters of New York/New Jersey Harbor Estuary. Mar. Chem. 109, 1–17. https://doi.org/10.1016/j.marchem.2007.09.005

Baya, P.A., Hollinsworth, J.L., Hintelmann, H., 2013. Evaluation and optimization of solid adsorbents for the sampling of gaseous methylated mercury species. Anal. Chim. Acta 786, 61–69. https://doi.org/10.1016/j.aca.2013.05.019

Benoit, J.M., Gilmour, C.C., Mason, R.P., Heyes, A., 1999a. Sulfide Controls on Mercury Speciation and Bioavailability to Methylating Bacteria in Sediment Pore Waters. Environ. Sci. Technol. 33, 951–957. https://doi.org/10.1021/es9808200

Benoit, J.M., Mason, R.P., Gilmour, C.C., 1999b. Estimation of mercury-sulfide speciation in sediment pore waters using octanol-water partitioning and implications for availability to methylating bacteria. Environ. Toxicol. Chem. 18, 2138–2141. https://doi.org/10.1002/etc.5620181004

Bianchi, D., Weber, T.S., Kiko, R., Deutsch, C., 2018. Global niche of marine anaerobic metabolisms expanded by particle microenvironments. Nat. Geosci. https://doi.org/10.1038/s41561-018-0081-0

Bloom, N., Fitzgerald, W.F., 1988. Determination of volatile mercury species at the picogram level by low-temperature gas chromatography with cold-vapour atomic fluorescence detection. Anal. Chim. Acta 208, 151–161. https://doi.org/10.1016/S0003-2670(00)80743-6

Bloom, N.S., Crecelius, E.A., 1983. Determination of mercury in seawater at sub-nanogram per liter levels. Mar. Chem. 14, 49–59. https://doi.org/10.1016/0304-4203(83)90069-5

Bloom, N.S., Effler, S.W., 1990. Seasonal variability in the Mercury speciation of Onondaga Lake (New York). Water. Air. Soil Pollut. 53, 251–265. https://doi.org/10.1007/BF00170741

Bloom, N.S., Moretto, L.M., Scopece, P., Ugo, P., 2004. Seasonal cycling of mercury and monomethyl mercury in the Venice Lagoon (Italy). Mar. Chem. 91, 85–99. https://doi.org/10.1016/j.marchem.2004.06.002

Bouchet, S., Goñi-Urriza, M., Monperrus, M., Guyoneaud, R., Fernandez, P., Heredia, C., Tessier, E., Gassie, C., Point, D., Guédron, S., Achá, D., Amouroux, D., 2018. Linking Microbial Activities and Low-Molecular-Weight Thiols to Hg Methylation in Biofilms and Periphyton from High-Altitude Tropical Lakes in the

Bolivian Altiplano. Environ. Sci. Technol. 52, 9758–9767. https://doi.org/10.1021/acs.est.8b01885
Bowman, K.L., Hammerschmidt, C.R., 2011. Extraction of monomethylmercury from seawater for low-femtomolar determination. Limnol. Oceanogr. Methods 9, 121–128. https://doi.org/10.4319/lom.2011.9.121
Bowman, K.L., Hammerschmidt, C.R., Lamborg, C.H., Swarr, G.J., Agather, A.M., 2016. Distribution of mercury species across a zonal section of the eastern tropical South Pacific Ocean (U.S. GEOTRACES GP16). Mar. Chem. 186, 156–166. https://doi.org/10.1016/j.marchem.2016.09.005
Chadwick, S.P., Babiarz, C.L., Hurley, J.P., Armstrong, D.E., 2013. Importance of hypolimnetic cycling in aging of "new" mercury in a northern temperate lake. Sci. Total Environ., Atmospheric Mercury, Air Pollution, and Associated Effects on Health: A Festschrift to Professor Jerry Keeler. 448, 176–188. https://doi.org/10.1016/j.scitotenv.2012.10.069
Chen, J., Hintelmann, H., Zheng, W., Feng, X., Cai, H., Wang, Zhuhong, Yuan, S., Wang, Zhongwei, 2016. Isotopic evidence for distinct sources of mercury in lake waters and sediments. Chem. Geol. 426, 33–44. https://doi.org/10.1016/j.chemgeo.2016.01.030
Christensen, G.A., Wymore, A.M., King, A.J., Podar, M., Hurt, R.A., Santillan, E.U., Soren, A., Brandt, C.C., Brown, S.D., Palumbo, A.V., Wall, J.D., Gilmour, C.C., Elias, D.A., 2016. Development and Validation of Broad-Range Qualitative and Clade-Specific Quantitative Molecular Probes for Assessing Mercury Methylation in the Environment. Appl. Environ. Microbiol. 82, 6068–6078. https://doi.org/10.1128/AEM.01271-16
Conaway, C.H., Squire, S., Mason, R.P., Flegal, A.R., 2003. Mercury speciation in the San Francisco Bay estuary. Mar. Chem. 80, 199–225. https://doi.org/10.1016/S0304-4203(02)00135-4
Driscoll, C., VAN, C., SCHOFIELD, C.L., MUNSON, R., HOLSAPPLE, J., 1994. THE MERCURY CYCLE AND FISH IN THE ADIRONDACK LAKES. Environ. Sci. Technol. 28, 136A-143A. https://doi.org/10.1021/es00052a721
Eckley, C.S., Hintelmann, H., 2006. Determination of mercury methylation potentials in the water column of lakes across Canada. Sci. Total Environ. 368, 111–125. https://doi.org/10.1016/j.scitotenv.2005.09.042
Eckley, C.S., Watras, C.J., Hintelmann, H., Morrison, K., Kent, A.D., Regnell, O., 2005. Mercury methylation in the hypolimnetic waters of lakes with and without connection to wetlands in northern Wisconsin. Can. J. Fish. Aquat. Sci. 62, 400–411. https://doi.org/10.1139/F04-205
Emerson, 1975. Gas exchange rates in small Canadian Shield lakes1 - Emerson - 1975 - Limnology and Oceanography - Wiley Online Library.
Fitzgerald, W.F., Engstrom, D.R., Mason, R.P., Nater, E.A., 1998. The Case for Atmospheric Mercury Contamination in Remote Areas. Environ. Sci. Technol. 32, 1–7. https://doi.org/10.1021/es970284w
Fitzgerald, W.F., Gill, G.A., 1979. Subnanogram determination of mercury by two-stage gold amalgamation and gas phase detection applied to atmospheric analysis. Anal. Chem. 51, 1714–1720. https://doi.org/10.1021/ac50047a030

Fitzgerald, W.F., Mason, R.P., Vandal, G.M., 1991. Atmospheric cycling and air-water exchange of mercury over mid-continental lacustrine regions. Water. Air. Soil Pollut. 56, 745–767. https://doi.org/10.1007/BF00342314

Gilmour, C.C., Bullock, A.L., McBurney, A., Podar, M., Elias, D.A., 2018. Robust Mercury Methylation across Diverse Methanogenic Archaea. mBio 9, e02403-17. https://doi.org/10.1128/mBio.02403-17

Gilmour, C.C., Henry, E.A., 1991. Mercury methylation in aquatic systems affected by acid deposition. Environ. Pollut. 71, 131–169. https://doi.org/10.1016/0269-7491(91)90031-Q

Gilmour, C.C., Henry, E.A., Mitchell, R., 1992. Sulfate stimulation of mercury methylation in freshwater sediments. Environ. Sci. Technol. 26, 2281–2287. https://doi.org/10.1021/es00035a029

Gilmour, C.C., Podar, M., Bullock, A.L., Graham, A.M., Brown, S.D., Somenahally, A.C., Johs, A., Hurt, R.A., Bailey, K.L., Elias, D.A., 2013. Mercury Methylation by Novel Microorganisms from New Environments. Environ. Sci. Technol. 47, 11810–11820. https://doi.org/10.1021/es403075t

Hammerschmidt, C.R., Fitzgerald, W.F., Lamborg, C.H., Balcom, P.H., Tseng, C.-M., 2006. Biogeochemical Cycling of Methylmercury in Lakes and Tundra Watersheds of Arctic Alaska. Environ. Sci. Technol. 40, 1204–1211. https://doi.org/10.1021/es051322b

Hampel, J.J., McCarthy, M.J., Gardner, W.S., Zhang, L., Xu, H., Zhu, G., Newell, S.E., 2018. Nitrification and ammonium dynamics in Taihu Lake, China: seasonal competition for ammonium between nitrifiers and cyanobacteria. Biogeosciences 15, 733–748. https://doi.org/10.5194/bg-15-733-2018

Herrin, R.T., Lathrop, R.C., Gorski, P.R., Andren, A.W., 1998. Hypolimnetic methylmercury and its uptake by plankton during fall destratification: A key entry point of mercury into lake food chains? Limnol. Oceanogr. 43, 1476–1486. https://doi.org/10.4319/lo.1998.43.7.1476

Hintelmann, H., Evans, R.D., 1997. Application of stable isotopes in environmental tracer studies – Measurement of monomethylmercury (CH3Hg+) by isotope dilution ICP-MS and detection of species transformation. Fresenius J. Anal. Chem. 358, 378–385. https://doi.org/10.1007/s002160050433

Hintelmann, H., Evans, R.D., Villeneuve, J.Y., 1995. Measurement of mercury methylation in sediments by using enriched stable mercury isotopes combined with methylmercury determination by gas chromatography–inductively coupled plasma mass spectrometry. J. Anal. At. Spectrom. 10, 619–624. https://doi.org/10.1039/JA9951000619

Horowitz, H.M., Jacob, D.J., Zhang, Y., Dibble, T.S., Slemr, F., Amos, H.M., Schmidt, J.A., Corbitt, E.S., Marais, E.A., Sunderland, E.M., 2017. A new mechanism for atmospheric mercury redox chemistry: implications for the global mercury budget. Atmospheric Chem. Phys. 17, 6353–6371. https://doi.org/10.5194/acp-17-6353-2017

Ingvorsen, K., Zeikus, J.G., Brock, T.D., 1981. Dynamics of Bacterial Sulfate Reduction in a Eutrophic Lake. Appl. Environ. Microbiol. 42, 1029–1036.

Johnsson, C., Sällsten, G., Schütz, A., Sjörs, A., Barregård, L., 2004. Hair mercury levels versus freshwater fish consumption in household members of Swedish angling societies. Environ. Res. 96, 257–263. https://doi.org/10.1016/j.envres.2004.01.005
Karagas, M.R., Choi, A.L., Oken, E., Horvat, M., Schoeny, R., Kamai, E., Cowell, W., Grandjean, P., Korrick, S., 2012. Evidence on the Human Health Effects of Low-Level Methylmercury Exposure. Environ. Health Perspect. 120, 799–806. https://doi.org/10.1289/ehp.1104494
Lam, P., Jensen, M.M., Lavik, G., McGinnis, D.F., Muller, B., Schubert, C.J., Amann, R., Thamdrup, B., Kuypers, M.M.M., 2007. Linking crenarchaeal and bacterial nitrification to anammox in the Black Sea. Proc. Natl. Acad. Sci. 104, 7104–7109. https://doi.org/10.1073/pnas.0611081104
Lamborg, C.H., Hammerschmidt, C.R., Gill, G.A., Mason, R.P., Gichuki, S., 2012. An intercomparison of procedures for the determination of total mercury in seawater and recommendations regarding mercury speciation during GEOTRACES cruises. Limnol. Oceanogr. Methods 10, 90–100. https://doi.org/10.4319/lom.2012.10.90
Landis, M.S., Vette, A.F., Keeler, G.J., 2002. Atmospheric Mercury in the Lake Michigan Basin: Influence of the Chicago/Gary Urban Area. Environ. Sci. Technol. 36, 4508–4517. https://doi.org/10.1021/es011216j
Lehnherr, I., Louis, V.L.S., Hintelmann, H., Kirk, J.L., 2011. Methylation of inorganic mercury in polar marine waters. Nat. Geosci. 4, 298–302. https://doi.org/10.1038/ngeo1134
Lyman, S.N., Gustin, M.S., 2008. Speciation of atmospheric mercury at two sites in northern Nevada, USA. Atmos. Environ. 42, 927–939. https://doi.org/10.1016/j.atmosenv.2007.10.012
Mason, R.P., Hammerschmidt, C.R., Lamborg, C.H., Bowman, K.L., Swarr, G.J., Shelley, R.U., 2017. The air-sea exchange of mercury in the low latitude Pacific and Atlantic Oceans. Deep Sea Res. Part Oceanogr. Res. Pap. 122, 17–28. https://doi.org/10.1016/j.dsr.2017.01.015
Mason, R.P., Morel, F.M.M., Hemond, H.F., 1995. The role of microorganisms in elemental mercury formation in natural waters. Water. Air. Soil Pollut. 80, 775–787. https://doi.org/10.1007/BF01189729
Mastrine, J.A., Bonzongo, J.-C.J., Lyons, W.B., 1999. Mercury concentrations in surface waters from fluvial systems draining historical precious metals mining areas ink southeastern U.S.A. Appl. Geochem. 14, 147–158. https://doi.org/10.1016/S0883-2927(98)00043-2
Matilainen, T., 1995. Involvement of bacteria in methylmercury formation in anaerobic lake waters. Water. Air. Soil Pollut. 80, 757–764.
Mergler, D., Anderson, H.A., Chan, L.H.M., Mahaffey, K.R., Murray, M., Sakamoto, M., Stern, A.H., 2007. Methylmercury Exposure and Health Effects in Humans: A Worldwide Concern. AMBIO J. Hum. Environ. 36, 3–11. https://doi.org/10.1579/0044-7447(2007)36[3:MEAHEI]2.0.CO;2
Meyer, A. L., 2014. Biogeochemistry of sulfur isotopes in Crystal Lake, Clark County, West-Central Ohio. Wright State University.
Ndu, U., Christensen, G.A., Rivera, N.A., Gionfriddo, C.M., Deshusses, M.A., Elias, D.A., Hsu-Kim, H., 2018. Quantification of Mercury Bioavailability for

Methylation Using Diffusive Gradient in Thin-Film Samplers. Environ. Sci. Technol. 52, 8521–8529. https://doi.org/10.1021/acs.est.8b00647
Newell, S.E., Babbin, A.R., Jayakumar, A., Ward, B.B., 2011. Ammonia oxidation rates and nitrification in the Arabian Sea: Arabian Sea ammonia oxidation and nitrification. Glob. Biogeochem. Cycles 25, n/a-n/a. https://doi.org/10.1029/2010GB003940
NWS, 2016. National Weather Service Climate [WWW Document]. URL https://w2.weather.gov/climate/index.php?wfo=iln (accessed 12.7.18).
Pak, K.-R., Bartha, R., 1998. Mercury Methylation and Demethylation in Anoxic Lake Sediments and by Strictly Anaerobic Bacteria. Appl. Environ. Microbiol. 64, 1013–1017.
Parks, J.M., Johs, A., Podar, M., Bridou, R., Hurt, R.A., Smith, S.D., Tomanicek, S.J., Qian, Y., Brown, S.D., Brandt, C.C., Palumbo, A.V., Smith, J.C., Wall, J.D., Elias, D.A., Liang, L., 2013. The Genetic Basis for Bacterial Mercury Methylation. Science 339, 1332–1335. https://doi.org/10.1126/science.1230667
Podar, M., Gilmour, C.C., Brandt, C.C., Soren, A., Brown, S.D., Crable, B.R., Palumbo, A.V., Somenahally, A.C., Elias, D.A., 2015. Global prevalence and distribution of genes and microorganisms involved in mercury methylation. Sci. Adv. 1, e1500675. https://doi.org/10.1126/sciadv.1500675
Poissant, L., Amyot, M., Pilote, M., Lean, D., 2000. Mercury water−Air exchange over the Upper St. Lawrence River and Lake Ontario. Environ. Sci. Technol. 34, 3069–3078. https://doi.org/10.1021/es990719a
Poulain, A.J., Amyot M., Findlay D., Telor S., Barkay T., Hintelmann H., 2004. Biological and photochemical production of dissolved gaseous mercury in a boreal lake. Limnol. Oceanogr. 49, 2265–2275. https://doi.org/10.4319/lo.2004.49.6.2265
Riscassi, A.L., Hokanson, K.J., Scanlon, T.M., 2011. Streamwater Particulate Mercury and Suspended Sediment Dynamics in a Forested Headwater Catchment. Water. Air. Soil Pollut. 220, 23–36. https://doi.org/10.1007/s11270-010-0731-3
Rolfhus, K.R., Sakamoto, H.E., Cleckner, L.B., Stoor, R.W., Babiarz, C.L., Back, R.C., Manolopoulos, H., Hurley, J.P., 2003. Distribution and Fluxes of Total and Methylmercury in Lake Superior. Environ. Sci. Technol. 37, 865–872. https://doi.org/10.1021/es026065e
Schaefer, J.K., Yagi, J., Reinfelder, J.R., Cardona, T., Ellickson, K.M., Tel-Or, S., Barkay, T., 2004. Role of the Bacterial Organomercury Lyase (MerB) in Controlling Methylmercury Accumulation in Mercury-Contaminated Natural Waters. Environ. Sci. Technol. 38, 4304–4311. https://doi.org/10.1021/es049895w
Schoellhamer, D.H., Mumley, T.E., Leatherbarrow, J.E., 2007. Suspended sediment and sediment-associated contaminants in San Francisco Bay. Environ. Res., Pollutants in the San Francisco Bay Estuary 105, 119–131. https://doi.org/10.1016/j.envres.2007.02.002
Sheehan, M.C., Burke, T.A., Navas-Acien, A., Breysse, P.N., McGready, J., Fox, M.A., 2014. Global methylmercury exposure from seafood consumption and risk of developmental neurotoxicity: a systematic review. Bull. World Health Organ. 92, 254-269F. https://doi.org/10.2471/BLT.12.116152

Siciliano, S.D., O'Driscoll, N.J., Lean, D.R.S., 2002. Microbial Reduction and Oxidation of Mercury in Freshwater Lakes. Environ. Sci. Technol. 36, 3064–3068. https://doi.org/10.1021/es010774v

Slemr, F., Schuster, G., Seiler, W., 1985. Distribution, speciation, and budget of atmospheric mercury. J. Atmospheric Chem. 3, 407–434. https://doi.org/10.1007/BF00053870

Smith, C.J., Nedwell, D.B., Dong, L.F., Osborn, A.M., 2006. Evaluation of quantitative polymerase chain reaction-based approaches for determining gene copy and gene transcript numbers in environmental samples. Environ. Microbiol. 8, 804–815. https://doi.org/10.1111/j.1462-2920.2005.00963.x

Soerensen, A.L., Mason, R.P., Balcom, P.H., Jacob, D.J., Zhang, Y., Kuss, J., Sunderland, E.M., 2014. Elemental Mercury Concentrations and Fluxes in the Tropical Atmosphere and Ocean. Environ. Sci. Technol. 48, 11312–11319. https://doi.org/10.1021/es503109p

Tseng, C.M., Lamborg, C., Fitzgerald, W.F., Engstrom, D.R., 2004. Cycling of dissolved elemental mercury in Arctic Alaskan lakes. Geochim. Cosmochim. Acta 68, 1173–1184. https://doi.org/10.1016/j.gca.2003.07.023

Vandal, G.M., Mason, R.P., Fitzgerald, W.F., 1991. Cycling of volatile mercury in temperate lakes. Water. Air. Soil Pollut. 56, 791–803. https://doi.org/10.1007/BF00342317

Verta, M., Matilainen, T., 1995. Methylmercury distribution and partitioning in stratified Finnish forest lakes. Water. Air. Soil Pollut. 80, 585–588. https://doi.org/10.1007/BF01189710

Vishnivetskaya, T.A., Hu, H., Nostrand, J.D.V., Wymore, A.M., Xu, X., Qiu, G., Feng, X., Zhou, J., Brown, S.D., Brandt, C.C., Podar, M., Gu, B., Elias, D.A., 2018. Microbial community structure with trends in methylation gene diversity and abundance in mercury-contaminated rice paddy soils in Guizhou, China. Environ. Sci. Process. Impacts 20, 673–685. https://doi.org/10.1039/C7EM00558J

Wanninkhof, R., Ledwell, J.R., Broecker, W.S., 1985. Gas Exchange-Wind Speed Relation Measured with Sulfur Hexafluoride on a Lake. Science 227, 1224–1226. https://doi.org/10.1126/science.227.4691.1224

Watras, C. J., Bloom, N.S., Claas, S.A., Morrison, K.A., Gilmour, C.C., Craig, S.R., 1995. Methylmercury production in the anoxic hypolimnion of a Dimictic Seepage Lake. Water. Air. Soil Pollut. 80, 735–745. https://doi.org/10.1007/BF01189725

Watras, C. J., Morrison, K.A., Host, J.S., Bloom, N.S., 1995. Concentration of mercury species in relationship to other site-specific factors in the surface waters of northern Wisconsin lakes. Limnol. Oceanogr. 40, 556–565. https://doi.org/10.4319/lo.1995.40.3.0556

Wollenberg, J.L., Peters, S.C., 2009. Mercury emission from a temperate lake during autumn turnover. Sci. Total Environ. 407, 2909–2918. https://doi.org/10.1016/j.scitotenv.2008.12.017

Woodruff, M. E., 1999. Isotope geochemistry of oxygen, hydrogen and carbon in Crystal Lakes, Medway, Clark County, Ohio. Wright State University.

FIGURES

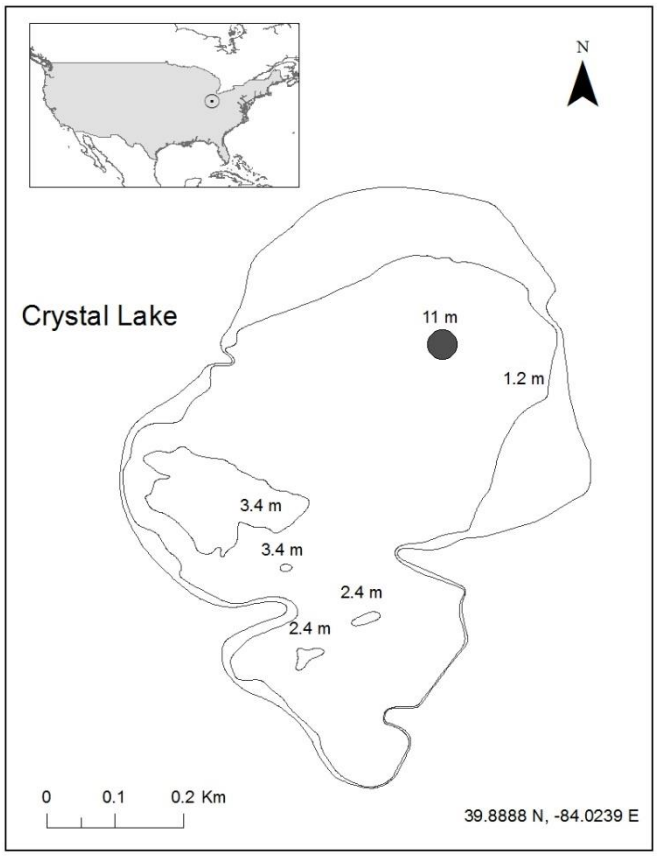

Figure 3.1. Map of the study location, Crystal Lake, Medway, Clark County, Ohio, USA. Circle designates the deepest part of the lake and sampling location.

A

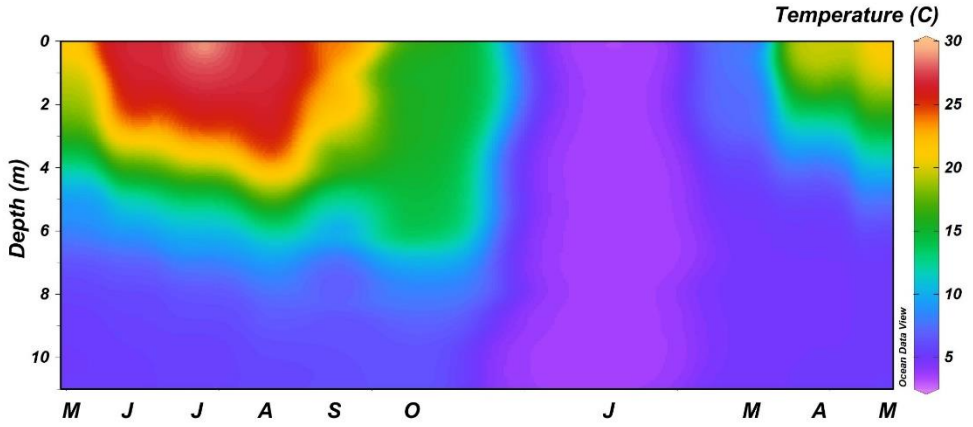
Temperature (C)
Depth (m)
0
2
4
6
8
10
M J J A S O J M A M
30
25
20
15
10
5
Ocean Data View

B

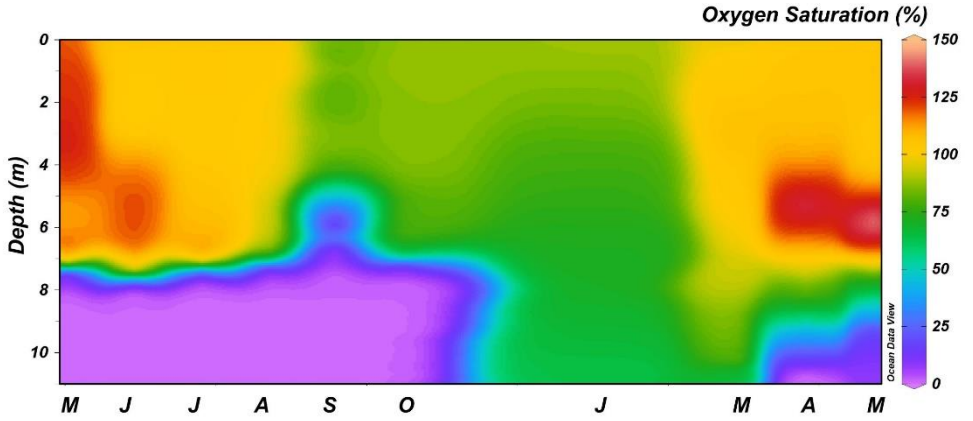
Oxygen Saturation (%)
Depth (m)
0
2
4
6
8
10
M J J A S O J M A M
150
125
100
75
50
25
0
Ocean Data View

C

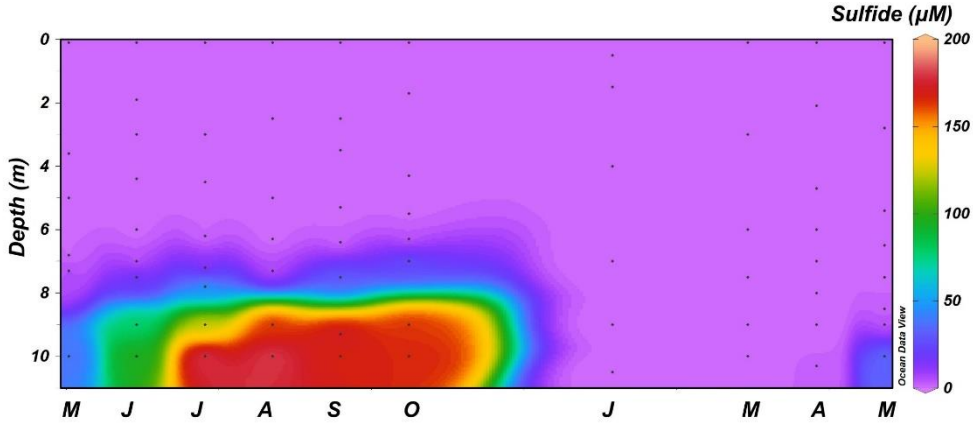
Sulfide (µM)
Depth (m)
0
2
4
6
8
10
M J J A S O J M A M
200
150
100
50
0
Ocean Data View

Figure 3.2. Depth-time diagrams of oxygen (A), temperature (B), and sulfide (C) in Crystal Lake from May 2016 through May 2017. Black dots in (C) indicate sampling depth, whereas data was collected throughout the entire vertical water column for oxygen (A) and temperature (B).

A

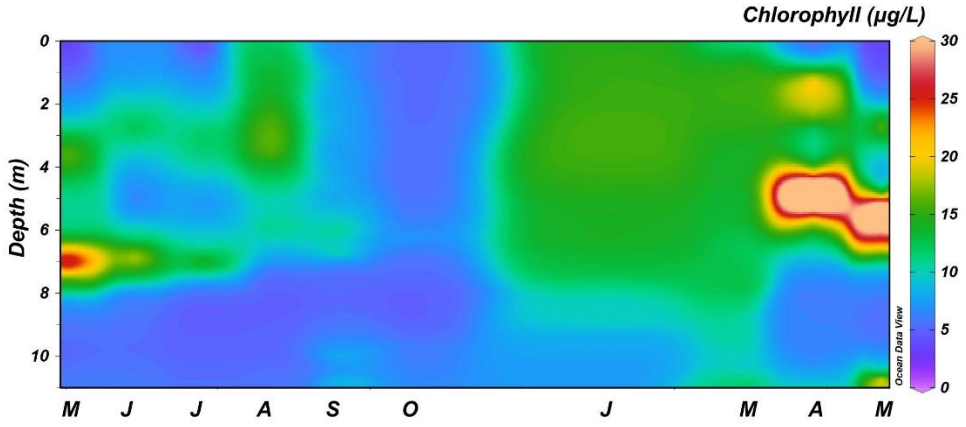

B

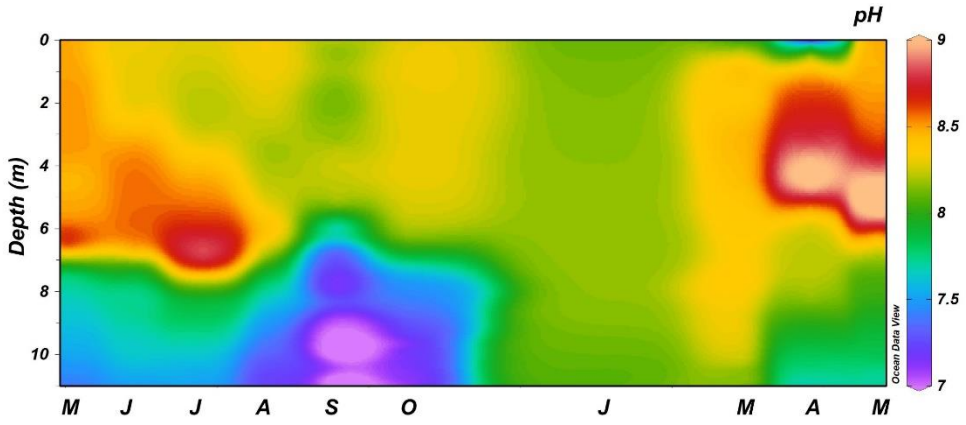

Figure 3.3. Depth-time diagrams of chlorophyll (A) and pH (B) for Crystal Lake, from May 2016 through May 2017.

A

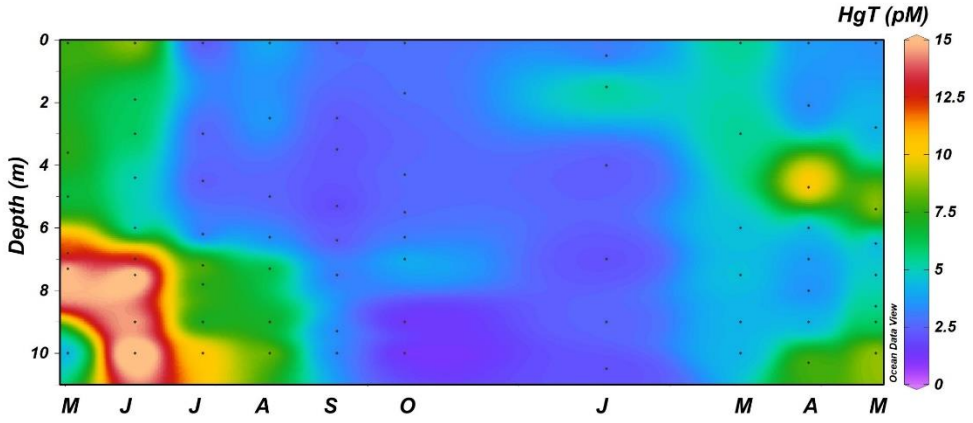
HgT (pM)
Depth (m)
0
2
4
6
8
10
M J J A S O J M A M
15
12.5
10
7.5
5
2.5
0
Ocean Data View

B

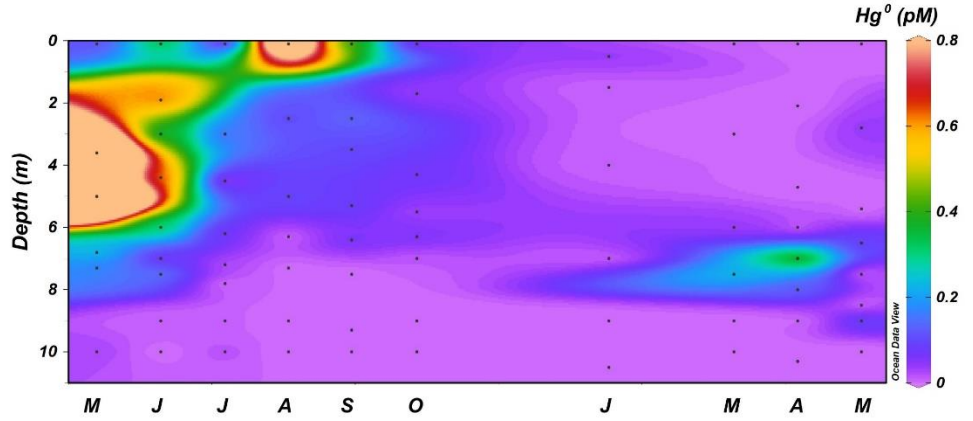
Hg⁰ (pM)
Depth (m)
0
2
4
6
8
10
M J J A S O J M A M
0.8
0.6
0.4
0.2
0
Ocean Data View

C

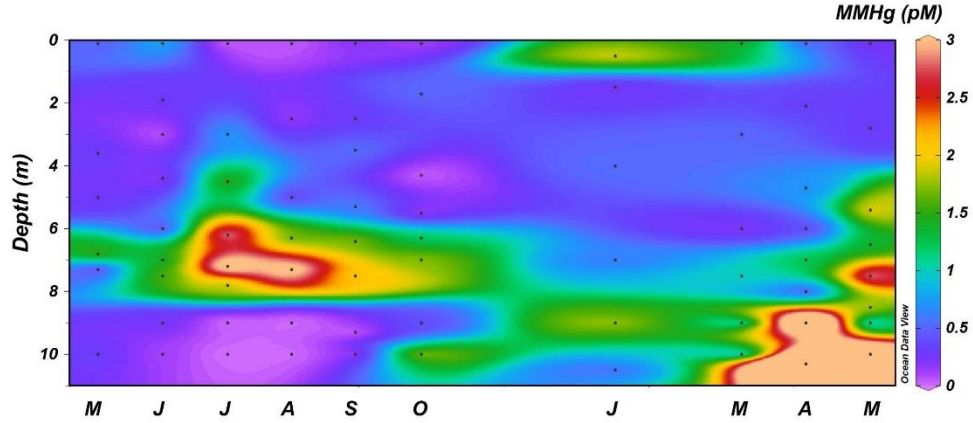
MMHg (pM)
Depth (m)
0
2
4
6
8
10
M J J A S O J M A M
3
2.5
2
1.5
1
0.5
0
Ocean Data View

Figure 3.4. Mercury species in Crystal Lake from May 2016 through May 2017, including unfiltered total mercury (HgT, A), elemental mercury (Hg^0, B), and unfiltered monomethylmercury (MMHg, C). Black dots indicate sample depth.

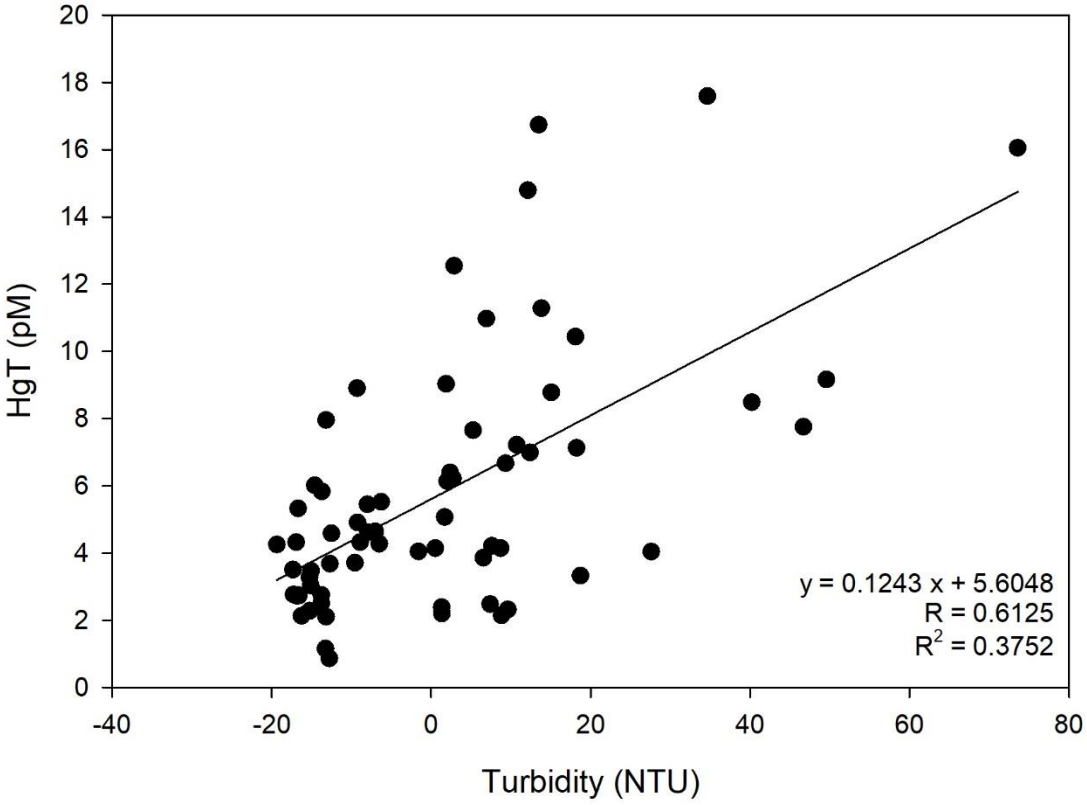

Figure 3.5. Unfiltered total mercury versus turbidity in Crystal Lake, p = <0.0001.

A

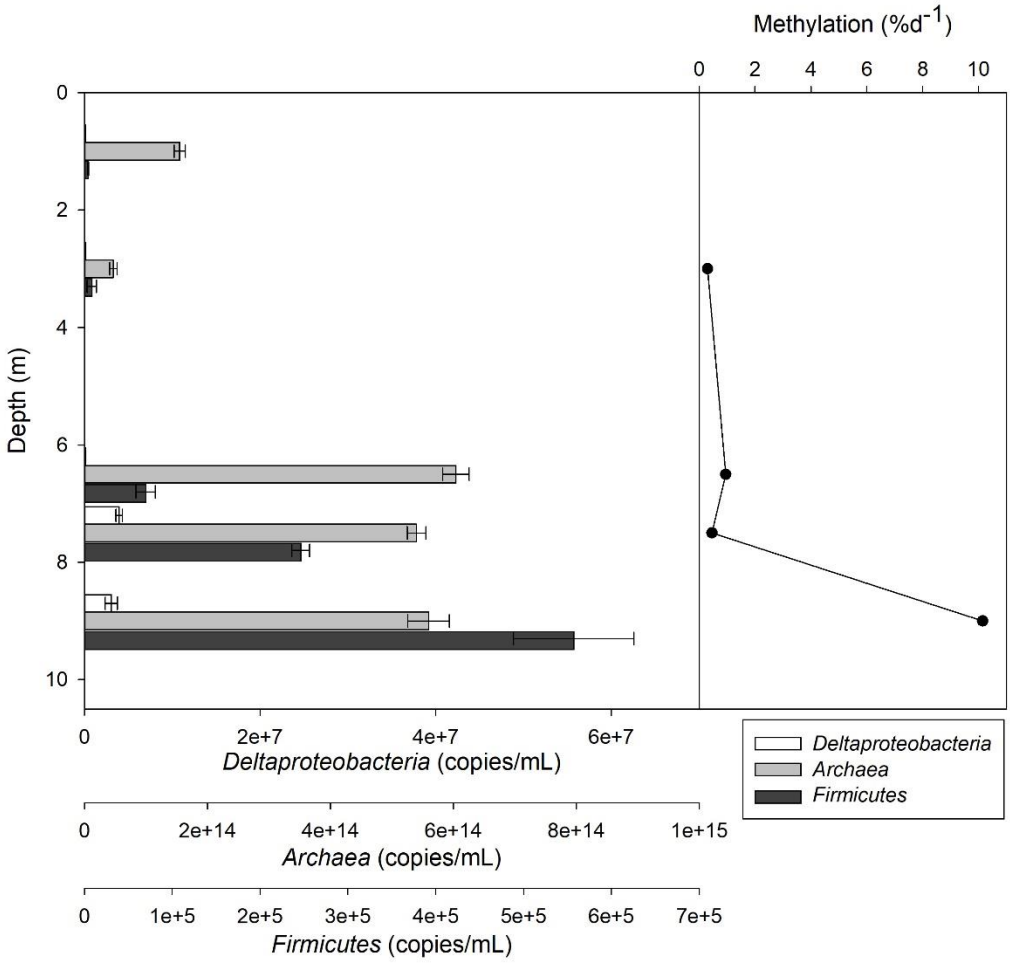
Methylation (%d-1)
0
2
4
6
8
10
Depth (m)
0
2
4
6
8
10
0
2e+7
4e+7
6e+7
Deltaproteobacteria (copies/mL)
0
2e+14
4e+14
6e+14
8e+14
1e+15
Archaea (copies/mL)
0
1e+5
2e+5
3e+5
4e+5
5e+5
6e+5
7e+5
Firmicutes (copies/mL)
Deltaproteobacteria
Archaea
Firmicutes

B

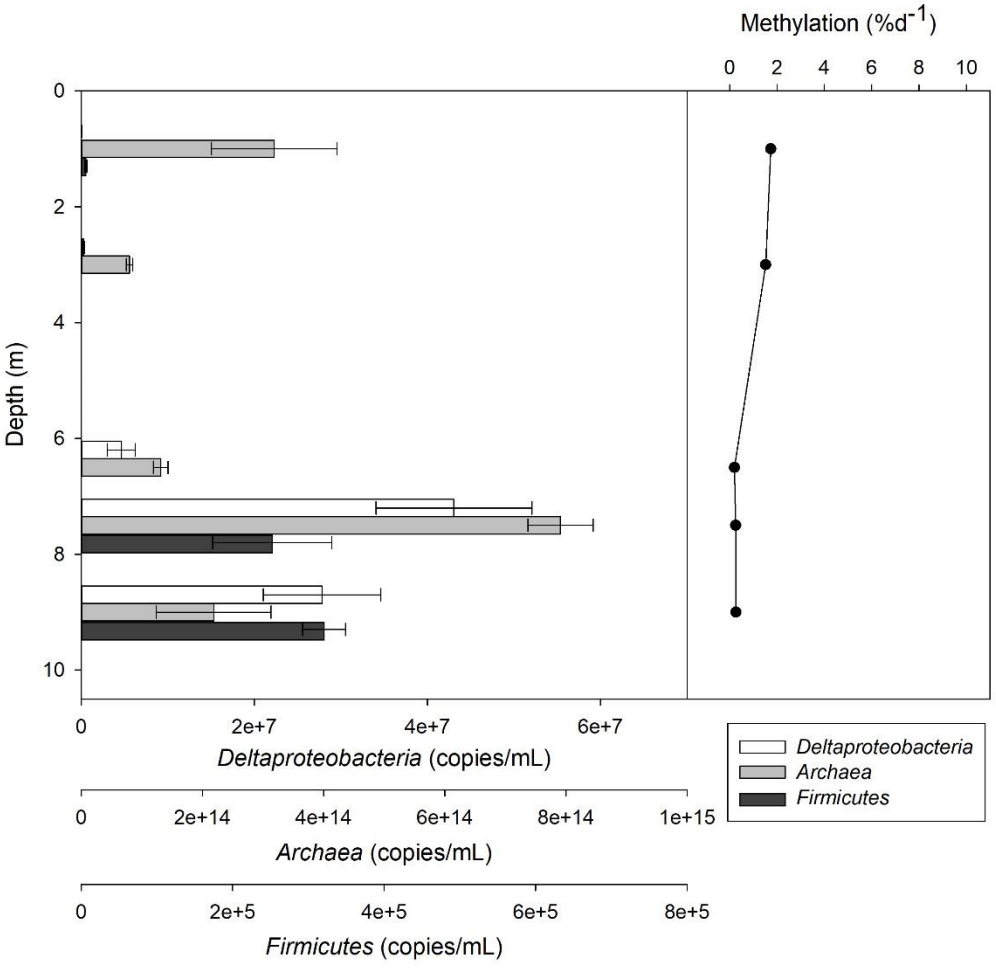

Figure 3.6. Mercury methylating gene abundance (*hgcA*) in the three known methylation clades and mercury methylation rates for August 2016 (A) and September 2016 (B) incubations.

TABLES

Table 3.1. PCR primers for amplification of *hgcAB* and qPCR primers for amplification of *hgcA*. From Christensen et al., 2016.

Primer Name	Sequence (5' to 3')	Amplicon Length (bp)
ORNL-HgcAB-uni-F	AAY GTC TGG TGY GCN GCV GG	818–1,020
ORNL-HgcAB-uni-R	CAB GCN CCR CAY TCC ATR CA	
ORNL-Delta-HgcA-F	GCC AAC TAC AAG MTG ASC TWC	107
ORNL-Delta-HgcA-R	CCS GCN GCR CAC CAG ACR TT	
ORNL-SRB-Firm-HgcA-F	TGG DCC GGT DAR AGC WAA RGA TA	167
ORNL-SRB-Firm-HgcA-R	AAA AGA GHA YBC CAA AAA TCA	
ORNL-Archaea-HgcA-F	AAY TAY WCN CTS AGY TTY GAY GC	125
ORNL-Archaea-HgcA-R	TCD GTC CCR AAB GTS CCY TT	

Table 3.2. Modified qPCR protocols for *hgcA* with primers from Christensen et al. 2016.

	Deltaproteobacteria	***Firmicutes***	***Archaea***
Initial denaturation	95 °C for 2 min	95 °C for 2 min	95 °C for 2 min
Denaturation	95 °C for 15 sec	95 °C for 10 sec	95 °C for 15 sec
Annealing	65°C for 33 sec	47 °C for 15 sec	50 °C for 30 sec
Extension	--	58 °C for 1 min	55 °C for 1 min
Number of cycles	50	35	50
Melt curve	65–95 °C	58–95 °C	55–95 °C
Forward primer conc.	375 nM	500 nM	250 Nm
Reverse primer conc.	375 nM	250 nM	250 nM

Table 3.3. Summary of data for Crystal Lake for the months of July, August, and September. Note that depths between the incubations and discreet measurements vary slightly. (ND = no data, <DL = below detection limit).

Month	Depth (m)	Methylation (% d^{-1})	n	*Archaea* (10^{14} *copies/mL)*	*Delta.* (10^{5} *copies/mL)*	*Firmicutes* (10^{4} *copies/mL)*	Depth (m)	Ambient MMHg (pM)	Sulfide (μM)	Temp (°C)	Chlor. (μg/L)	pH
July	1		5	ND	ND	ND	0.1	0.0	0.0	29.5	1.4	8.3
July	3	0.16	2	ND	ND	ND	3	0.8	0.0	23.7	13.0	8.3
July	6.5	0.10	4	ND	ND	ND	6.2	3.1	0.0	10.2	9.1	8.7
July	7.5	0.33	4	ND	ND	ND	7.8	1.7	52	6.7	6.4	8.2
July	9	4.29	3	ND	ND	ND	9	0.0	125	5.8	4.9	7.8
August	1		0	1.5	1.0	0.4	0.1	0.0	0	26.9	10.2	8.4
August	3	0.30	2	0.5	1.3	0.8	2.5	0.1	0	26.9	17.0	8.3
August	6.5	0.95	5	6	1.2	7	6.3	1.6	0	11.9	11.0	8.4
August	7.5	0.46	2	5.4	3.9	24.6	7.3	3.3	4	9.0	5.7	8.0
August	9	10.14	3	5.6	3.1	55.7	9	0.0	166	6.7	4.9	7.5
September	1	1.74	3	3.1	0.6	0.6	0.1	0.2	0	24.2	6.0	8.3
September	3	1.53	4	0.8	2.6	<DL	2.5	0.3	0	20.7	7.9	8.1
September	6.5	0.21	4	1.3	4.6	<DL	6.4	1.8	0	8.4	11.2	7.3
September	7.5	0.26	2	7.9	43.1	25.2	7.5	2.1	31	6.4	5.1	7.1
September	9	0.27	1	<DL	99.2	32.1	9.3	0.0	174	6.3	6.4	6.9

Table 3.4. Pearson product moment correlation for methylation potential and gene copy number of *hgcA* in *Deltaproteobacteria*, *Archaea*, and *Firmicutes*. Listed from top to bottom are Pearson's correlation coefficient (*r*), *p*-value, and number of samples.

	Delta.	*Arch.*	*Firm.*
Methylation Potential	-0.237 0.54 9	0.247 0.521 9	0.704 0.0772 7
Delta.		0.463 0.178 10	0.357 0.385 8
Arch.			0.469 0.241 8
Firm.			

Chapter 4: MERCURY METHYLATION IN COASTAL WATERS OF THE NORTHWEST ATLANTIC OCEAN

4.1. Abstract

Mercury (Hg) cycling on the continental shelf has been widely studied because monomethylmercury (MMHg) produced on the shelf enters coastal food webs. Hg transformation potentials were measured in water along the northwest Atlantic continental shelf and slope. Water samples from the deep chlorophyll maximum and near the sediment were amended with isotopically enriched ^{200}Hg and $CH_3{}^{201}Hg$ to examine Hg methylation and demethylation potentials. Samples for DNA were collected at the same depths as the Hg incubation samples and *hgcA*, a functional gene required for Hg methylation, was quantified. Methylation potentials at shelf stations averaged 0.08 ± 0.14% d^{-1} in the deep chlorophyll maximum and 0.24 ± 0.15% d^{-1} near sediments, with no significant difference between depths. No methylation was measured in oligotrophic water off the shelf. Demethylation potentials were below detection limit at all depths and stations, and estimated to be uniform across stations and depths at a rate of <2% d^{-1}. To characterize the microbial communities involved with biotic methylation, three inhibitor treatments were added to incubations. Chloramphenicol (a broad spectrum anti-microbial) almost entirely inhibited methylation, suggesting microbially-mediated methylation accounted for almost all of the methylation at these sites. BESA (sodium 2-bromoethanesulfonate: a methanogenesis inhibitor) reduced methylation potentials to 72 ± 10% at Station 1 and 65 ± 18% at Station 2, suggesting methanogens contributed to

MMHg production. Sodium molybdate (sulfate reduction inhibitor) had varying results, but did not significantly differ from control samples. Methylation/demethylation experiments were also executed with additions of carbon sources, including pyruvate and dimethyl sulfoxide. Pyruvate reduced methylation to 21± 4% at Station 1, and it was undetected at Station 2. Dimethyl sulfoxide (DMSO) reduced Hg methylation to 65 ± 5% and 61 ± 13% of controls at Stations 1 and 2, respectively. Quantitative PCR abundance of *hgcA* showed *Archaea* was the most abundant clade, and archaeal gene copies were detected in all samples. *Firmicutes* were detected above the sediment at the station closest to shore, while *Deltaproteobacteria* were not found at any station or depth. Together, inhibitor experiments and *Archaea* gene copy abundance suggest that methanogens are either directly or indirectly involved with Hg methylation in coastal waters of the northwest Atlantic Ocean and may be important methylators in the pelagic water column.

4.2. Introduction

Humans are exposed to monomethylmercury (MMHg), a bioaccumulative neurotoxin, mostly from the consumption of seafood (Sunderland, 2007). MMHg is synthesized in the ocean via both biotic and abiotic reactions occurring in sediment (Hammerschmidt et al., 2004; Hammerschmidt and Fitzgerald, 2006a, 2004; Hollweg et al., 2010, 2009) and the water column (Lehnherr et al., 2011; Monperrus et al., 2007). Marine coastal systems (Fitzgerald et al., 2007) and low-oxygen waters (Bowman et al., 2015, 2016; Mason et al., 2012; Sunderland et al., 2009) are suspected of being important zones for mercury (Hg) methylation. Coastal fisheries are sources of seafood to local anglers and can impact Hg accumulation in local populations (Lincoln et al., 2011; Sunderland, 2007). Near-shore fisheries are important to the economy and estimates suggest coastal environments supply 38% of the biosphere's monetary value (Costanza et al., 1997), so there are both financial and health incentives to understand near-shore Hg cycling.

Earlier work focused on Hg cycling in sediments under the premise that Hg cycling in the near-shore environment is a large source of MMHg to the coastal ecosystems (Hammerschmidt et al., 2004; Hammerschmidt and Fitzgerald, 2006b, 2006a; Hollweg et al., 2009, 2010). Coastal food webs are important routes of Hg exposure to local anglers and regional consumers (Mahaffey et al., 2009). A better understanding of near-shore water column Hg methylation can elucidate possible mechanisms of methylation in both the neritic and pelagic ocean. Although little is known about water-column Hg methylation (Lehnherr et al., 2011; Monperrus et al., 2007), it has been

hypothesized to be an important source of MMHg in the open ocean (Fitzgerald et al., 2007; Mason and Fitzgerald, 1991).

Recent identification of the gene pair responsible for Hg methylation has vastly improved understanding of biotic Hg methylation. The gene pair *hgcAB* is present in three clades of Hg-methylating bacteria and archaea: *Deltaproteobacteria*, *Firmicutes*, and *Archaea* (Gilmour et al., 2013). Polymerase chain reaction (PCR) primer sets can be used to identify the presence of the gene pair and quantify abundance of clade-specific *hgcA* (Christensen et al., 2016). These tools have been used to characterize bacterial and archaeal Hg-methylating communities in a couple environments, including rice paddy soil in China (Vishnivetskaya et al., 2018), and biofilms and periphyton in Bolivian lakes (Bouchet et al., 2018). Metagenomic screening of oceanic samples confirmed the presence of *hgcAB* in the ocean, but it was rarely detected in the water column and more abundant in sediments (Podar et al., 2015).

We sampled water from the northwest Atlantic shelf and slope to study Hg methylation with the following objectives: (1) determine Hg methylation potentials; (2) perform inhibitor and substrate addition incubations to compare relative Hg methylation relative to controls; and (3) characterize and quantify the potential for Hg methylating communities with DNA. Here we present coupled Hg methylation and genomic data and discuss their interrelation with regard to MMHg cycling in the water column.

4.3. Methods

4.3.1. Sampling

Seawater was sampled from the northwest Atlantic Ocean in summer of 2017 (Aug 20–29, 2017) from three stations (Figure 4.1). Stations 1 and 2 were near-shore shelf stations, with water column depths of 57 and 46 m, respectively. Station 4 was on the continental slope (depth 2510 m). Water was sampled from two depths at each station. Shallow samples were collected from each station at the deep chlorophyll maximum (at 14, 5, and 54 m, respectively). A second, deeper sample was collected either overlying the sediment (50 and 40 m at Stations 1 and 2), or at Station 4, from the oxygen minimum (320 m). Water was sampled by deploying a trace-metal clean rosette attached to a non-metallic hydrowire. The rosette was fitted with 8-L Teflon-coated X-Niskin bottles (Munson et al., 2015). Upon retrieval of the rosette, X-Niskin bottles were transferred to a clean lab and subsampled with clean sampling methods for Hg (Lamborg et al., 2012).

Water samples for Hg methylation potentials were collected either above the sediment interface (Stations 1 and 2) or within the oxygen minimum (Station 4). Water above sediment was amended with one of five treatments, and each treatment was prepared in quadruplicate. Three inhibitor treatments included additions of 28 mM sodium molybdate (sulfate reduction inhibitor; Cleckner et al., 1999; Compeau and Bartha, 1985; Gilmour et al., 1992; Hamelin et al., 2011), 0.25 mM chloramphenicol (a broad spectrum anti-microbial; Cleckner et al., 1999), and 30 mM sodium 2-bromoethanesulfonate (BESA; a methanogenesis inhibitor; Hamelin et al., 2011). Two treatments received carbon additions, which included either 100 mM dimethyl sulfoxide

(DMSO) or 50 mM pyruvate. Substrate amendments were added in excess as compared to environmental concentrations (Obernosterer et al., 1999; Simó et al., 2000), but pyruvate additions were of similar order of magnitude as culture studies (Bridou et al., 2011; Compeau and Bartha, 1985; Graham et al., 2012). Control samples were unamended and collected from the same depths as the treatment samples. All water samples, including controls and treatments from all depths, were amended with additions of 10 pM $^{200}Hg^{2+}$ and 1 pM $CH_3{}^{201}Hg$ prior to incubation. Water overlying the sediment and from the oxygen minimum was incubated for 24 hours in the dark at 4 °C, to mimic in situ conditions. Water from the deep chlorophyll maximum was incubated at in situ conditions in a sunlit ship-board incubator with continuous-flow surface water, where light intensity and temperature were monitored with a data logger (Onset HOBO Pendant). At the end of the incubation, 1 pM $CH_3{}^{199}Hg$ was added to samples for isotope dilution analysis of $CH_3{}^{200}Hg$ (Hintelmann et al., 1995; Hintelmann and Evans, 1997). Samples were acidified to 1% with H_2SO_4 to prevent further biological transformations of Hg and stored in the dark until MMHg extraction and analysis.

DNA was concentrated from seawater on Sterivex filters (0.22 μm, Millipore). DNA was collected from the same depths as incubation samples. Water volumes filtered for DNA analysis varied from 0.4 to 5.0 L. Filters were preserved with RNAlater® (Invitrogen) and stored at −80 °C until extraction (Hampel et al., 2018).

4.3.2. Methylmercury Analysis

Methylmercury was quantitatively extracted from acidified seawater samples to determine Hg methylation potentials. The pH of water was neutralized with KOH, buffered to pH 4.9 with acetate, amended with 0.3 mM ascorbic acid, and MMHg was

ethylated with sodium tetraethylborate (Bowman and Hammerschmidt, 2011; Munson et al., 2014). Derivatized MMHg (as methylethylmercury) was purged from seawater with Hg-free N_2, collected on Tenax and analyzed by isotope-dilution gas chromatography inductively coupled plasma mass-spectrometry (Perkin Elmer Elan 9000; Hintelmann et al., 1995; Hintelmann and Evans, 1997). Isotope recovery was calculated as described by Hintelmann and Evans (1997). Methylation potentials were calculated as the fraction of added ^{200}Hg transformed into $CH_3{}^{200}Hg$ during the 24-hour incubation period (Hintelmann et al., 2000). Ambient MMHg concentration was estimated from $CH_3{}^{202}Hg$ measurements and its relative isotopic abundance (29.9%; Nogaro and Hammerschmidt, 2013). The method detection limit for $CH_3{}^{200}Hg$ formation was 0.02% d^{-1} and was calculated as described by Hintelmann and Evans (1997). The detection limit for $CH_3{}^{201}Hg$ demethylation is constrained by the error associated with the isotopic addition technique, which was 2% d^{-1} (Eckley and Hintelmann, 2006).

4.3.3. Quantitative polymerase chain reaction analysis

DNA was extracted from 0.2 μm Sterivex filters (EMD Millipore) before quantification of *hgcA* by quantitative polymerase chain reaction (qPCR). Sterivex filters were rinsed with phosphate buffer to remove residual RNAlater, and genomic material was extracted with Puregene® Core Kit A (Qiagen) with some modifications (Hampel et al., 2018; Newell et al., 2011). Sterivex filters were rinsed with phosphate buffered saline 1X solution prior to addition of 0.9 mL lysis buffer and 4 μL Proteinase K. Filters were incubated sequentially for one hour each at 55 and 65 °C. The extraction solution was removed and new aliquots of lysis buffer and Proteinase K were added prior to repeating the incubation (Hampel et al., 2018). The purity and amount of DNA extracted was

quantified spectrophotometrically (NanoDrop ND 2000, Thermo Scientific). Samples were screened for *hgcAB* with broad range primers for polymerase chain reaction (PCR; Table 4.1; Christensen et al., 2016). After confirming the presence of *hgcAB*, clade-specific primers were used to amplify *hgcA* in *Delatproteobacteria*, methanogenic *Archaea*, and *Firmicutes* (Table 4.1). Standards for qPCR were prepared from respective *hgcA* fragments. Primer specificity was confirmed with a single band by gel electrophoresis (Band length in Table 4.1). Bands were cut from the gel and cleaned with Wizard® SV Gel & PCR Clean-Up System (Promega). The cleaned *hgcA* fragment was cloned with TOPO™ TA Cloning Kit (Invitrogen), and assimilated into a cell plasmid (One Shot™, Invitrogen). The plasmid containing *hgcA* was isolated with the UltraClean® Standard Mini Plasmid Prep Kit (Mo Bio Laboratories Inc.).

Sample assays included all samples to minimize set-to-set differentiation between analyses. Each assay contained three no-template controls (NTC), and triplicate standards and samples containing 0.05–20 ng of DNA. Standards were prepared from serial dilutions of the isolated plasmid, and ranged in efficiency from 90 to 110%, with R^2 values greater than 0.9. Primer efficiency of the *Archaea* assay was 71%, which was similar to the cited primer efficiency of the organism (*Methanomethylovorans hollandica*; 73%; Christensen et al., 2016). The qPCR amplification mixture contained Luna® qPCR Mastermix (NEB Labs). qPCR protocols were optimized for sample and primer concentration, and denaturation, annealing, and extension times (Table 4.2; Christensen et al., 2016). The NTC for both *Deltaproteobacteria* and *Firmicutes* assays were not detected. The NTC for *Archaea* was detected five cycles after the lowest standard, at cycle 45, suggesting that any non-specific products formed on or after cycle 45 (Lam et

al., 2007). Automatic settings on the thermocycler (Eppendorf Realplex) determined the threshold cycle value. Gene abundance was calculated by multiplying the quantity of DNA in the sample (*ng*) by Avagadro's number, and dividing it by the number of base pairs (*bp*) in the fragment multiplied by average mass of a DNA fragment (Equation 1).

$$Gene\ abundance = \frac{ng \cdot 6.0221\times10^{23}\frac{molecules}{mol}}{bp \cdot 10^{9}\frac{ng}{g} \cdot 650\frac{g}{mol}} \quad \text{Equation 1}$$

Gene abundance was normalized to sample volume, assuming 100% extraction efficiency. Assay detection limits (not method detection limits) were calculated from the lowest standard concentration required to bracket *hgcA* within our seawater samples. Assay detection limits were 55100 copies mL^{-1} for *Deltaproteobacteria*, 19700 copies mL^{-1} for *Firmicutes*, and 1.3×10^{10} copies mL^{-1} for *Archaea*. Detection limits for *Deltaproteobacteria* and *Firmicutes* were similar to those previously published (Christensen et al., 2016), while the large *Archaea* detection limit may be due to formation of multiple products from the 500-fold degeneracy of the primer (Christensen et al., 2016).

4.4. Results and Discussion

4.4.1. Water physicochemistry

Water at all stations and all depths was fully oxic (Figure 4.2). The deep chlorophyll maximum was coincident with the O_2 maxima at Stations 1, 2 and 4. Station 4 had a local oxygen minimum at 320 m, where O_2 declined to 130 μmol $kg^{-}1$, about half of surface O_2 levels. At Station 1, maxima of fluorescence and O_2 were coincident with

the deep chlorophyll maximum, whereas fluorescence and O_2 were unrelated. Photosynthetically active radiation (PAR) declined with depth. All depths sampled for incubations had PAR less than 13% of the surface irradiance (Table 4.3). Salinity at Station 4 ranged from 34.9–36.2, whereas that at Stations 1 and 2 ranged from 31.4 to 32.7, reflective of greater freshwater inputs most likely from continental runoff.

4.4.2. Ambient Hg

Mercury concentrations were greater on the shelf (Stations 1 and 2) than on the Slope (Station 4). Unfiltered total Hg (HgT) averaged 1.4 ± 0.31 pM at Station 1, 1.5 ± 0.71 pM at Station 2, and 0.59 ± 0.15 pM at Station 4 (Lamborg et al., unpublished data), consistent with results from nearby stations occupied during the U.S. GEOTRACES cruise in 2011 (Bowman et al., 2015). The vertical distribution of HgT at Station 1 exhibited a nutrient-type distribution: HgT was low at the surface, had a subsurface maximum at the deep chlorophyll maximum, and decreasing concentrations below the deep chlorophyll maximum, with an increase near the sediment. This pattern is consistent with other Hg measurements on the shelf and suggests sediments are a source of HgT to the lower water column (Bowman et al., 2015). Stations 2 and 4 had scavenged-type profiles of HgT, with lower surface water concentrations than Station 1, a subsurface minimum, and increasing concentrations below 100 m. Distributions and concentrations were similar to past work on the North Atlantic shelf and continental margin (Bowman et al., 2015).

Surface Hg^0 concentrations decreased with distance from shore. Station 1 had the greatest Hg^0 concentrations, averaging 0.24 ± 0.06 pM. In contrast, Stations 2 and 4 had mean Hg^0 concentrations of 0.12 ± 0.01 pM and 0.13 ± 0.06 pM, respectively. All three

profiles exhibited nutrient-type distributions, with low Hg^0 at the surface, subsurface maxima in the deep chlorophyll maximum, and decreasing concentrations below the mid-depth Hg^0 maxima. Hg^0 profiles tended to follow fluorescence profiles, suggesting either autotrophic (Poulain et al., 2004; Schaefer et al., 2004) or heterotrophic formation of Hg^0 (Mason et al., 1995; Poulain et al., 2004). If the latter is true, then heterotrophic formation of Hg^0 is dependent on primary producers. Vertical distributions and concentration ranges are typical of near-shore environments in the North Atlantic (Bowman et al., 2015; Mason et al., 1998; Rolfhus and Fitzgerald, 2001).

4.4.3. Mercury methylation potentials

Mercury methylation was detected in seawater at Stations 1 and 2, but not at Station 4. Methylation potentials at Stations 1 and 2 ranged from 0.06–0.31% d^{-1} (Figure 4.3). These values are slightly lower than methylation potentials measured in the Canadian Arctic Archipelago (0.06–1.3% d^{-1}; Lehnherr et al., 2011) and much less than those measured in the Mediterranean Sea (<0.02–6.3% d^{-1}; Monperrus et al., 2007). Mercury methylation potentials in water overlying sediment were not significantly different than in the deep chlorophyll maximum at Station 1 (Two- tailed *t*-test; $p = 0.11$; Figure 4.3). Mercury methylation potentials at Station 2 had high variability between water overlying sediment and the deep chlorophyll maximum, but methylation potentials were not significantly different between depths (Two-tailed *t*-test; $p = 0.656$). Among all replicate samples at Stations 1 and 2, average Hg methylation potentials were 0.08 ± 0.14% d^{-1} in the deep chlorophyll maximum and 0.24 ± 0.15% d^{-1} in water overlying the sediment. These values are an order of magnitude lower than methylation potentials measured in sediments from Long Island Sound, Chesapeake Bay, and mid-Atlantic

continental shelf and slope (Hammerschmidt and Fitzgerald, 2004; Hollweg et al., 2010, 2009). Water-column Hg methylation potentials are likely less than those in sediment due to lower concentrations of organic matter and microbes, including methylating microorganisms. The only station along the continental slope, Station 4, had no quantifiable Hg methylation at either the deep chlorophyll maximum or oxygen minimum. Hg methylation likely occurred in these oligotrophic water, but at a rate below our detection limit (0.02% d^{-1}).

4.4.4. Mercury demethylation

Demethylation of MMHg was below the detection limit (<2% d^{-1}) among all sites and depths. Such low rates are less than those measured in dark incubations in the Mediterranean Sea (2.8–10.9% d^{-1}; Monperrus et al., 2007), photodemethylation rates in surface Mediterranean Sea water (3.2–16.9% d^{-1}; Monperrus et al., 2007), and demethylation in the Canadian Arctic Archipelago (23–59% d^{-1}; Lehnherr et al., 2011). Demethylation in the Canadian Arctic Archipelago was relatively consistent among sampling sites and depths (Lehnherr et al., 2011).

4.4.5. qPCR results

hgcA DNA was detected in coastal waters of the northwest Atlantic Ocean (Figure 4.4). *Deltaproteobacteria* copies were below detection limit for all sites and depths. *Firmicutes* were only detected in water overlying the sediment at Station 1. Most Hg methylating *Firmicutes* are strictly anaerobic bacteria that use sulfate, iron, and carbon as electron acceptors, but a few *Firmicutes* are syntrophic and fermentative (Gilmour et al., 2013). This suggests that we would not expect to detect a high abundance of *Firmicutes* in oxic water, but some cells may have been suspended with sediment. Methanogenic

archaeal *hgcA* was detected in all samples, with a greater number of copies in the deep chlorophyll maximum than in water over sediment. While our data cannot corroborate whether active transcription of *hgcAB* occurs at these sites, if the gene was actively transcribed, archaeal Hg methylation could be a possible mechanism for MMHg production in oxic water.

Previous research found *hgcA*-like sequences in both seawater and marine sediments, but was unable to confirm active Hg methylation. *hgcA*-like sequences were found in the pelagic water column of the South Atlantic Ocean (Podar et al., 2015), and in the Transpolar Drift and water overlying sediment in the Arctic Ocean (Bowman et al., in prep). In both cases, these *hgcA*-like genes were unrelated to seawater MMHg concentrations, suggesting they may be either incapable of Hg methylation or not active in the water column. Moreover, *hgcA* abundance in marine sediment was not correlated with Hg methylation potential (Ndu et al., 2018), suggesting that *hgcA* alone may be insufficient for understanding Hg methylation in marine systems. The gene pair *hgcAB* has been found in coastal and estuarine sediment (Gilmour et al., 2013; Podar et al., 2015), which, if actively transcribed may be a better indicator of Hg methylation potential.

4.4.6. Effects of metabolic inhibitors and substrates on Hg methylation

Inhibitor and carbon addition incubations yielded large variability among the three stations, but little significant difference. No Hg methylation was detected in the inhibitor treatments at Station 4, which was similar to absence of measureable MMHg production in control samples. Water from Stations 1 and 2 that were amended with BESA had slightly suppressed methylation potentials as compared to the aphotic controls,

but were not statistically different from the controls likely due to the small sample size. BESA inhibits methanogenesis (Cleckner et al., 1999; Gilmour et al., 1998; Pak and Bartha, 1998), and the mean decrease of Hg methylation at Station 1 was 72 ± 10% and 65± 18% at Station 2 suggests that methanogens were responsible for some MMHg production. This conclusion is supported by the detection of methangenic archaeal *hgcA* at these stations, and suggests methanogens may methylate Hg in oxic waters.

Molybdate amendment affected Hg methylation differently at Stations 1 and 2. At Station 1, Hg methylation increased by 18± 7%, on average compared to controls, while MMHg production at Station 2 was reduced to 39± 14%, but neither of the differences were significantly different from control samples. Molybdate inhibits sulfate reduction and Hg methylation by sulfate reducing bacteria (SRB; Achá et al., 2011; Cleckner et al., 1999; Compeau and Bartha, 1985; Ekstrom et al., 2003; Fleming et al., 2006; Gilmour et al., 1998, 1992; Hamelin et al., 2011; King, Jeffery K. et al., 1999; Pak and Bartha, 1998; Sørensen et al., 1981; Yu et al., 2012). Inhibition by molybdate may allow other microbes to outcompete SRB and methylate Hg at Station 1. Molybdate is also hypothesized to inhibit MMHg demethylation (Oremland et al., 1991), but we cannot confirm this speculation as demethylation potentials were below detection limits. SRB were not significant methylators at Station 1 but are likely part of the Hg methylating community at Station 2, even if the *Deltaproteobacteria hgcA* gene was below detection.

Chloramphenicol amended seawater had reduced methylation compared to controls. Methylation at Station 1 was either completely suppressed or it was below detection limit, and results were significantly different than the control (Mann-Whitney Rank Sum Test, $p = 0.100$). At Station 2, chloramphenicol was not significantly different

from zero, MMHg formation was reduced to 7 ± 9% of the control (Mann-Whitney Rank Sum Test, $p = 0.100$). Of the inhibitors used in this study, chloramphenicol was the most effective at suppressing Hg methylation at both sites. Chloramphenicol is a broad spectrum anti-microbial, which inhibits protein synthesis and methanogens (Hamelin et al., 2011), and has been used to determine the contribution of methanogens to Hg methylation (Cleckner et al., 1999; Goñi-Urriza et al., 2015; Hamelin et al., 2011). MMHg produced at Station 2 may be a result of bacterial resistance to chloramphenicol (Cleckner et al., 1999) or abiotic production. Overall, this data suggests Hg methylation at these depths is primarily driven by microbial processes and largely methanogenesis. Methanogens may either methylate Hg or indirectly stimulate MMHg production by other microbes that benefit from products of methanogenesis. The ubiquity and abundance of *Archaea hgcA* copies also indicate that methanogens are important methylators at these sites. Although there is site-to-site variation in microbial population, this data suggests methanogens have an important role in methylating Hg in the coastal northwest Atlantic Ocean.

Contrary to culture studies, addition of pyruvate reduced Hg methylation. At Station 1 Hg methylation was reduced to 21 ± 4% of controls, and methylation at Station 2 was not detected. In culture studies, pyruvate was found to increase MMHg synthesis (Compeau and Bartha, 1985; Gilmour et al., 2013; Schaefer et al., 2011). When compared to culture studies, the efficacy of pyruvate as a carbon donor seems reduced during in-situ Hg methylation incubations. While Choi and Bartha (1993) postulated that the methyl group in MMHg may originate from pyruvate, there are likely many carbon donors in natural waters. Indeed, pyruvate additions may not yield direct MMHg

synthesis in-situ because it can either be an electron donor (Gilmour et al., 2011) or an electron acceptor (Bridou et al., 2011). Although pyruvate may be an important carbon donor for MMHg formation in culture, it may be used in natural waters for other biochemical reactions before Hg methylation. Reduced methylation (as compared to controls) may result from pyruvate stimulating microbes that outcompete Hg methylating bacteria and archaea. Pyruvate may have also catalyzed reactions whose products interfered with Hg methylation. Lastly, pyruvate additions may have stimulated microbes responsible for Hg demethylation, but it remained below detection limits.

DMSO additions did not increase the methylation potential of water overlying sediment. DMSO decreased Hg methylation potentials at Stations 1 and 2, Hg methylation potentials were 65 ± 5% and 61 ± 13% of controls, respectively. DMSO was added as a precursor to dimethyl sulfide, which is used by some Hg methylating methanogens (Gilmour et al., 2013; Lomans et al., 1999). Bacteria and archaea metabolize DMSO via DMSO reductase to form dimethyl sulfide (McEwan et al., 2002). DMSO was added to indirectly stimulate MMHg synthesis. MMHg production did not increase, likely for similar reasons discussed above. Non-methylating microbes likely outcompeted methylating archaea, and decreased MMHg production. Additional research (e.g., by performing methylation incubations with various forms of dissolved organic matter) should be conducted to determine if methylation in the ocean is limited by carbon donor availability.

4.5. Conclusions

Mercury methylation potentials were measured in northwest Atlantic Ocean shelf waters and averaged 0.08 ± 0.14% d^{-1} in deep chlorophyll maximum waters and 0.24 ± 0.15% d^{-1} in water overlying the sediment. Results from inhibitor experiments and clade-specific *hgcA* DNA quantification suggest that methanogens may help methylate Hg in oxic coastal waters. These results add to our current understanding of coastal MMHg formation (Hammerschmidt et al., 2004; Hammerschmidt and Fitzgerald, 2004, 2006a, 2006b; Hollweg et al., 2009, 2010; Lehnherr et al., 2011; Monperrus et al., 2007) which can lead to a better understanding of open ocean Hg methylation.

4.6. Acknowledgments

We thank chief scientist Colleen Hansel and the captain and crew of the R/V *Endeavour* cruise 604. Carl Lamborg and Katlin Bowman shared Hg concentration results. Lindsay Starr, Kortney Mullen, Lamborg, and Bowman helped with sampling. We thank Justyna Hampel, Daniel Hoffman, Desi Niewinski and Megan Reed for help with PCR.

4.7. References

Achá, D., Hintelmann, H., Yee, J., 2011. Importance of sulfate reducing bacteria in mercury methylation and demethylation in periphyton from Bolivian Amazon region. Chemosphere 82, 911–916. https://doi.org/10.1016/j.chemosphere.2010.10.050

Bouchet, S., Goñi-Urriza, M., Monperrus, M., Guyoneaud, R., Fernandez, P., Heredia, C., Tessier, E., Gassie, C., Point, D., Guédron, S., Achá, D., Amouroux, D., 2018. Linking Microbial Activities and Low-Molecular-Weight Thiols to Hg Methylation in Biofilms and Periphyton from High-Altitude Tropical Lakes in the Bolivian Altiplano. Environ. Sci. Technol. 52, 9758–9767. https://doi.org/10.1021/acs.est.8b01885

Bowman, K.L., Hammerschmidt, C.R., 2011. Extraction of monomethylmercury from seawater for low-femtomolar determination. Limnol. Oceanogr. Methods 9, 121–128. https://doi.org/10.4319/lom.2011.9.121

Bowman, K.L., Hammerschmidt, C.R., Lamborg, C.H., Swarr, G., 2015. Mercury in the North Atlantic Ocean: The U.S. GEOTRACES zonal and meridional sections. Deep Sea Res. Part II Top. Stud. Oceanogr. 116, 251–261. https://doi.org/10.1016/j.dsr2.2014.07.004

Bowman, K.L., Hammerschmidt, C.R., Lamborg, C.H., Swarr, G.J., Agather, A.M., 2016. Distribution of mercury species across a zonal section of the eastern tropical South Pacific Ocean (U.S. GEOTRACES GP16). Mar. Chem. 186, 156–166. https://doi.org/10.1016/j.marchem.2016.09.005

Bridou, R., Monperrus, M., Gonzalez, P.R., Guyoneaud, R., Amouroux, D., 2011. Simultaneous determination of mercury methylation and demethylation capacities of various sulfate-reducing bacteria using species-specific isotopic tracers. Environ. Toxicol. Chem. 30, 337–344.

Christensen, G.A., Wymore, A.M., King, A.J., Podar, M., Hurt, R.A., Santillan, E.U., Soren, A., Brandt, C.C., Brown, S.D., Palumbo, A.V., Wall, J.D., Gilmour, C.C., Elias, D.A., 2016. Development and Validation of Broad-Range Qualitative and Clade-Specific Quantitative Molecular Probes for Assessing Mercury Methylation in the Environment. Appl. Environ. Microbiol. 82, 6068–6078. https://doi.org/10.1128/AEM.01271-16

Cleckner, L.B., Gilmour, C.C., Hurley, J.P., Krabbenhoft, D.P., 1999. Mercury methylation in periphyton of the Florida Everglades. Limnol. Oceanogr. 44, 1815–1825. https://doi.org/10.4319/lo.1999.44.7.1815

Compeau, G.C., Bartha, R., 1985. Sulfate-Reducing Bacteria: Principal Methylators of Mercury in Anoxic Estuarine Sediment. Appl Env. Microbiol 50, 498–502.

Costanza, R., d'Arge, R., Groot, R. de, Farber, S., Grasso, M., Hannon, B., Limburg, K., Naeem, S., O'Neill, R.V., Paruelo, J., Raskin, R.G., Sutton, P., Belt, M. van den, 1997. The value of the world's ecosystem services and natural capital. Nature 387, 253–260. https://doi.org/10.1038/387253a0

Eckley, C.S., Hintelmann, H., 2006. Determination of mercury methylation potentials in the water column of lakes across Canada. Sci. Total Environ. 368, 111–125. https://doi.org/10.1016/j.scitotenv.2005.09.042

Ekstrom, E.B., Morel, F.M.M., Benoit, J.M., 2003. Mercury Methylation Independent of the Acetyl-Coenzyme A Pathway in Sulfate-Reducing Bacteria. Appl Env. Microbiol 69, 5414–5422. https://doi.org/10.1128/AEM.69.9.5414-5422.2003

Fitzgerald, W.F., Lamborg, C.H., Hammerschmidt, C.R., 2007. Marine Biogeochemical Cycling of Mercury. Chem. Rev. 107, 641–662. https://doi.org/10.1021/cr050353m

Fleming, E.J., Mack, E.E., Green, P.G., Nelson, D.C., 2006. Mercury Methylation from Unexpected Sources: Molybdate-Inhibited Freshwater Sediments and an Iron-Reducing Bacterium. Appl. Environ. Microbiol. 72, 457–464. https://doi.org/10.1128/AEM.72.1.457-464.2006

Gilmour, C.C., Elias, D.A., Kucken, A.M., Brown, S.D., Palumbo, A.V., Schadt, C.W., Wall, J.D., 2011. Sulfate-Reducing Bacterium Desulfovibrio desulfuricans ND132 as a Model for Understanding Bacterial Mercury Methylation. Appl. Environ. Microbiol. 77, 3938–3951. https://doi.org/10.1128/AEM.02993-10

Gilmour, C.C., Henry, E.A., Mitchell, R., 1992. Sulfate stimulation of mercury methylation in freshwater sediments. Environ. Sci. Technol. 26, 2281–2287. https://doi.org/10.1021/es00035a029

Gilmour, C.C., Podar, M., Bullock, A.L., Graham, A.M., Brown, S.D., Somenahally, A.C., Johs, A., Hurt, R.A., Bailey, K.L., Elias, D.A., 2013. Mercury Methylation by Novel Microorganisms from New Environments. Environ. Sci. Technol. 47, 11810–11820. https://doi.org/10.1021/es403075t

Gilmour, C.C., Riedel, G.S., Ederington, M.C., Bell, J.T., Gill, G.A., Stordal, M.C., 1998. Methylmercury concentrations and production rates across a trophic gradient in the northern Everglades. Biogeochemistry 40, 327–345. https://doi.org/10.1023/A:1005972708616

Goñi-Urriza, M., Corsellis, Y., Lanceleur, L., Tessier, E., Gury, J., Monperrus, M., Guyoneaud, R., 2015. Relationships between bacterial energetic metabolism, mercury methylation potential, and hgcA/hgcB gene expression in Desulfovibrio dechloroacetivorans BerOc1. Environ. Sci. Pollut. Res. 22, 13764–13771. https://doi.org/10.1007/s11356-015-4273-5

Graham, A.M., Aiken, G.R., Gilmour, C.C., 2012. Dissolved Organic Matter Enhances Microbial Mercury Methylation Under Sulfidic Conditions. Environ. Sci. Technol. 46, 2715–2723. https://doi.org/10.1021/es203658f

Hamelin, S., Amyot, M., Barkay, T., Wang, Y., Planas, D., 2011. Methanogens: Principal Methylators of Mercury in Lake Periphyton. Environ. Sci. Technol. 45, 7693–7700. https://doi.org/10.1021/es2010072

Hammerschmidt, C.R., Fitzgerald, W.F., 2006a. Methylmercury cycling in sediments on the continental shelf of southern New England. Geochim. Cosmochim. Acta 70, 918–930. https://doi.org/10.1016/j.gca.2005.10.020

Hammerschmidt, C.R., Fitzgerald, W.F., 2006b. Bioaccumulation and Trophic Transfer of Methylmercury in Long Island Sound. Arch. Environ. Contam. Toxicol. 51, 416–424. https://doi.org/10.1007/s00244-005-0265-7

Hammerschmidt, C.R., Fitzgerald, W.F., 2004. Geochemical Controls on the Production and Distribution of Methylmercury in Near-Shore Marine Sediments. Environ. Sci. Technol. 38, 1487–1495. https://doi.org/10.1021/es034528q

Hammerschmidt, C.R., Fitzgerald, W.F., Lamborg, C.H., Balcom, P.H., Visscher, P.T., 2004. Biogeochemistry of methylmercury in sediments of Long Island Sound. Mar. Chem. 90, 31–52. https://doi.org/10.1016/j.marchem.2004.02.024

Hampel, J.J., McCarthy, M.J., Gardner, W.S., Zhang, L., Xu, H., Zhu, G., Newell, S.E., 2018. Nitrification and ammonium dynamics in Taihu Lake, China: seasonal competition for ammonium between nitrifiers and cyanobacteria. Biogeosciences 15, 733–748. https://doi.org/10.5194/bg-15-733-2018

Hintelmann, H., Evans, R.D., 1997. Application of stable isotopes in environmental tracer studies – Measurement of monomethylmercury (CH3Hg+) by isotope dilution ICP-MS and detection of species transformation. Fresenius J. Anal. Chem. 358, 378–385. https://doi.org/10.1007/s002160050433

Hintelmann, H., Evans, R.D., Villeneuve, J.Y., 1995. Measurement of mercury methylation in sediments by using enriched stable mercury isotopes combined with methylmercury determination by gas chromatography–inductively coupled plasma mass spectrometry. J. Anal. At. Spectrom. 10, 619–624. https://doi.org/10.1039/JA9951000619

Hintelmann, H., Keppel-Jones, K., Evans, R.D., 2000. Constants of mercury methylation and demethylation rates in sediments and comparison of tracer and ambient mercury availability. Environ. Toxicol. Chem. 19, 2204–2211. https://doi.org/10.1002/etc.5620190909

Hollweg, T.A., C. C. Gilmour, Mason, R.P., 2010. Mercury and methylmercury cycling in sediments of the mid-Atlantic continental shelf and slope. Limnol. Oceanogr. 55, 2703–2722. https://doi.org/10.4319/lo.2010.55.6.2703

Hollweg, T.A., Gilmour, C.C., Mason, R.P., 2009. Methylmercury production in sediments of Chesapeake Bay and the mid-Atlantic continental margin. Mar. Chem. 114, 86–101. https://doi.org/10.1016/j.marchem.2009.04.004

King, Jeffery K., Saunders, F. M, Lee, R. F., Jahnke, R. A., 1999. Coupling mercury methylation rates to sulfate reduction rates in marine sediments. Environ. Toxicol. Chem. 18, 1362–1369.

Lam, P., Jensen, M.M., Lavik, G., McGinnis, D.F., Muller, B., Schubert, C.J., Amann, R., Thamdrup, B., Kuypers, M.M.M., 2007. Linking crenarchaeal and bacterial nitrification to anammox in the Black Sea. Proc. Natl. Acad. Sci. 104, 7104–7109. https://doi.org/10.1073/pnas.0611081104

Lamborg, C.H., Hammerschmidt, C.R., Gill, G.A., Mason, R.P., Gichuki, S., 2012. An intercomparison of procedures for the determination of total mercury in seawater and recommendations regarding mercury speciation during GEOTRACES cruises. Limnol. Oceanogr. Methods 10, 90–100. https://doi.org/10.4319/lom.2012.10.90

Lehnherr, I., Louis, V.L.S., Hintelmann, H., Kirk, J.L., 2011. Methylation of inorganic mercury in polar marine waters. Nat. Geosci. 4, 298–302. https://doi.org/10.1038/ngeo1134

Lincoln, R.A., Shine, J.P., Chesney, E.J., Vorhees, V.D.J., Grandjean, P., Senn, D.B., 2011. Fish Consumption and Mercury Exposure among Louisiana Recreational Anglers. Environ. Health Perspect. 119, 245–251. https://doi.org/10.1289/ehp.1002609

Lomans, B.P., Maas, R., Luderer, R., Pol, A., 1999. Isolation and Characterization of Methanomethylovorans hollandica gen. nov., sp. nov., Isolated from Freshwater Sediment, a Methylotrophic Methanogen Able To Grow on Dimethyl Sulfide and Methanethiol 65, 10.

Mahaffey, K., Clickner, R., Jeffries, R., 2009. Adult women's blood mercury concentrations vary regionally in the United States: association with patterns of fish consumption (NHANES 1999-2004). Environ. Health Perspect. 117, 47–53. https://doi.org/10.1289/ehp.11674

Mason, R.P., Choi, A.L., Fitzgerald, W.F., Hammerschmidt, C.R., Lamborg, C.H., Soerensen, A.L., Sunderland, E.M., 2012. Mercury biogeochemical cycling in the ocean and policy implications. Environ. Res., Mercury in Marine Ecosystems: Sources to Seafood Consumers 119, 101–117. https://doi.org/10.1016/j.envres.2012.03.013

Mason, R.P., Fitzgerald, W.F., 1991. Mercury speciation in open ocean waters. Water. Air. Soil Pollut. 56, 779–789. https://doi.org/10.1007/BF00342316

Mason, R.P., Morel, F.M.M., Hemond, H.F., 1995. The role of microorganisms in elemental mercury formation in natural waters. Water. Air. Soil Pollut. 80, 775–787. https://doi.org/10.1007/BF01189729

Mason, R.P., Rolfhus, K.R., Fitzgerald, W.F., 1998. Mercury in the North Atlantic. Mar. Chem. 61, 37–53. https://doi.org/10.1016/S0304-4203(98)00006-1

McEwan, A.G., Ridge, J.P., McDevitt, C.A., Hugenholtz, P., 2002. The DMSO Reductase Family of Microbial Molybdenum Enzymes; Molecular Properties and Role in the Dissimilatory Reduction of Toxic Elements. Geomicrobiol. J. 19, 3–21.

Monperrus, M., Tessier, E., Amouroux, D., Leynaert, A., Huonnic, P., Donard, O.F.X., 2007. Mercury methylation, demethylation and reduction rates in coastal and marine surface waters of the Mediterranean Sea. Mar. Chem., Mercury Cycling in Surface and Deep Waters of the Mediterranean Sea 107, 49–63. https://doi.org/10.1016/j.marchem.2007.01.018

Munson, K.M., Babi, D., Lamborg, C.H., 2014. Determination of monomethylmercury from seawater with ascorbic acid-assisted direct ethylation. Limnol. Oceanogr. Methods 12, 1–9. https://doi.org/10.4319/lom.2014.12.1

Munson, K.M., Lamborg, C.H., Swarr, G.J., Saito, M.A., 2015. Mercury species concentrations and fluxes in the Central Tropical Pacific Ocean. Glob. Biogeochem. Cycles 29, 656–676. https://doi.org/10.1002/2015GB005120

Ndu, U., Christensen, G.A., Rivera, N.A., Gionfriddo, C.M., Deshusses, M.A., Elias, D.A., Hsu-Kim, H., 2018. Quantification of Mercury Bioavailability for Methylation Using Diffusive Gradient in Thin-Film Samplers. Environ. Sci. Technol. 52, 8521–8529. https://doi.org/10.1021/acs.est.8b00647

Newell, S.E., Babbin, A.R., Jayakumar, A., Ward, B.B., 2011. Ammonia oxidation rates and nitrification in the Arabian Sea: Arabian Sea ammonia oxidation and nitrification. Glob. Biogeochem. Cycles 25, n/a-n/a. https://doi.org/10.1029/2010GB003940

Nogaro, G., Hammerschmidt, C.R., 2013. Influence of benthic macrofauna on microbial production of methylmercury in sediments on the New England continental shelf. Hydrobiologia 701, 289–299. https://doi.org/10.1007/s10750-012-1286-7

Obernosterer, I., Kraay, G., de Ranitz, E., Herndl, G., 1999. Concentrations of low molecular weight carboxylic acids and carbonyl compounds in the Aegean Sea (Eastern Mediterranean) and the turnover of pyruvate. Aquat. Microb. Ecol. 20, 147–156. https://doi.org/10.3354/ame020147

Oremland, R.S., Culbertson, C.W., Winfrey, M.R., 1991. Methylmercury Decomposition in Sediments and Bacterial Cultures: Involvement of Methanogens and Sulfate Reducers in Oxidative Demethylation. Appl Env. Microbiol 57, 130–137.

Pak, K.-R., Bartha, R., 1998. Mercury Methylation and Demethylation in Anoxic Lake Sediments and by Strictly Anaerobic Bacteria. Appl. Environ. Microbiol. 64, 1013–1017.

Podar, M., Gilmour, C.C., Brandt, C.C., Soren, A., Brown, S.D., Crable, B.R., Palumbo, A.V., Somenahally, A.C., Elias, D.A., 2015. Global prevalence and distribution of genes and microorganisms involved in mercury methylation. Sci. Adv. 1, e1500675–e1500675. https://doi.org/10.1126/sciadv.1500675

Poulain, A.J., Amyot M., Findlay D., Telor S., Barkay T., Hintelmann H., 2004. Biological and photochemical production of dissolved gaseous mercury in a boreal lake. Limnol. Oceanogr. 49, 2265–2275. https://doi.org/10.4319/lo.2004.49.6.2265

Rolfhus, K.R., Fitzgerald, W.F., 2001. The evasion and spatial/temporal distribution of mercury species in Long Island Sound, CT-NY. Geochim. Cosmochim. Acta 65, 407–418. https://doi.org/10.1016/S0016-7037(00)00519-6

Schaefer, J.K., Rocks, S.S., Zheng, W., Liang, L., Gu, B., Morel, F.M.M., 2011. Active transport, substrate specificity, and methylation of Hg(II) in anaerobic bacteria. Proc. Natl. Acad. Sci. 108, 8714–8719. https://doi.org/10.1073/pnas.1105781108

Schaefer, J.K., Yagi, J., Reinfelder, J.R., Cardona, T., Ellickson, K.M., Tel-Or, S., Barkay, T., 2004. Role of the Bacterial Organomercury Lyase (MerB) in Controlling Methylmercury Accumulation in Mercury-Contaminated Natural Waters. Environ. Sci. Technol. 38, 4304–4311. https://doi.org/10.1021/es049895w

Simó, R., Pedrós-Alió, C., Malin, G., Grimalt, J., 2000. Biological turnover of DMS, DMSP and DMSO in contrasting open-sea waters. Mar. Ecol. Prog. Ser. 203, 1–11. https://doi.org/10.3354/meps203001

Sørensen, J., Christensen, D., Jørgensen, B.B., 1981. Volatile Fatty Acids and Hydrogen as Substrates for Sulfate-Reducing Bacteria in Anaerobic Marine Sediment. Appl Env. Microbiol 42, 5–11.

Sunderland, E.M., 2007. Mercury Exposure from Domestic and Imported Estuarine and Marine Fish in the U.S. Seafood Market. Environ. Health Perspect. 235.

Sunderland, E.M., Krabbenhoft, D.P., Moreau, J.W., Strode, S.A., Landing, W.M., 2009. Mercury sources, distribution, and bioavailability in the North Pacific Ocean: Insights from data and models. Glob. Biogeochem. Cycles 23, GB2010. https://doi.org/10.1029/2008GB003425

Vishnivetskaya, T.A., Hu, H., Nostrand, J.D.V., Wymore, A.M., Xu, X., Qiu, G., Feng, X., Zhou, J., Brown, S.D., Brandt, C.C., Podar, M., Gu, B., Elias, D.A., 2018. Microbial community structure with trends in methylation gene diversity and abundance in mercury-contaminated rice paddy soils in Guizhou, China. Environ. Sci. Process. Impacts 20, 673–685. https://doi.org/10.1039/C7EM00558J

Yu, R.-Q., Flanders, J.R., Mack, E.E., Turner, R., Mirza, M.B., Barkay, T., 2012. Contribution of Coexisting Sulfate and Iron Reducing Bacteria to Methylmercury Production in Freshwater River Sediments. Environ. Sci. Technol. 46, 2684–2691. https://doi.org/10.1021/es2033718

FIGURES

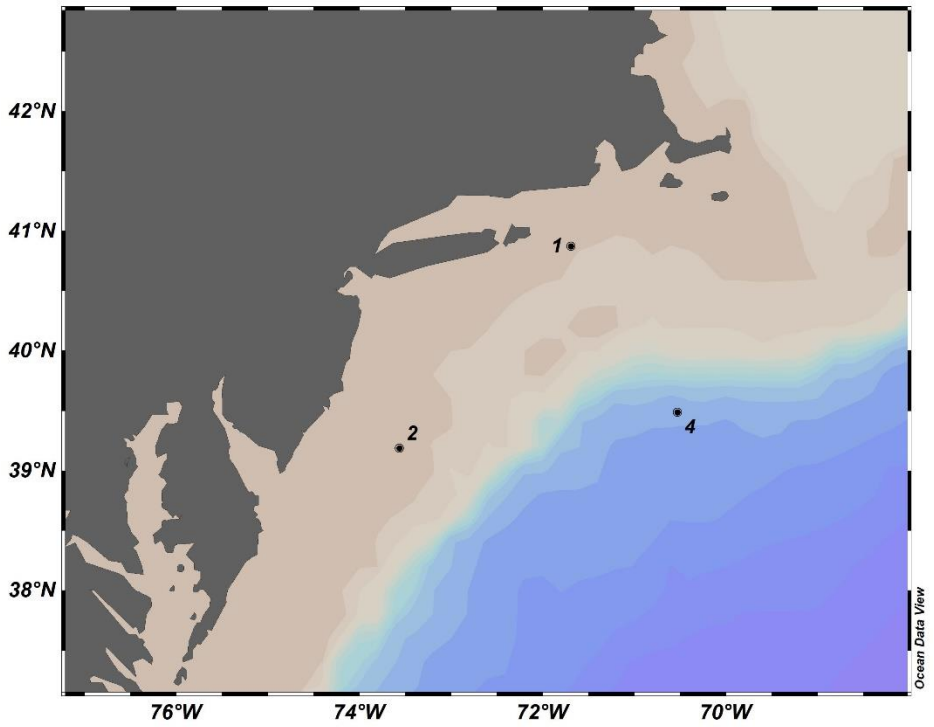

Figure 4.1. Map of seawater sampling locations. Color contours indicate differences in bathymetry and Stations indicated by points.

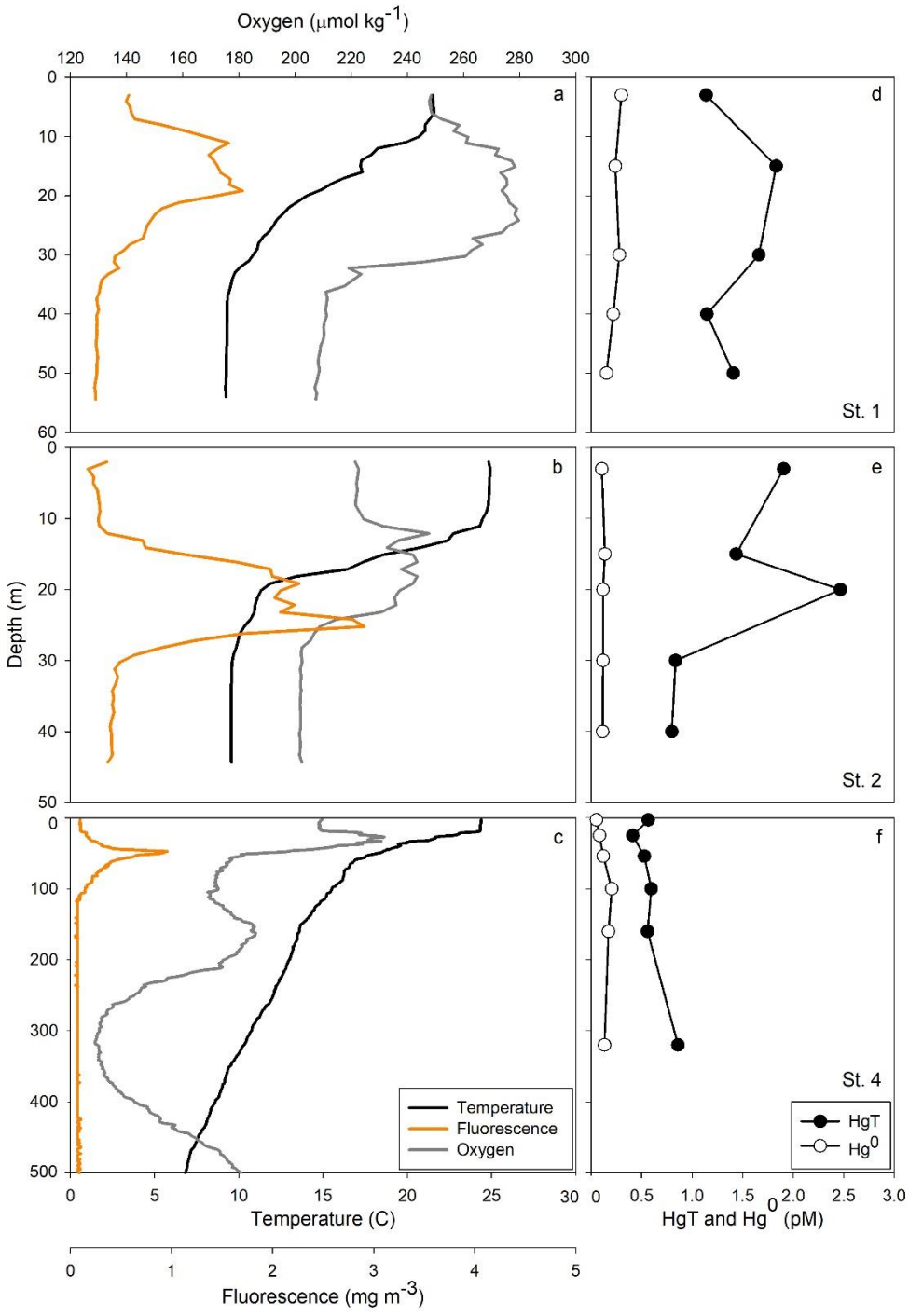

Figure 4.2. Temperature, oxygen and fluorescence at Stations 1, 2 and 4 (a, b, c), and total mercury (HgT) and elemental mercury (Hg^0) profiles (d, e, f; Lamborg et al., unpublished).

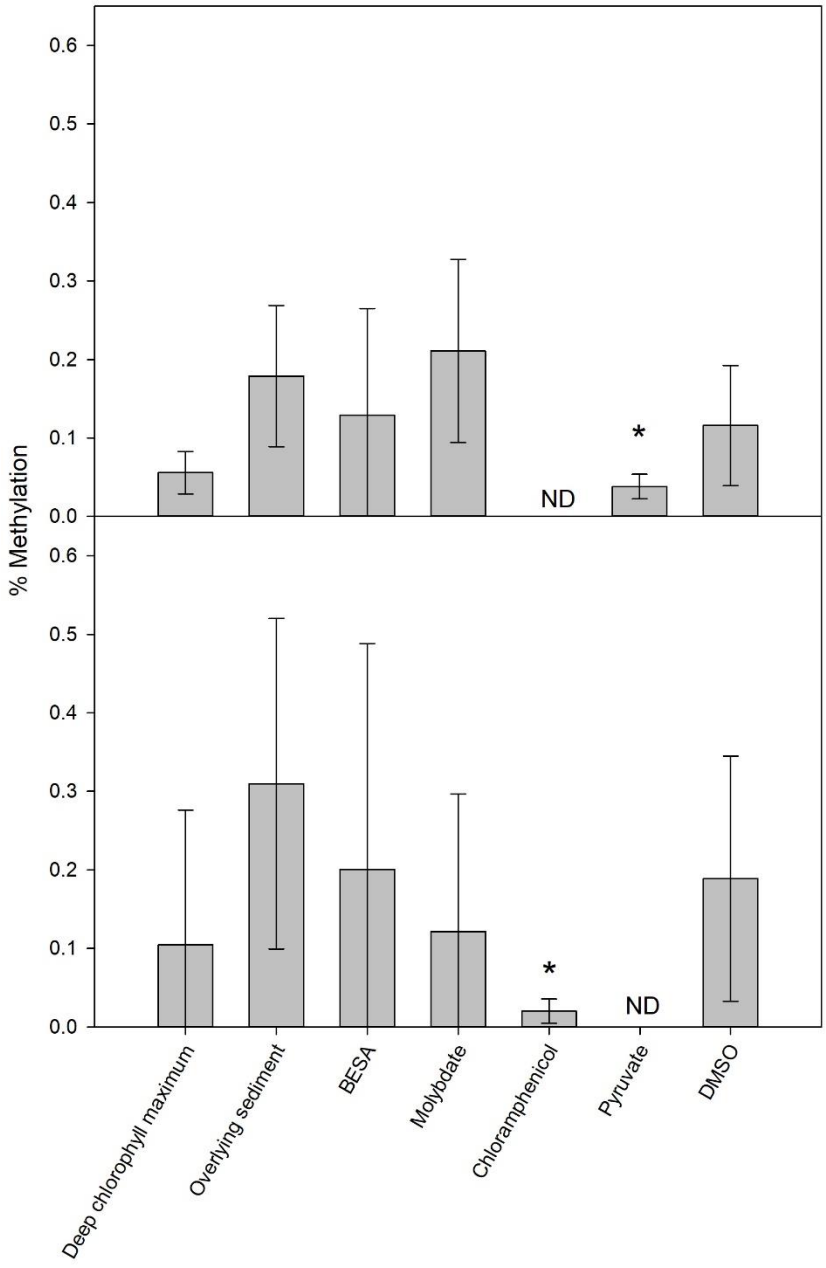
% Methylation
0.6
0.5
0.4
0.3
0.2
0.1
0.0
*
ND
0.6
0.5
0.4
0.3
0.2
0.1
0.0
*
ND
Deep chlorophyll maximum
Overlying sediment
BESA
Molybdate
Chloramphenicol
Pyruvate
DMSO

Figure 4.3. Mercury methylation potentials at Stations 1 (top) and 2 (bottom). Error bars indicate ± 1 standard deviation. The deep chlorophyll maximum and water overlying sediment were incubated without any treatment additions. Additional water was sampled at the bottom of the water column and amended with one of five treatments: 30 mM sodium 2-bromoethanesulfonate (BESA), 28 mM sodium molybdate, 0.25 mM chloramphenicol, 50 mM pyruvate, and 100 mM dimethyl sulfoxide (DMSO). Treatments significantly different from the control samples (overlying sediment) are marked with * for $p \leq 0.100$, and ND denotes no methylation was detected among the four replicates.

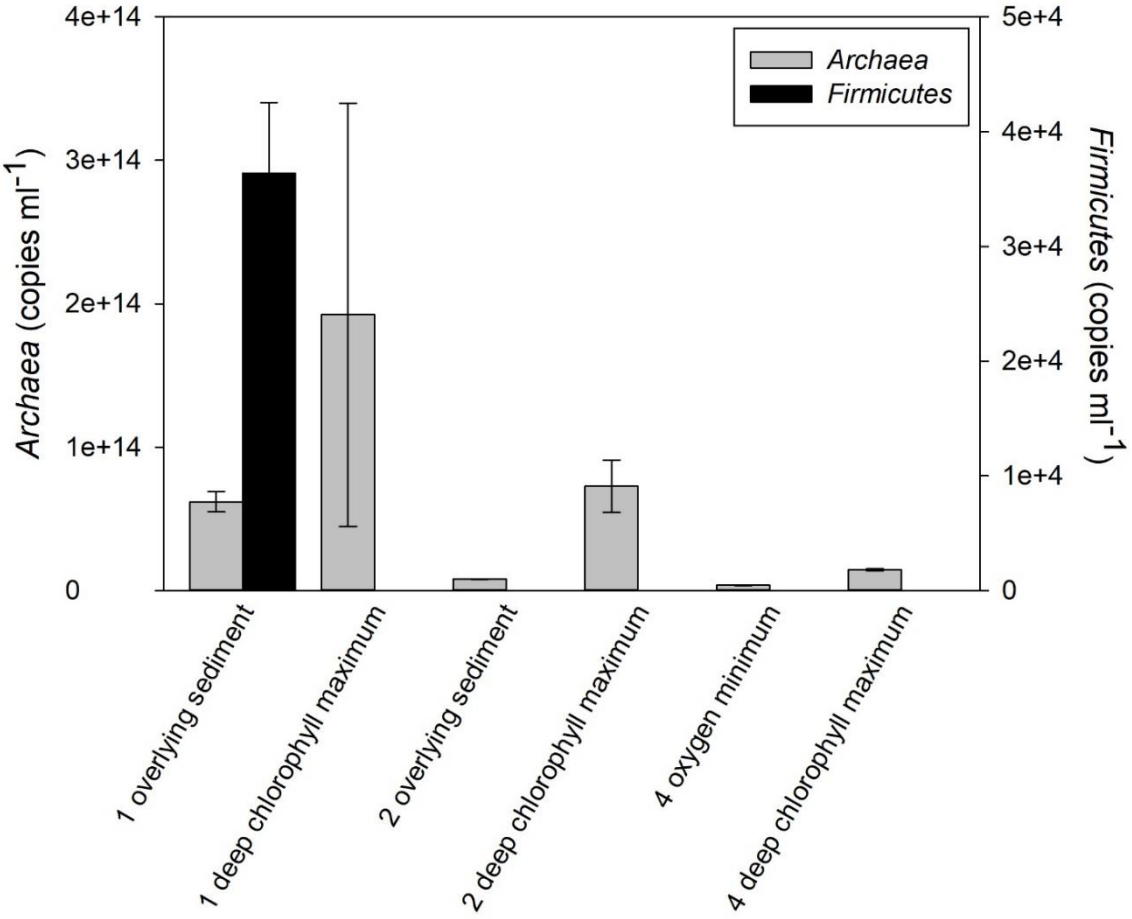

Figure 4.4. qPCR results for *hgcA* DNA in *Firmicutes* and *Archaea* in the deep chlorophyll maximum and above sediment at Stations 1 and 2, and the oxygen minimum at Station 4. Error bars indicate ± 1 standard deviation.

TABLES

Table 4.1. PCR primers from *HgcAB* screening, and qPCR primers for amplification of *hgcA* in the three Hg methylating clades, *Deltaproteobacteria*, *Firmicutes*, and *Archaea* (Christensen et al., 2016).

Primer Name	Sequence (5' to 3')	Amplicon Length (bp)
ORNL-HgcAB-uni-F	AAY GTC TGG TGY GCN GCV GG	818–1,020
ORNL-HgcAB-uni-R	CAB GCN CCR CAY TCC ATR CA	
ORNL-Delta-HgcA-F	GCC AAC TAC AAG MTG ASC TWC	107
ORNL-Delta-HgcA-R	CCS GCN GCR CAC CAG ACR TT	
ORNL-SRB-Firm-HgcA-F	TGG DCC GGT DAR AGC WAA RGA TA	167
ORNL-SRB-Firm-HgcA-R	AAA AGA GHA YBC CAA AAA TCA	
ORNL-Archaea-HgcA-F	AAY TAY WCN CTS AGY TTY GAY GC	125
ORNL-Archaea-HgcA-R	TCD GTC CCR AAB GTS CCY TT	

Table 4.2. Modified qPCR protocols for detection of *hgcA* with clade-specific primers (Christensen et al., 2016).

	Deltaproteobacteria	***Firmicutes***	***Archaea***
Initial denaturation	95 °C for 2 min	95 °C for 2 min	95 °C for 2 min
Denaturation	95 °C for 15 sec	95 °C for 10 sec	95 °C for 15 sec
Annealing	65°C for 33 sec	47 °C for 15 sec	50 °C for 30 sec
Extension	--	58 °C for 1 min	55 °C for 1 min
Number of cycles	50	35	50
Melt curve	65–95 °C	58–95 °C	55–95 °C
Forward primer conc.	375 nM	500 nM	250 nM
Reverse primer conc.	375 nM	250 nM	250 nM

Table 4.3. Temperature and light comparison between in-situ conditions and incubation conditions for seawater from the deep chlorophyll maximum.

	In situ		Incubator	
Station	T (°C)	%PAR	T (°C)	Illuminance (lux)
1	17.3	12	25.1	7234
2	11.3	4	25.8	8444
4	17.5	4	20.3	5239

*Average illuminance over 24 hour incubation period

Chapter 5: CONCLUSIONS AND FUTURE DIRECTIONS

The primary goal of this work was to improve understanding of Hg cycling and methylation in the water column. Water was sampled from three diverse systems: the Arctic Ocean, and Atlantic Ocean margin, and Crystal Lake (Medway, Ohio). In the Arctic Ocean, my goal was to measure Hg speciation and distribution. Freshwater work in Crystal Lake examined Hg speciation and distribution, and quantified methylation potentials and methylator abundance. Lastly, work in the northwest Atlantic Ocean improved understanding of Hg cycling in coastal waters and identified microbes that may be involved in methylation in oxic waters.

5.1. Water column methylation

> Hypothesis 1: Mercury methylation occurs in the oxic water column of lakes and coastal marine ecosystems.

Mercury methylation in oxic waters was observed in both Crystal Lake and the northwest Atlantic Ocean. Methylation potentials in the northwest Atlantic Ocean were less than half of those measured in Crystal Lake. On average, Hg methylation occurs more quickly in Crystal Lake (1.6 ± 0.27 % d^{-1}; ± 1 SE) than in northwest Atlantic shelf waters (0.16 ± 0.11 % d^{-1}; ± 1 SD). The microbial community within the the oxygen minimum over the continental slope at Station 4 did not methylate a detectable amount of Hg, suggesting that in addition to shelf sediment, shelf waters are an important source of MMHg to near-

shore fisheries (Hammerschmidt and Fitzgerald, 2006). In comparison, the methylation potential in Crystal Lake's anoxic hypolimnion was 50 times greater than the methylation potential of Atlantic shelf waters. Methylation potentials of the two sites were reflected in ambient MMHg concentrations at both sites, with greater Crystal Lake mean MMHg concentration (1.0 ± 0.15 pM, ± 1 SE) than in the northwest Atlantic Ocean (0.095 ± 0.098 pM ± 1 SD).

5.2. Influence of sea ice on surface Hg distribution

> Hypothesis 2: Sea ice cover alters Hg speciation and concentration in the upper water column, compared to open (ice-free) water.

Sea ice affected some species of Hg. Hg^0 was supersaturated in ice-covered waters. Ice-covered waters likely accumulate Hg^0 due to limited gas exchange with the atmosphere. Under-ice Hg^0 measurements were among the highest measurements made throughout the GN01 transect. The fraction of HgT as Hg^0 was greater in ice-covered waters as opposed to ice-free waters. Ice cover did not impact on HgT, but MMHg concentrations were elevated in ice-covered waters. Increased MMHg content could be a result of under-ice methylating communities (Gionfriddo et al., 2016), or reduced photodemethylation due to ice cover. DMHg was not elevated under the ice, suggesting either ice does not prevent DMHg from degassing in the same manner as Hg^0, or mechanisms affecting DMHg concentration are not affected by ice cover.

5.3. Arctic circulation patters influence Hg abundance and speciation

> Hypothesis 3: Hg speciation and vertical distributions result from water circulation and age differences between the Makarov, Canada, and Fram Basins.

Seawater circulation dictated Hg speciation and distribution more than age. Pacific inflow through the Bering Strait brings filtered and particulate HgT and particulate MMHg into the central Arctic Ocean. We estimated the Bering Strait supplies 4–71 kmol HgT yr^{-1}. The Transpolar Drift (TPD) is another source of Hg to the Arctic Ocean, as it brings relatively young Siberian Shelf water to the central Arctic Ocean. The TPD introduced higher HgT and Hg^0 concentrations to surface waters, but had no effect on MMHg. DMHg was negatively impacted by meteoric water brought by the TPD, suggesting DMHg concentrations were influenced by marine processes. Intermediate and deep water circulation mobilized HgT and MMHg from sills and pelagic sediments. We did not find a difference in Hg species concentrations between Canadian Basin Deep Water and Eurasian Basin Deep Water even though the two water masses differ in age by almost 200 years. Lastly, methylated Hg species were unrelated to apparent oxygen utilization, phosphate, and nitrate concentrations, which in the Arctic are formed over the shelf, suggesting MMHg is formed in situ.

5.4. Sulfide controls on Hg methylation in Crystal Lake

> Hypothesis 4: Interactions between sulfide and Hg in the hypolimnion of Crystal Lake form HgS complexes that decrease in situ MMHg concentrations, but do not affect methylation potential.

In early spring, the MMHg maximum in Crystal Lake was in the hypolimnion. As sulfide concentrations increased from spring to summer, hypolimnetic MMHg decreased. When sulfide levels exceeded 100 μM, MMHg was not detected in filtered hypolimnetic water. In the summer and fall, the MMHg maximum was at the oxic/anoxic boundary. During July, August, and September, methylation potentials were measured in the hypolimnion.

Crystal Lake bottom water had an average methylation potential of 4.9 ± 3.0 % d^{-1} (± 1 SE). These results suggest that ambient Hg formed Hg-S complexes that were unavailable to methylating bacteria (Benoit et al., 2001a, 2001b, 1999; Gilmour et al., 2018). Additions of labile Hg(II) were likely methylated before equilibrating with sulfide.

5.5. Methylation community composition

Goal: Investigate the diversity, abundance, and distribution of methylating communities in the water columns of the North Atlantic Ocean and Crystal Lake.

Hypothesis 5: There will be a greater abundance of hgcAB genes where higher methylation rates are measured.

hgcA was present in all DNA samples from Crystal Lake and northwest Atlantic Ocean shelf waters. Methylation potentials in Crystal Lake had a positive correlation with *Firmicutes* gene copy number. A low positive correlation was found for *Archaea*, and a negative correlation was found for *Deltaproteobacteria* and methylation potentials in Crystal Lake. These results suggest *Firmicutes* are the primary methylators in Crystal Lake.

Clade-specific *hgcA* abundance provided some insight to the diversity of methylating communities among sites. In oxic waters in both Crystal Lake and the northwest Atlantic Ocean, *Archaeal hgcA* was found, suggesting methanogens may play a role in Hg methylation in oxic waters. Communities of *Archaea* seem to be important in both environments, likely due to their diverse presence in two out of six classes, and their ubiquity in different environments (Gilmour et al., 2013). In culture, methanogens

produce methylation rates equal to *Deltaproteobacteria* (Gilmour et al., 2018), which may support methylation potentials measured in northwest Atlantic shelf waters.

5.6. Future directions

These studies have improved our understanding of Hg distribution and methylation in marine and freshwater systems, but knowledge gaps remain, especially regarding biotic Hg methylation. First, improving the method of assessing methylating communities by collecting either RNA or cDNA for qPCR would identify and quantify active methylating clades, as opposed to DNA, which confirms presence but not necessarily activity. Genomic sequencing should also be used to identify methylators and potential methylators in the environment. Gene sequencing may identify alternate biotic pathways of Hg methylation. Community diversity analyses from sequencing data may identify syntrophic organisms and potential reaction mechanisms leading to MMHg formation.

Chemical analyses can also be improved to better understand Hg cycling. First, MMHg demethylation potentials should be constrained by extending the incubation period to 48 or 62 hours (Eckley et al., 2005). Method improvements to lower detection limits for both methylation and demethylation would be ideal for studies in seawater. More work in low oxygen waters and oxygen minimum zones is necessary, because these areas have been identified as potentially important regions for methylation. Lastly, DMHg cycling measurements can identify controlling factors and mechanisms of formation.

As for the Arctic Ocean, data from the three Arctic GEOTRACES cruises needs to be compiled and synthesized. Prior to 2015, there was little Hg data in the Arctic Ocean. Now, three datasets can describe Hg sources and cycling in the Arctic Ocean and neighboring seas. Together, we can begin to test many of the hypotheses regarding anomalously high MMHg in Arctic mammals. Although we have more data, many questions remain unanswered. Temperature dependence of biological uptake and partitioning rates should be investigated to evaluate whether plankton in colder climates accumulate Hg more quickly than in warmer waters. Methylation over broad Arctic shelves should be studied. In locations where large fluxes of Hg enter the Arctic, methylating microbial communities should be characterized. Describing Hg speciation and distribution in the Arctic is not enough to understand the complexity involved with cycling and accumulation of Hg. This work provides a good framework for future studies and understanding of Hg cycling and methylation in a changing world.

5.7. References

Benoit, J.M., Gilmour, C.C., Mason, R.P., 2001a. Aspects of Bioavailability of Mercury for Methylation in Pure Cultures of Desulfobulbus propionicus (1pr3). Appl. Environ. Microbiol. 67, 51–58. https://doi.org/10.1128/AEM.67.1.51-58.2001

Benoit, J.M., Gilmour, C.C., Mason, R.P., 2001b. The Influence of Sulfide on Solid-Phase Mercury Bioavailability for Methylation by Pure Cultures of *Desulfobulbus propionicus* (1pr3). Environ. Sci. Technol. 35, 127–132. https://doi.org/10.1021/es001415n

Benoit, J.M., Gilmour, C.C., Mason, R.P., Heyes, A., 1999. Sulfide Controls on Mercury Speciation and Bioavailability to Methylating Bacteria in Sediment Pore Waters. Environ. Sci. Technol. 33, 951–957. https://doi.org/10.1021/es9808200

Eckley, C.S., Watras, C.J., Hintelmann, H., Morrison, K., Kent, A.D., Regnell, O., 2005. Mercury methylation in the hypolimnetic waters of lakes with and without connection to wetlands in northern Wisconsin. Can. J. Fish. Aquat. Sci. 62, 400–411. https://doi.org/10.1139/F04-205

Gilmour, C.C., Bullock, A.L., McBurney, A., Podar, M., Elias, D.A., 2018. Robust Mercury Methylation across Diverse Methanogenic Archaea. mBio 9, e02403-17. https://doi.org/10.1128/mBio.02403-17

Gilmour, C.C., Podar, M., Bullock, A.L., Graham, A.M., Brown, S.D., Somenahally, A.C., Johs, A., Hurt, R.A., Bailey, K.L., Elias, D.A., 2013. Mercury Methylation by Novel Microorganisms from New Environments. Environ. Sci. Technol. 47, 11810–11820. https://doi.org/10.1021/es403075t

Gionfriddo, C.M., Tate, M.T., Wick, R.R., Schultz, M.B., Zemla, A., Thelen, M.P., Schofield, R., Krabbenhoft, D.P., Holt, K.E., Moreau, J.W., 2016. Microbial mercury methylation in Antarctic sea ice. Nat. Microbiol. 1, 16127.

Hammerschmidt, C.R., Fitzgerald, W.F., 2006. Methylmercury cycling in sediments on the continental shelf of southern New England. Geochim. Cosmochim. Acta 70, 918–930. https://doi.org/10.1016/j.gca.2005.10.020